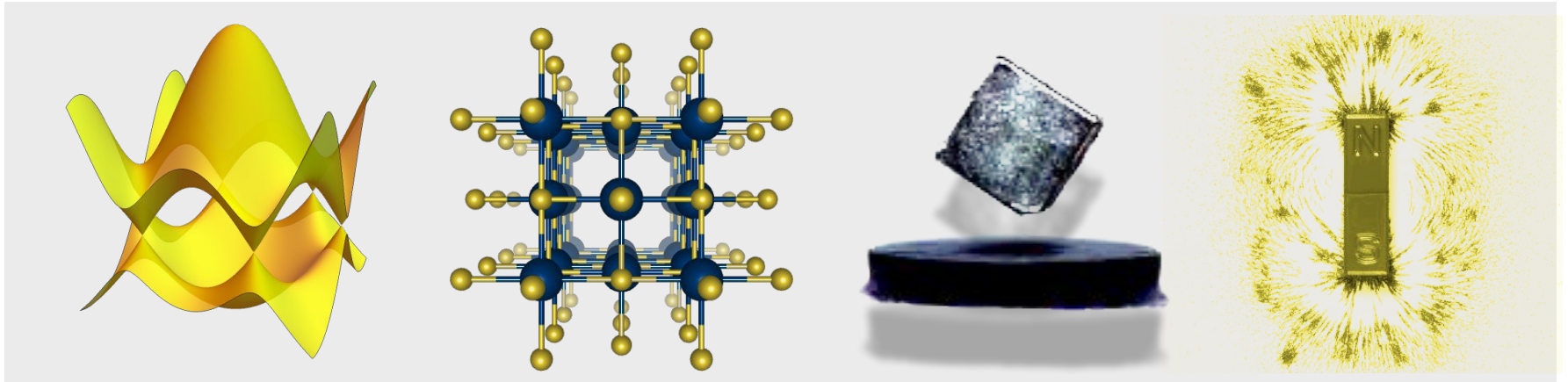


ESCOLA SÉRGIO MASCARENHAS DE FÍSICA DA MATÉRIA CONDENSADA

Aula 4 - 18 de Julho

Propriedades Magnéticas



História

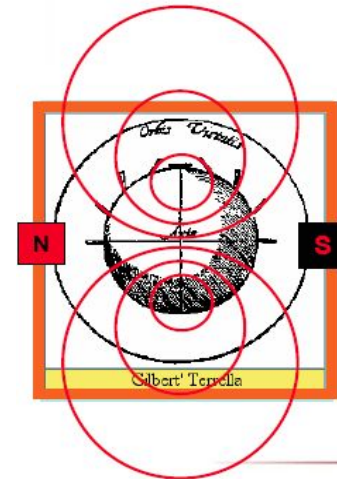
- O termo surge da antiga cidade grega de Magnésia, onde muitos magnetos naturais eram achados. Hoje nos referimos a esses materiais como ímãs, que contém magnetita, um ferromagneto natural (Fe_3O_4).
- Plínio, o velho (23-79 DC) descreveu uma montanha próxima ao Rio Indu que era inteiramente feita de uma pedra que atraía o ferro.
- Os chineses, já em 121 DC sabiam que uma haste de ferro aproximada desses magnetos naturais adquiriria e reteria as propriedades magnéticas... e que essa haste, ao ser suspensa por um fio, se alinharia na direção norte-sul.

Primórdios...

- **Lodestone:** rocha magnetizada
 - Rica em magnetita (Fe_3O_4)
 - "lead stone" indicar o caminho"
 - Chineses e europeus 800AC



- 1600 *De Magnete*, de William Gilbert:
 - Primeiro tratado científico de magnetismo.
 - Observação do campo de dipolo para diferentes formas de ímã.
 - A terra é um grande ímã



Curiosidades...



- Sob o travesseiro de uma “esposa infiel” levaria à confissão do crime durante o sono.
- Magnetismo animal: poder de curar...
- Dr. James Graham: "Royal Patagonian Magnetic Bed" (50 guinés/noite)



Indicações: dores nos ombros, cabeça, nuca, braços, queda de cabelo, problemas faciais e que transpiram muito na cabeça.

“O campo magnético proporciona o equilíbrio energético”



Rabatan com imãs e photon



CUIDADO!!!!
Efeito interrompido por
ALHO ou CEBOLA



Magnetoterapia

- **O que é o Magnetismo:**

:: O magnetismo é uma força gravitacional emitida do centro do globo terrestre. Alguns físicos propõem que existe um gigantesco magneto permanente no centro da Terra ou uma corrente elétrica que é responsável pelo campo magnético da Terra, transformando-a num imenso imã, energia esta chamada de geomagnetismo, que atua sobre todos os seres vivos trazendo grandes benefícios para saúde. (Magnetoterapia pág. 37/1999).

www.unimagcolchoes.com.br/m



- Travesseiros Terapêuticos ZiFF - Proporcionam um sono profundo e revitalizador, respeitando a anatomia da cabeça, dos ombros e, principalmente, sem forçar a coluna, ajudando a prevenir uma série de problemas à sua saúde, pela melhor posição circulação. <http://www.ziff.com.br/>



Magnetoterapia

- **"Magnetismo Humano Sutil"**
- Ministrado pelo autor, ininterruptamente desde 1973, com material integralmente elaborado por ele, inclusive 42 slides.
- www.portaluz.com.br/curso_magnetismo.htm



A decorative header at the top of the slide features a horizontal band with a light gray background. On this band, there are several semi-transparent icons: a diamond on a pedestal, a molecular structure, a yellow flower-like shape, and a circular disc. Below this band, there are two larger, semi-transparent gray rectangular blocks, one on the left and one on the right, which appear to be part of a larger graphic or design.

Sabia-se que os fenômenos existiam e foram desenvolvidas aplicações interessantes.

Mas ninguém os entendia!

Finalmente, a Ciência!

- Somente em 1819 é que foi encontrada uma conexão entre os fenômenos elétricos e magnéticos. O Cientista Danês Hans Christian Oersted observou que uma agulha de uma bússola na vizinhança de um fio que transportava corrente elétrica era defletida.
- Em 1831, Michael Faraday descobriu que uma corrente momentânea aparecia em um circuito quando a corrente em um circuito próximo era iniciada ou parada.
- Logo depois, ele descobriu que o movimento de um ímã em direção a ou saindo de um circuito podia produzir o mesmo efeito. Aparentemente, Joseph Henry havia descoberto esses fenômenos antes, mas não conseguiu publicá-los.

A conexão foi estabelecida

Oersted mostrou que efeitos magnéticos podiam ser produzido ao mover cargas elétricas; Faraday e Henry mostraram que as correntes elétricas podiam ser produzidas por ímãs em movimento.

Então...

Conexões...

Todos os fenômenos
magnéticos resultam
de forças entre
cargas elétricas em
movimento!

Olhando com mais detalhe

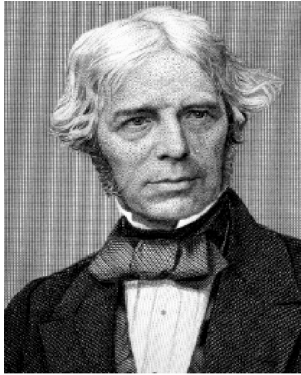
- Ampère foi o primeiro a sugerir em 1820 que as propriedades da matéria eram devidas a minúsculas correntes atômicas.
- Todos os átomos exibem fenômenos magnéticos
- O meio no qual as cargas se movem tem efeito profundo nas forças magnéticas observadas.

O que podemos aprender sobre magnetismo?

1. Há pólos norte e pólos sul.
2. Pólos iguais se repelem, e pólos opostos se atraem.
3. Forças magnéticas atraem somente materiais magnéticos.
4. Forças magnéticas atuam a distância.
5. Enquanto estão magnetizados, os magnetos temporários atuam como magnetos permanentes.

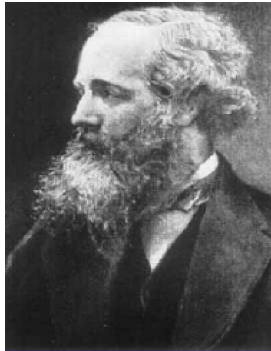
Lista Top Ten

6. Uma espira com uma corrente elétrica fluindo através dela torna-se um magneto.
7. Colocar ferro dentro de uma bobina com corrente aumenta a força do eletroímã.
8. Um campo magnético variável induz uma corrente elétrica em um condutor.
9. Uma partícula carregada não sente a força magnética quando se movimenta paralelamente a um campo magnético, mas quando se move perpendicular a esse campo ela sente uma força que é perpendicular tanto ao campo quanto à direção de movimento.
10. Um fio condutor de corrente em um campo magnético perpendicular sente uma força na direção perpendicular tanto ao fio quanto ao campo.



Michael Faraday

- 1820 Oersted: efeito magnético das correntes
- 1820-21 Ampère:
 - atribui o magnetismo da matéria a "correntes moleculares"
- 1831 Faraday: campo variável induz corrente elétrica em um circuito
- 1864 Maxwell: teoria eletromagnética:



James Clerk Maxwell

$$\nabla \cdot \vec{B} = 0 ,$$

$$\nabla \times \vec{E} + \partial \vec{B} / \partial t = 0 ,$$

$$\nabla \cdot \vec{D} = \rho ,$$

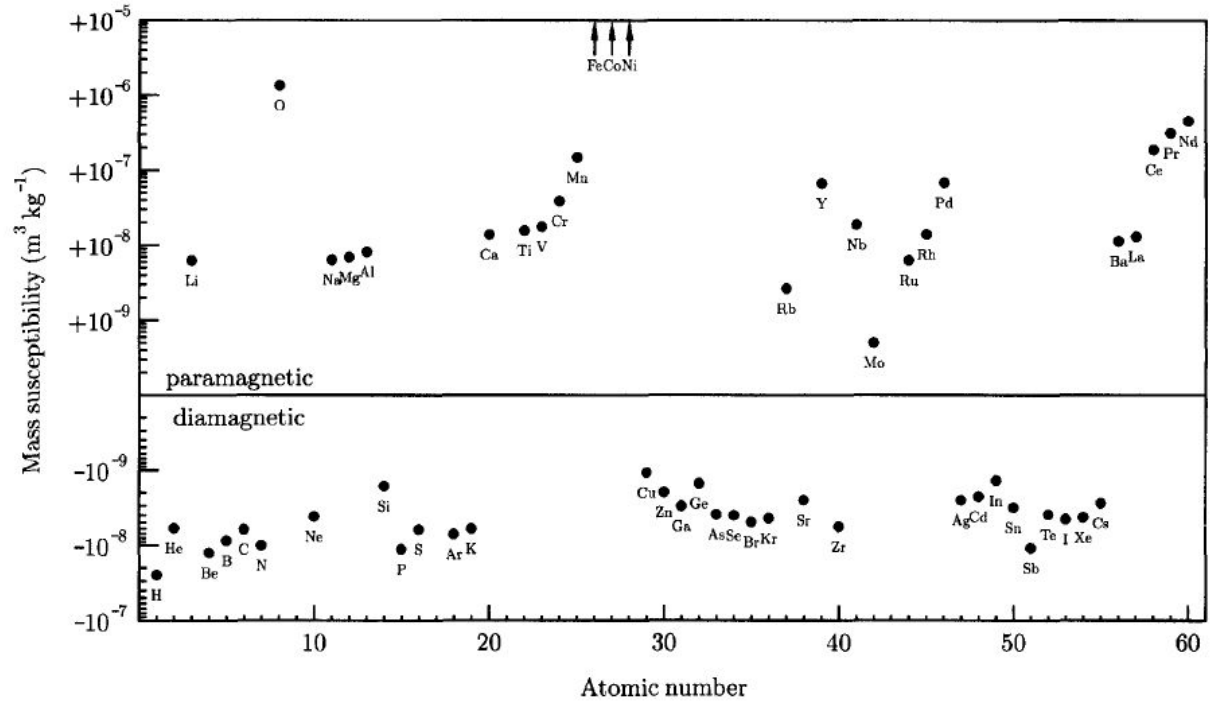
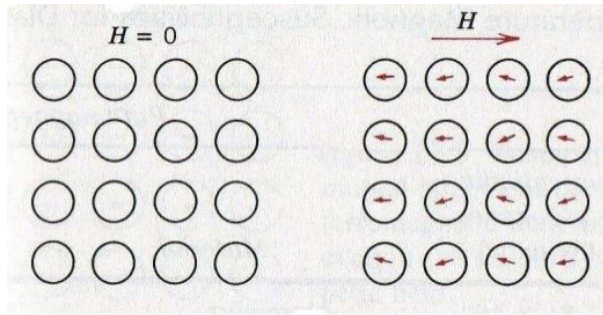
$$\nabla \times \vec{H} - \partial \vec{D} / \partial t = \vec{J} .$$

- 1897 descoberta do eletron
- Sec XX : Teoria Quântica (1925-1930)
(Heisenberg, Dirac, Schrödinger, Pauli)

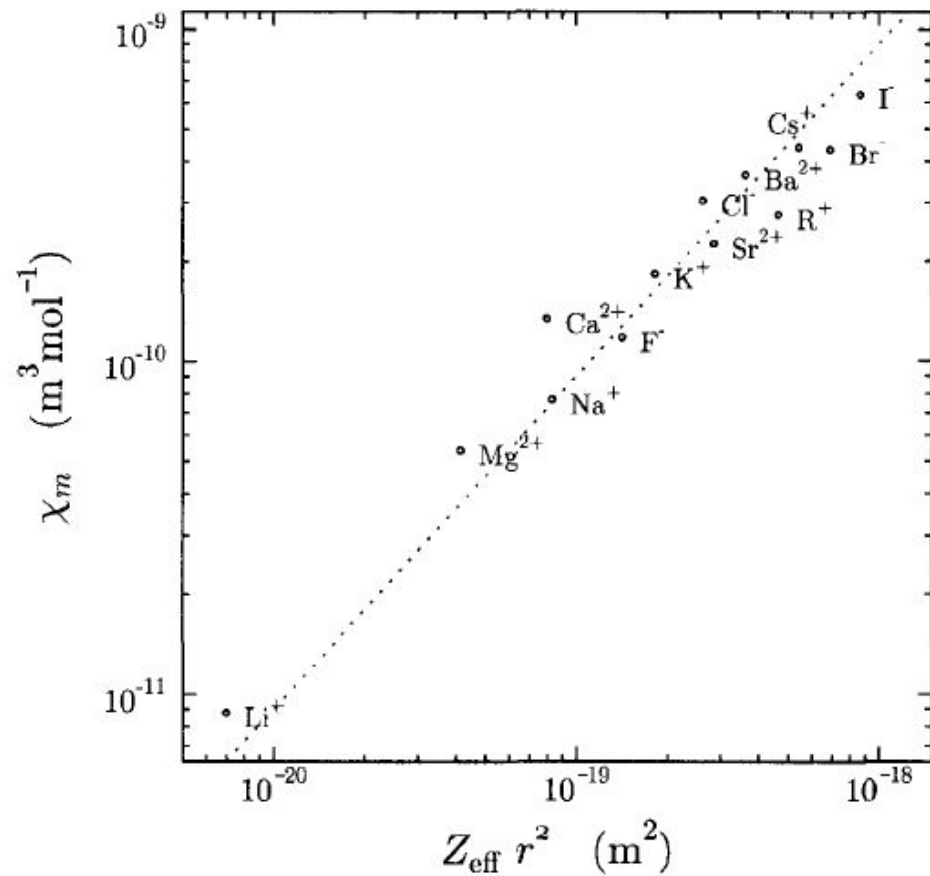


Andre-Marie Ampere

Diamagnetismo



$$\sum_{i=1}^{Z_{\text{eff}}} \langle r_i^2 \rangle \approx Z_{\text{eff}} r^2.$$



Grafito pirolitico

PHYSICAL REVIEW

VOLUME 123, NUMBER 5

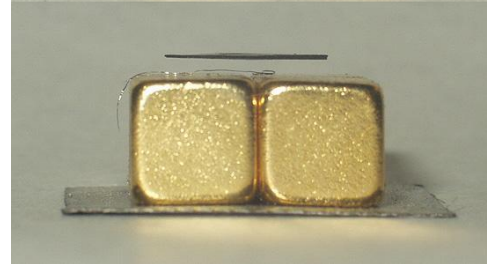
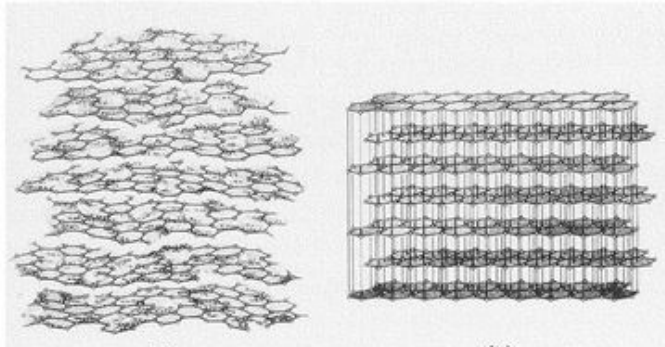
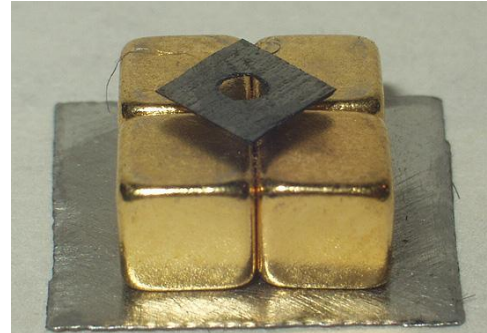
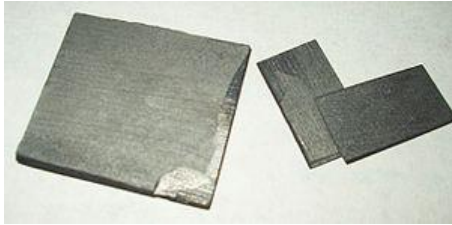
SEPTEMBER 1, 1961

Diamagnetic Susceptibility of Pyrolytic Graphite*

D. B. FISCHBACH

Jet Propulsion Laboratory, California Institute of Technology, Pasadena, California

(Received April 12, 1961)



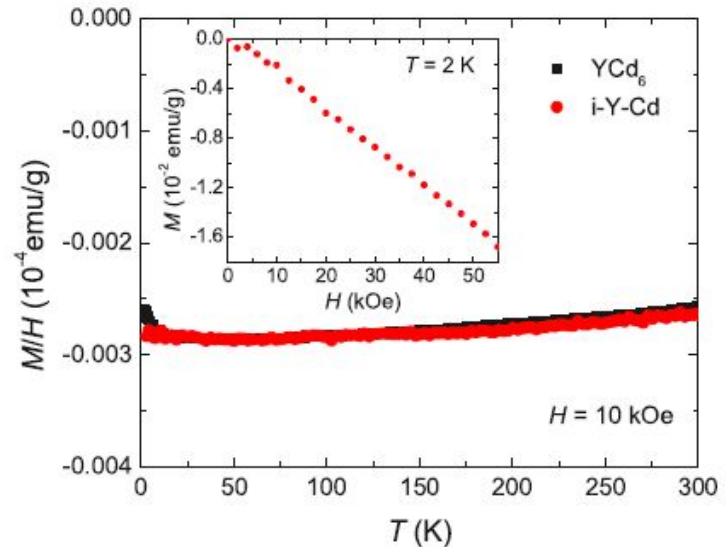
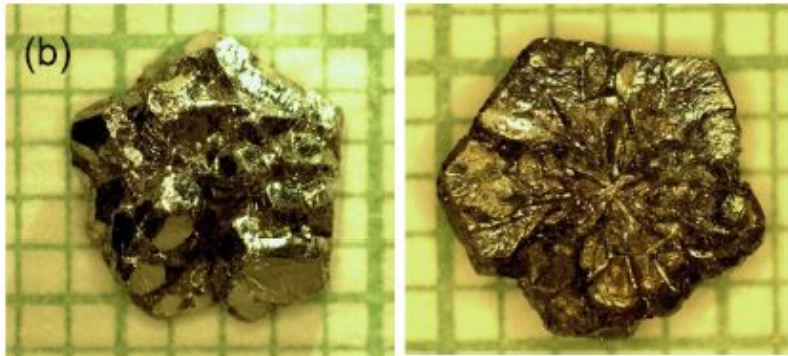
Magnetic and transport properties of *i-R*-Cd icosahedral quasicrystals ($R=Y, Gd-Tm$)

Tai Kong,¹ Sergey L. Bud'ko,¹ Anton Jesche,¹ John McArthur,² Andreas Kreyssig,¹
Alan I. Goldman,¹ and Paul C. Canfield^{1,*}

¹Ames Laboratory, US DOE, and Department of Physics and Astronomy, Iowa State University, Ames, Iowa 50011, USA

²Quantum Design Japan, 1-11-16 Takamatsu, Toshima ku, Tokyo 171-0042, Japan

(Received 17 June 2014; revised manuscript received 5 July 2014; published 18 July 2014)



Unusual evolution from a superconducting to an antiferromagnetic ground state in $Y_{1-x}Gd_xPb_3$ ($0 \leq x \leq 1$)

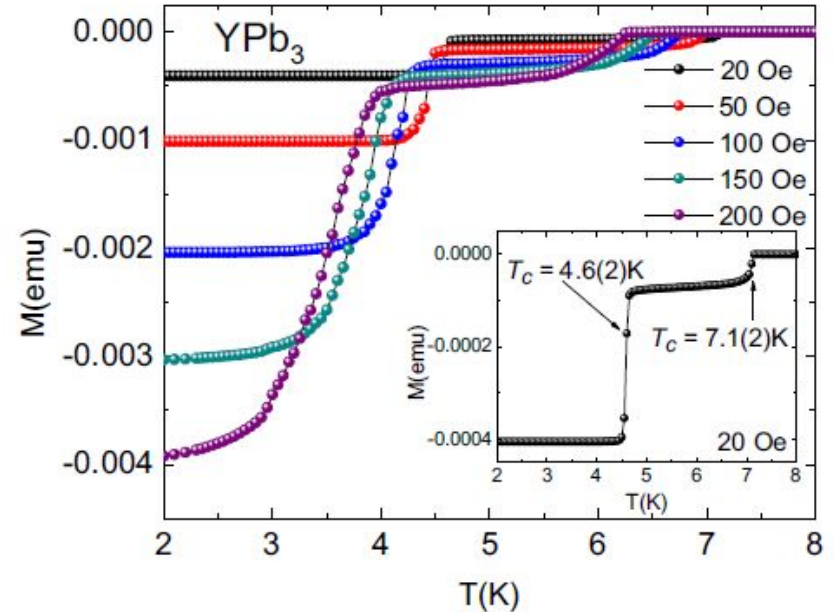
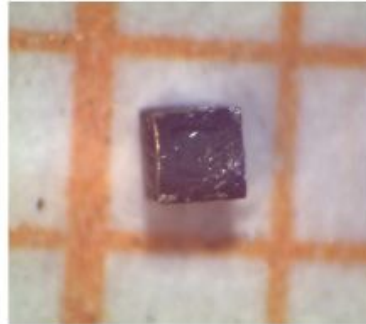
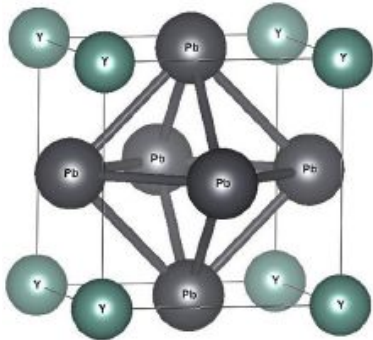
M. Cabrera-Baez,^{1,*} V. C. Denis,² L. Mendonça-Ferreira,² M. Carlone,³ P. A. Venegas,⁴ M. A. Avila,² and C. Rettori^{1,2}

¹Instituto de Física "Gleb Wataghin," UNICAMP, Campinas, São Paulo 13083-859, Brazil

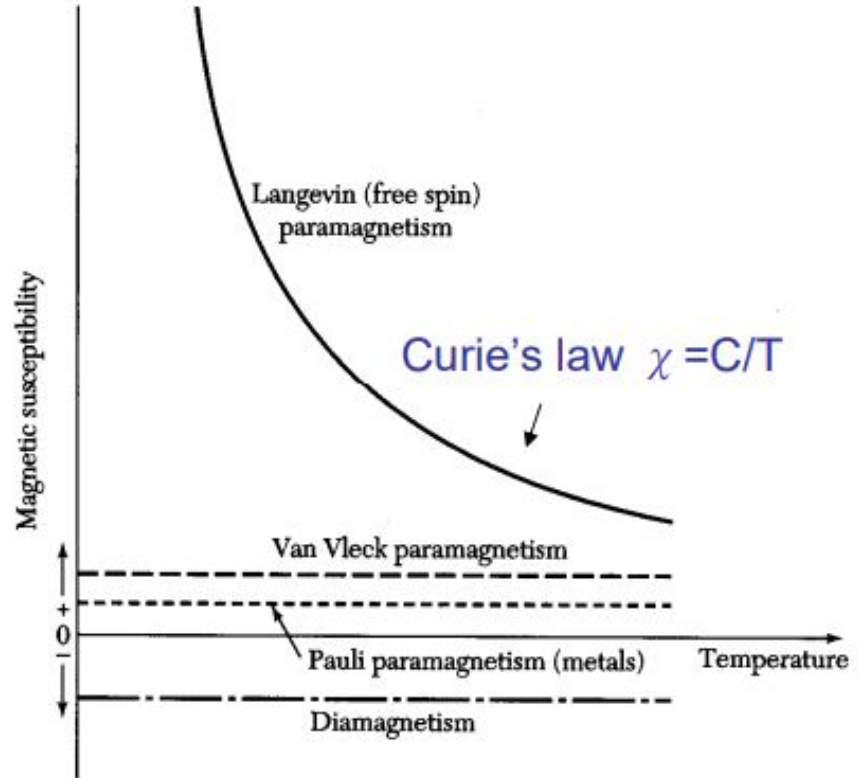
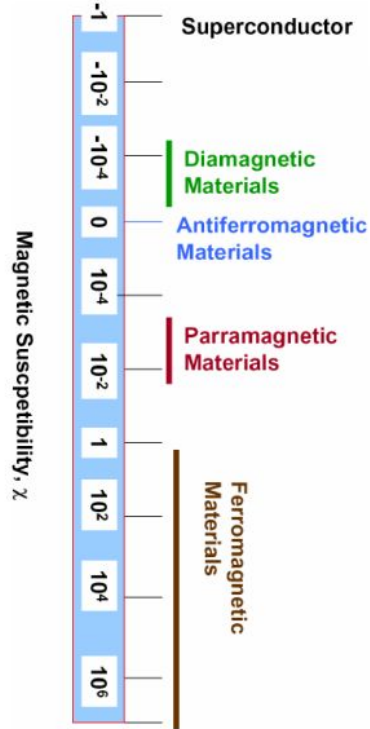
²CCNH, Universidade Federal do ABC, Santo André, São Paulo 09210-580, Brazil

³Programa de Pós-Graduação em Ciência e Tecnologia de Materiais, Faculdade de Ciências, Universidade Estadual Paulista - UNESP, Bauru, São Paulo 17033-360, Brazil

⁴Departamento de Física, Faculdade de Ciências, Universidade Estadual Paulista, Bauru, São Paulo 17033-360, Brazil



Susceptibilidade em escala



Atomic susceptibility

$$H = \sum_i \left(\frac{p_i^2}{2m} + V_i \right) + \mu_B (\vec{L} + g\vec{S}) \cdot \vec{H} + \frac{e^2}{2mc} \sum_i A_i^2, \quad \mu_B = \frac{e\hbar}{2mc}$$
$$= H_0 + \Delta H$$

Order of magnitude

- $\mu_B (\vec{L} + g\vec{S}) \cdot \vec{H} \approx \mu_B H \approx \hbar\omega_c$
 $\approx 10^{-4} eV$ when $H = 1 \text{ T}$
- $\vec{A}_i = \frac{H}{2} (-y_i, x_i, 0)$
 $\frac{e^2}{2mc} \sum_i A_i^2 \approx \left(\frac{eH}{mc} \right)^2 ma_0^2, \quad a_0 \equiv \frac{\hbar^2}{me^2}$
 $\approx \frac{(\hbar\omega_c)^2}{e^2 / a_0} \approx 10^{-5}$ of the linear term at $H = 1 \text{ T}$

$$J = 6 \quad {}^7F_6 \text{ ————— } E_6 = 21\lambda$$

$$J = 5 \quad {}^7F_5 \text{ ————— } E_5 = 15\lambda$$

$$J = 4 \quad {}^7F_4 \text{ ————— } E_4 = 10\lambda$$

$$J = 3 \quad {}^7F_3 \text{ ————— } E_3 = 6\lambda$$

$$J = 2 \quad {}^7F_2 \text{ ————— } E_2 = 3\lambda$$

$$J = 1 \quad {}^7F_1 \text{ ————— } E_1 = \lambda$$

$$J = 0 \quad {}^7F_0 \text{ ————— } E_0 = 0$$

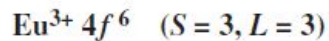


Fig. 1. Energy levels of the lowest multiplet 7F_J of trivalent Eu^{3+} ions in the absence of the external field. These separations are caused by the spin-orbit interaction $\lambda \mathbf{L} \cdot \mathbf{S}$. The magnitude of λ indicates the energy difference between the ground state and the first excited state.

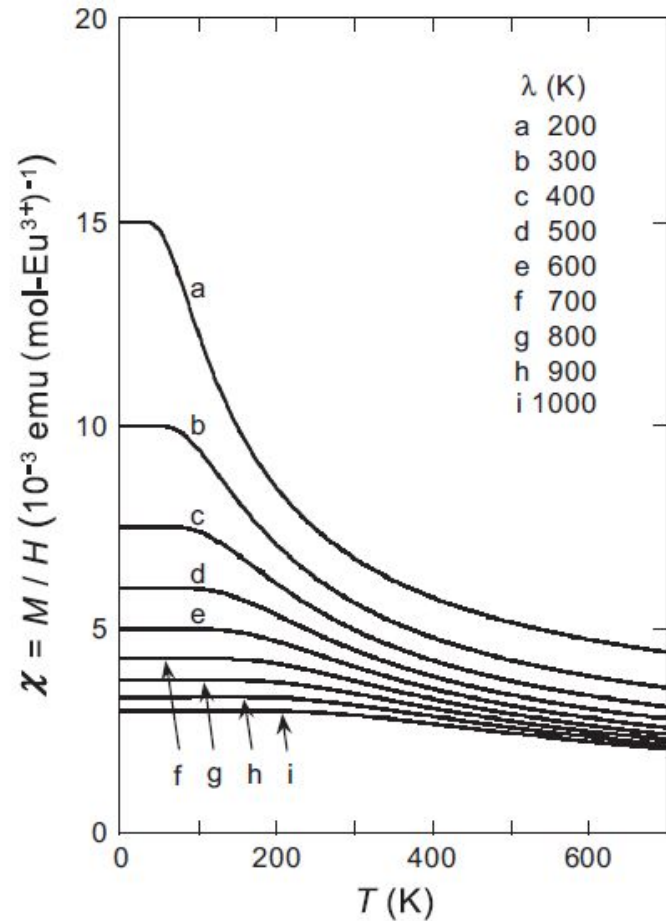
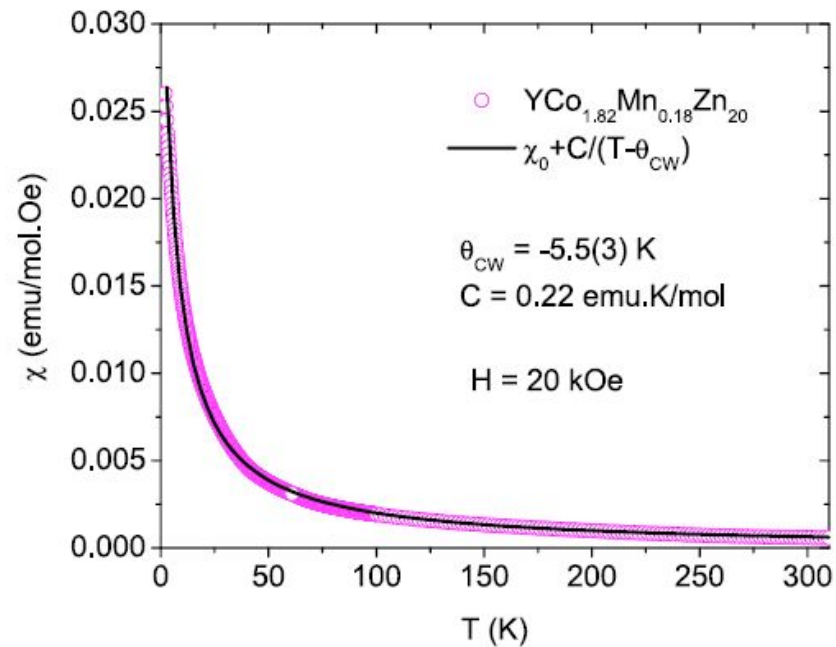
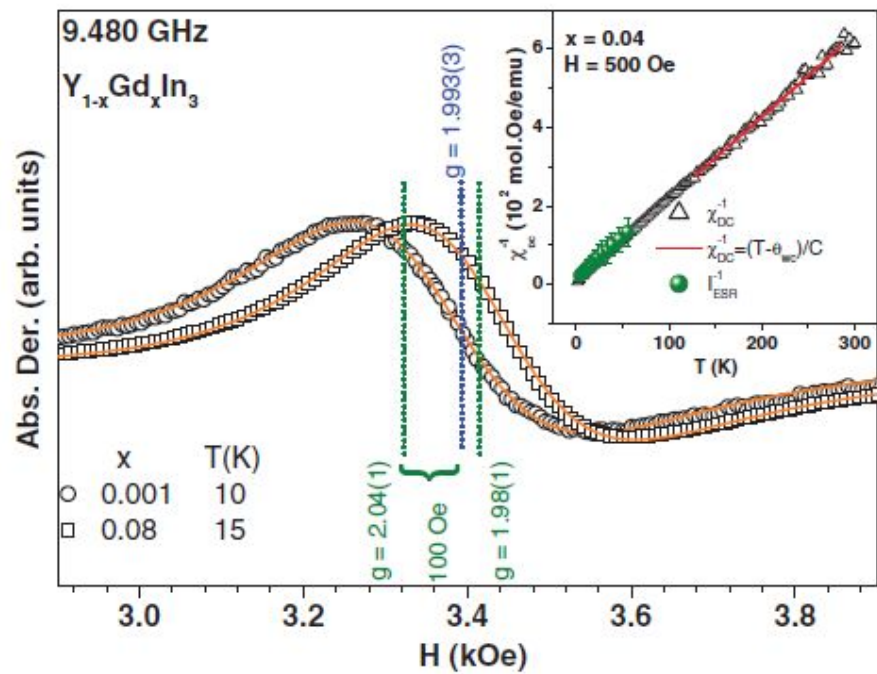
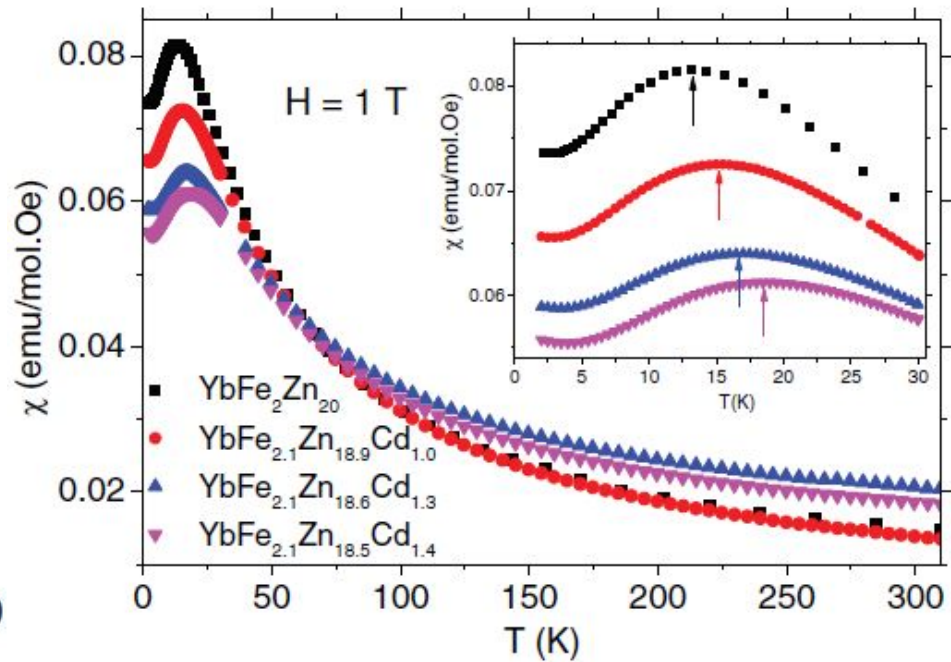
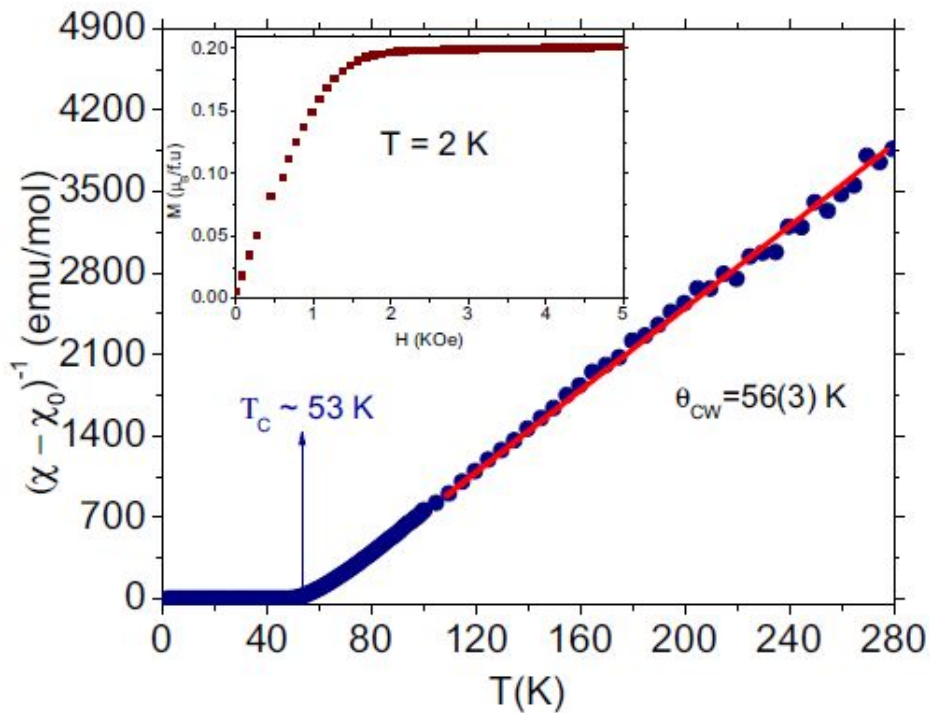
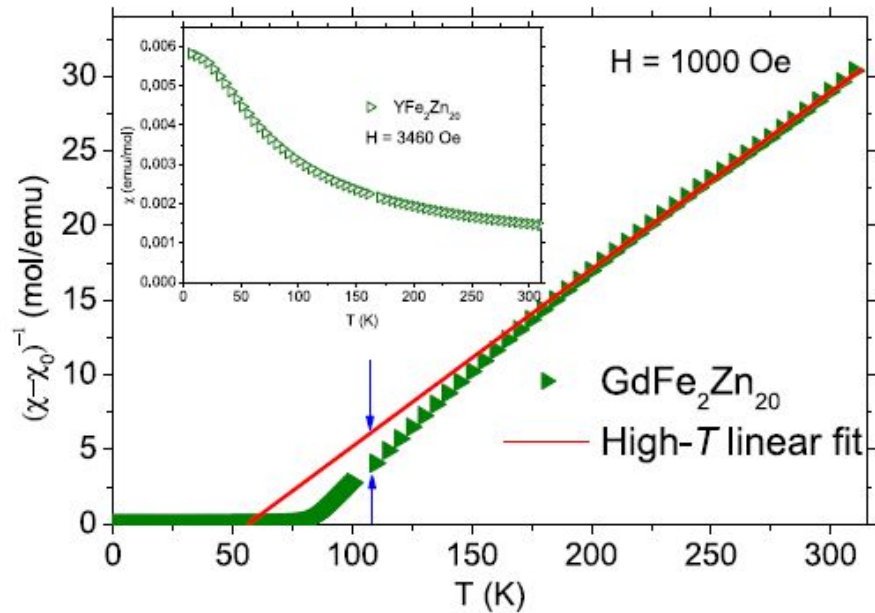
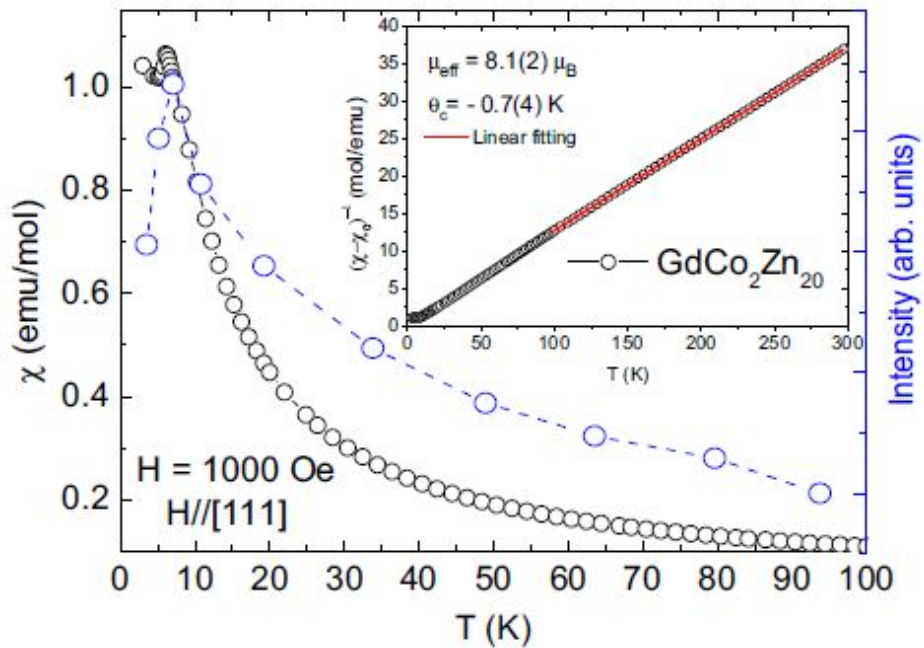


Table 4.6. The 4 *f* ions. The paramagnetic moment m_{eff} and the saturation moment m_0 are in units of μ_B

$4f^n$		S	L	J	g	$m_0 = gJ$	$m_{eff} = g\sqrt{J(J+1)}$	m_{eff}^{exp}
1	Ce ³⁺	$\frac{1}{2}$	3	$\frac{5}{2}$	$\frac{6}{7}$	2.14	2.54	2.5
2	Pr ³⁺	1	5	4	$\frac{4}{5}$	3.20	3.58	3.5
3	Nd ³⁺	$\frac{3}{2}$	6	$\frac{9}{2}$	$\frac{8}{11}$	3.27	3.52	3.4
4	Pm ³⁺	2	6	4	$\frac{3}{5}$	2.40	2.68	
5	Sm ³⁺	$\frac{5}{2}$	5	$\frac{5}{2}$	$\frac{2}{7}$	0.71	0.85	1.7
6	Eu ³⁺	3	3	0	0	0	0	3.4
7	Gd ³⁺	$\frac{7}{2}$	0	$\frac{7}{2}$	2	7.0	7.94	8.9
8	Tb ³⁺	3	3	6	$\frac{3}{2}$	9.0	9.72	9.8
9	Dy ³⁺	$\frac{5}{2}$	5	$\frac{15}{2}$	$\frac{4}{3}$	10.0	10.65	10.6
10	Ho ³⁺	2	6	8	$\frac{5}{4}$	10.0	10.61	10.4
11	Er ³⁺	$\frac{3}{2}$	6	$\frac{15}{2}$	$\frac{6}{5}$	9.0	9.58	9.5
12	Tm ³⁺	1	5	6	$\frac{7}{6}$	7.0	7.56	7.6
13	Yb ³⁺	$\frac{1}{2}$	3	$\frac{7}{2}$	$\frac{8}{7}$	4.0	4.53	4.5







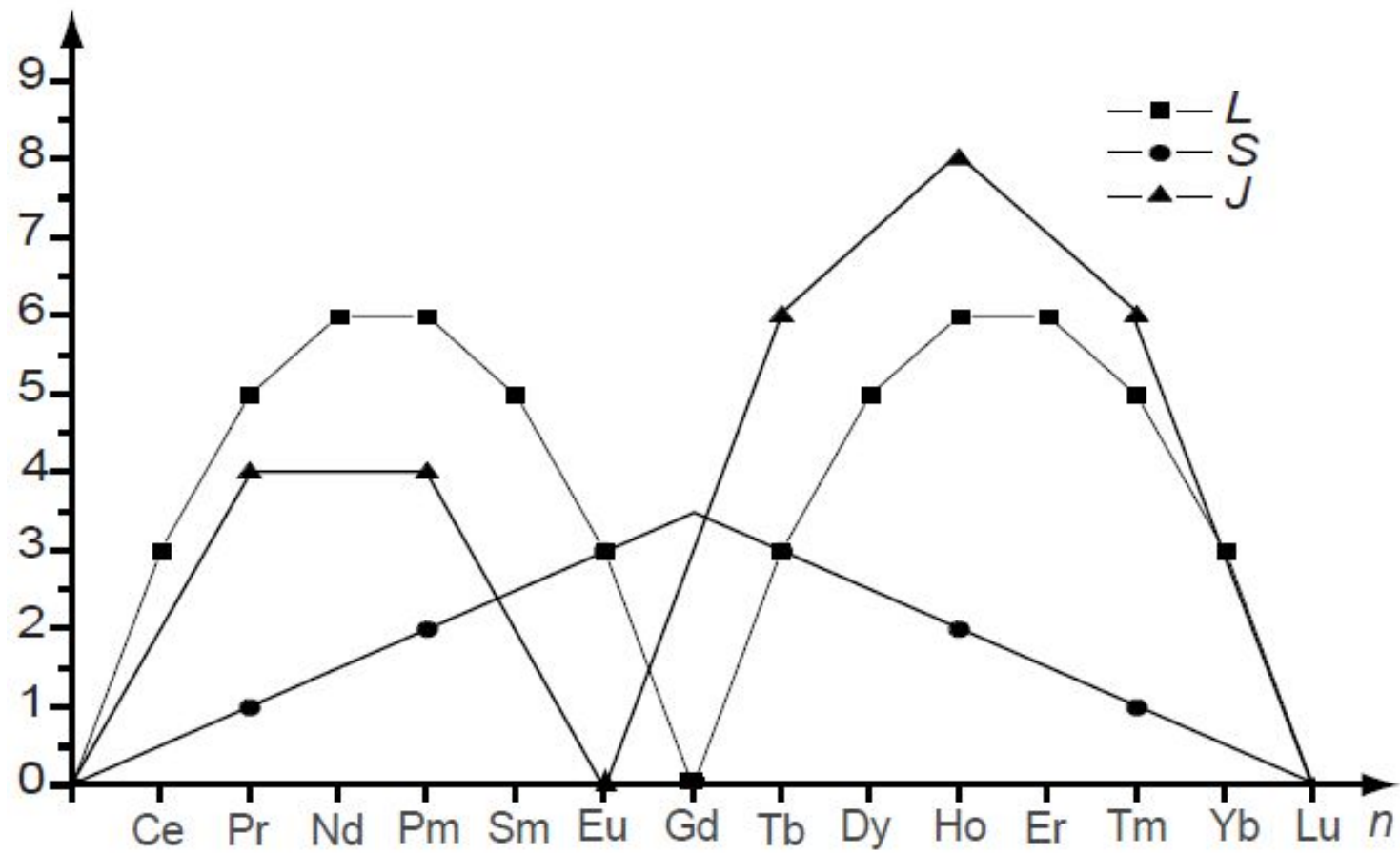
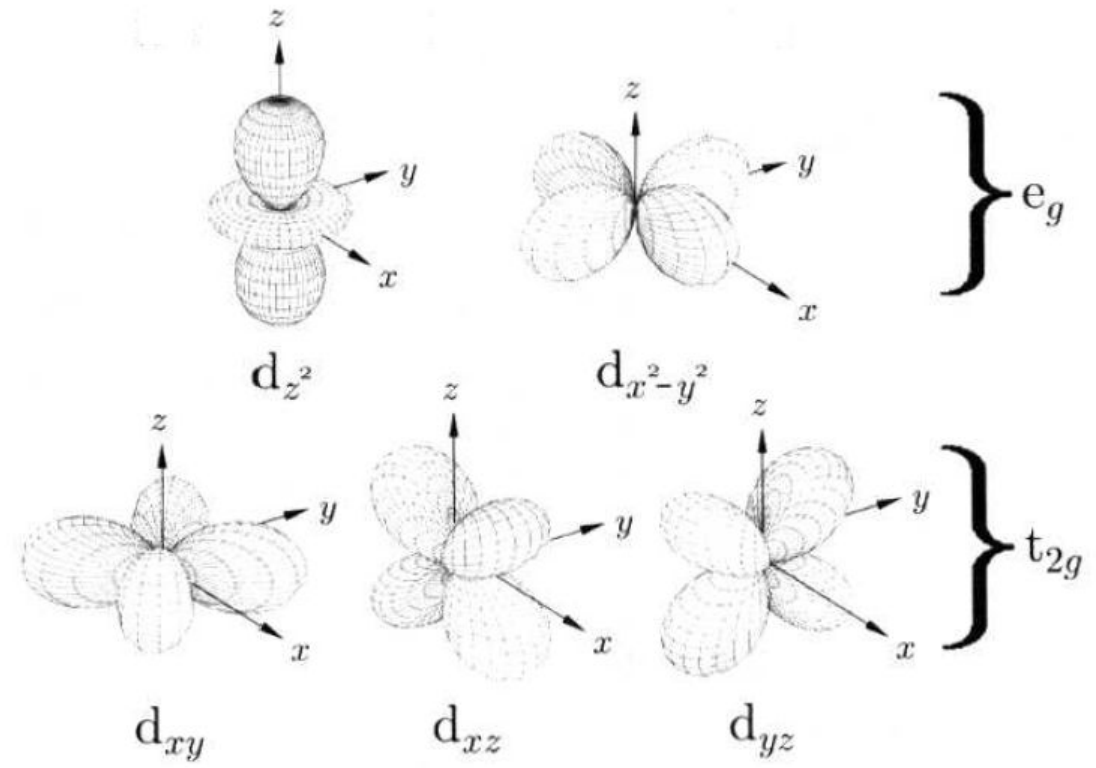
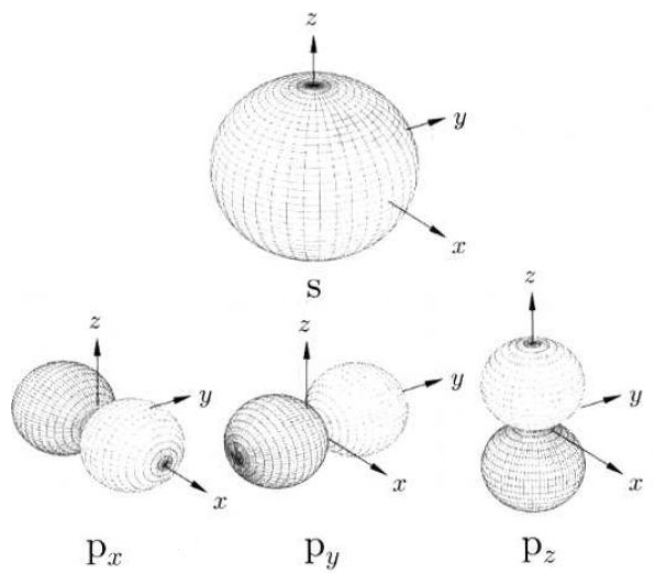


Table 4.7. The 3d ions. m_{eff} is in units of μ_B

$3d^n$		S	L	J	g	$m_{eff} = \frac{g\sqrt{J(J+1)}}{g\sqrt{J(J+1)}}$	$m_{eff} = \frac{g\sqrt{S(S+1)}}{g\sqrt{S(S+1)}}$	m_{eff}^{exp}
1	Ti ³⁺ , V ⁴⁺	$\frac{1}{2}$	2	$\frac{3}{2}$	$\frac{4}{5}$	1.55	1.73	1.7
2	Ti ²⁺ , V ³⁺	1	3	2	$\frac{2}{3}$	1.63	2.83	2.8
3	V ²⁺ , Cr ³⁺	$\frac{3}{2}$	3	$\frac{3}{2}$	$\frac{2}{5}$	0.78	3.87	3.8
4	Cr ²⁺ , Mn ³⁺	2	2	0			4.90	4.9
5	Mn ²⁺ , Fe ³⁺	$\frac{5}{2}$	0	$\frac{5}{2}$	2	5.92	5.92	5.9
6	Fe ²⁺ , Co ³⁺	2	2	4	$\frac{3}{2}$	6.71	4.90	5.4
7	Co ²⁺ , Ni ³⁺	$\frac{3}{2}$	3	$\frac{9}{2}$	$\frac{4}{3}$	6.63	3.87	4.8
8	Ni ³⁺	1	3	4	$\frac{5}{4}$	5.59	2.83	3.2
9	Cu ²⁺	$\frac{1}{2}$	2	$\frac{5}{2}$	$\frac{6}{5}$	3.55	1.73	1.9

Table 4.5. Spin-orbit coupling constants for ions in the $3d$ and $4f$ series, in kelvin. $\Delta\varepsilon$ is the energy of the first excited multiplet

	Ion	λ	Λ	$\Delta\varepsilon$
$3d^1$	Sc^{2+}	124	124	310
$3d^2$	Ti^{2+}	176	88	264
$3d^3$	V^{2+}	246	82	205
$3d^4$	Cr^{2+}	340	85	85
$3d^6$	Fe^{2+}	656	-164	656
$3d^7$	Co^{2+}	818	-272	1224
$3d^8$	Ni^{2+}	987	-494	3948
$4f^1$	Ce^{3+}	920	920	3220
$4f^2$	Pr^{3+}	1080	540	2700
$4f^3$	Nd^{3+}	1290	430	2365
$4f^4$	Pm^{3+}	1540	380	1900
$4f^5$	Sm^{3+}	1730	350	1225
$4f^6$	Eu^{3+}	1950	330	330
$4f^8$	Tb^{3+}	2450	-410	2460
$4f^9$	Dy^{3+}	2730	-550	4125
$4f^{10}$	Ho^{3+}	3110	-780	6240
$4f^{11}$	Er^{3+}	3510	-1170	8775
$4f^{12}$	Tm^{3+}	3800	-1900	11400
$4f^{13}$	Yb^{3+}	4140	-4140	14490



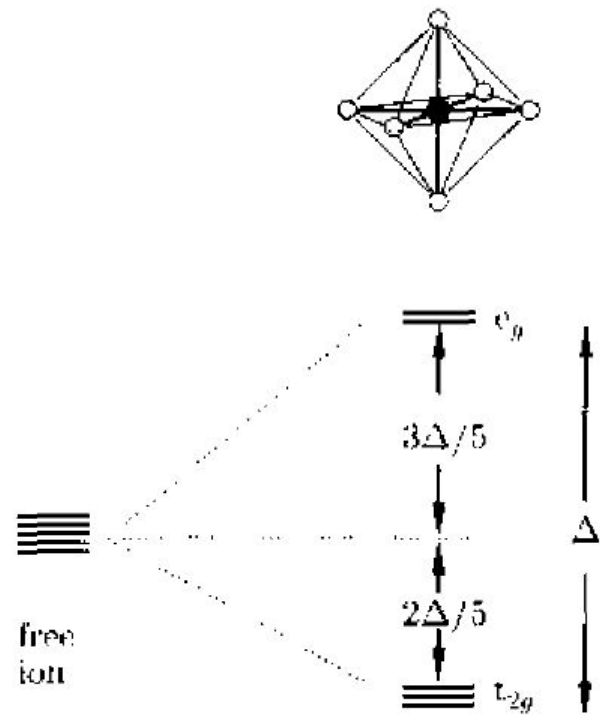
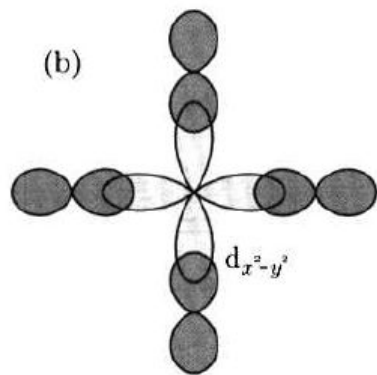
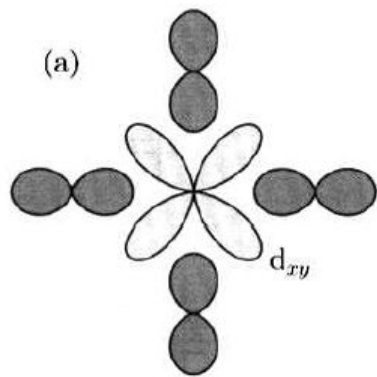
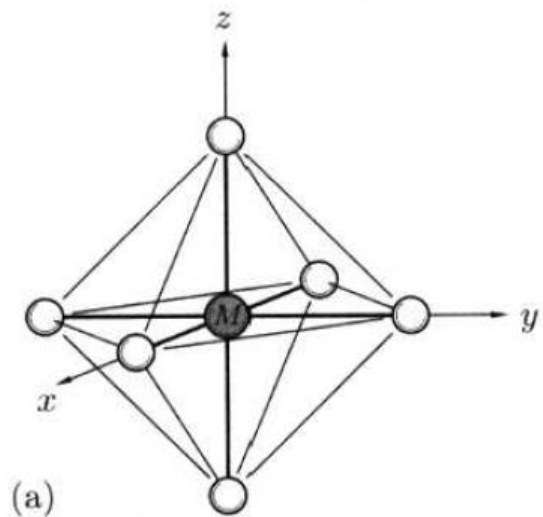


Table 4.9. The splitting of the one-electron levels in different symmetry

ℓ	Cubic	Tetragonal	Trigonal	Rhombohedral
s	0	1	1	1
p	1	3	1, 2	1, 1, 1
d	2	2, 3	1, 1, 1, 2	1, 1, 1, 1, 1
f	3	1, 3, 3	1, 1, 1, 2, 2	1, 1, 1, 1, 1, 1, 1

Figure 4.13

The effect of a tetragonal distortion of octahedral symmetry on the one-electron energy levels.

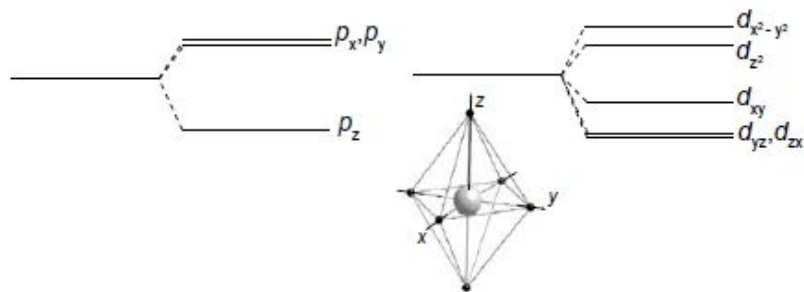
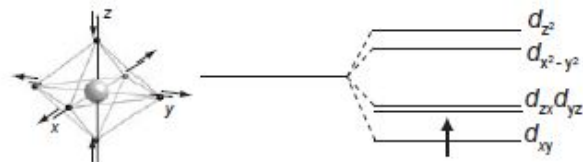


Figure 4.14

Jahn-Teller distortion of an octahedral site containing a d^1 ion.



Classificação

- Origem dos momentos magnéticos
- Tipo de interação entre os momentos

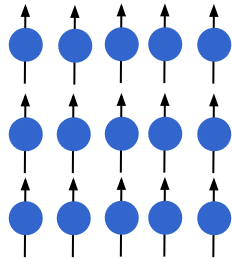
- Magnetismo Fraco

- Diamagnetos
- Paramagnetos

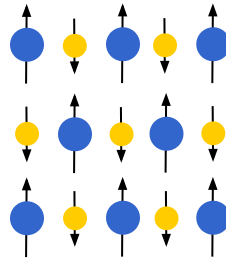
- Magnetismo Forte

- Materiais Ordenados:

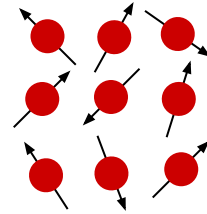
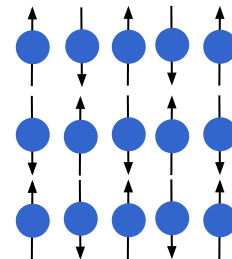
- **Ferromagnetos**

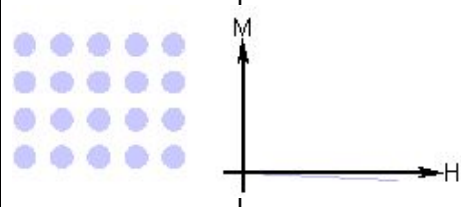
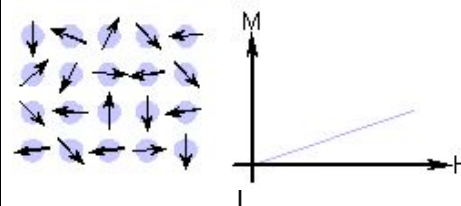
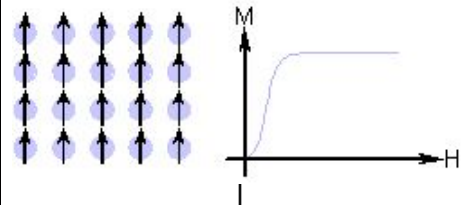
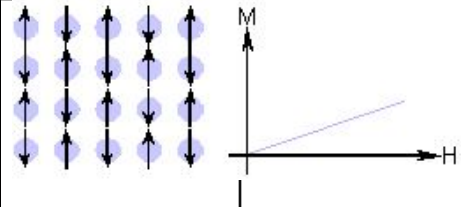
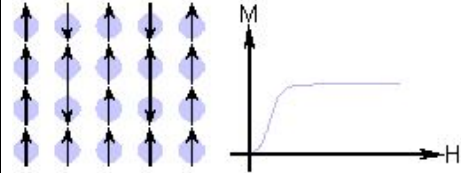


- **Ferrimagnetos**



- **Antiferromagnetos**



<i>Type of Magnetism</i>	<i>Susceptibility</i>	<i>Atomic / Magnetic Behaviour</i>	<i>Example / Susceptibility</i>
Diamagnetism	Small & negative.	Atoms have no magnetic moment	 -2.74×10^{-6} -0.77×10^{-6}
Paramagnetism	Small & positive.	Atoms have randomly oriented magnetic moments	 0.19×10^{-6} 21.04×10^{-6} 66.10×10^{-6}
Ferromagnetism	Large & positive, function of applied field, microstructure dependent.	Atoms have parallel aligned magnetic moments	 $\sim 100,000$
Antiferromagnetism	Small & positive.	Atoms have mixed parallel and anti-parallel aligned magnetic moments	 3.6×10^{-6}
Ferrimagnetism	Large & positive, function of applied field, microstructure dependent	Atoms have anti-parallel aligned magnetic moments	 ~ 3

Diamagnetos

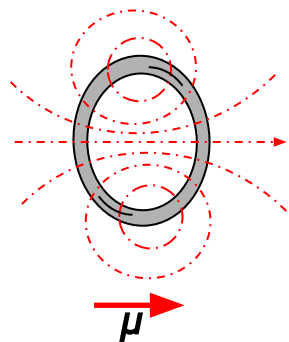
- Não possuem momento permanente

• Origem: variação do momento orbital dos elétrons

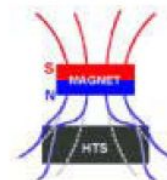
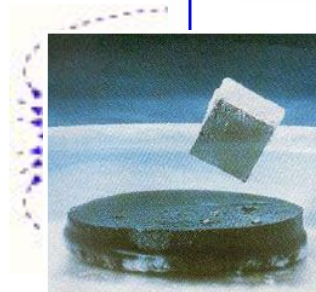
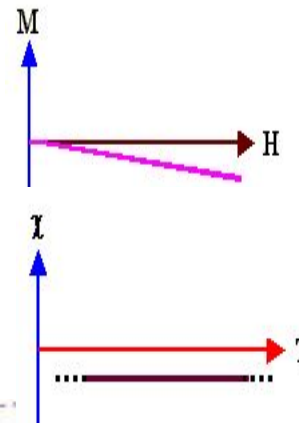
(Lei de Lenz) induzida pela ação de um campo magnético

- Resposta se opõe ao campo →

$$\chi = \frac{M}{H} (\approx 10^{-6})$$

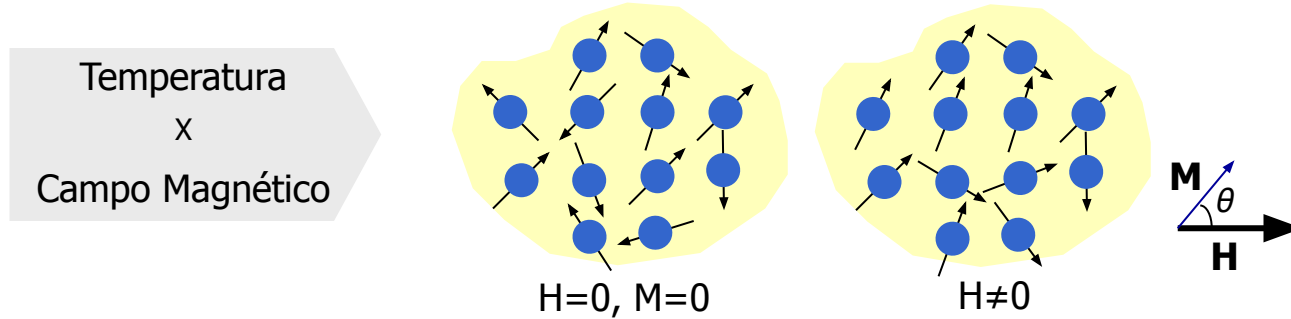


- Todo material apresenta diamagnetismo
- Resulta do efeito de um campo VARIÁVEL sobre os elétrons



Paramagnetismo

- Possuem momento magnético permanente
- Não há interação entre momentos
- $\chi > 0$ porém pequena ($10^{-5} - 10^{-3}$) (tende a alinhar com o campo)



- Langevin (Clássica): momentos idênticos que não interagem e apontam em qualquer direção

Campo
Magnético

$$E = - \underline{\mu} \cdot \underline{B}$$

$$= - \mu \cos \theta B$$

Projeção do momento na direção de B

- E^{\min} : momentos alinhados com \underline{B}
- Competição com agitação térmica

Paramagnetismo Quântico

Campo Magnético

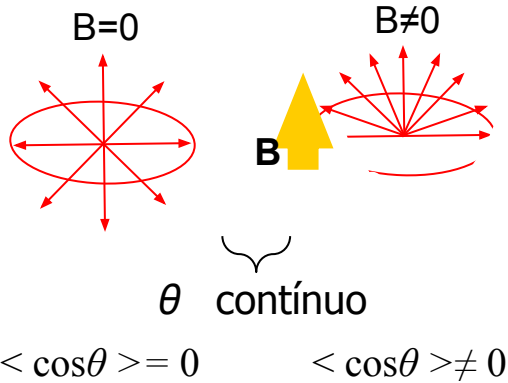
x

Temperatura

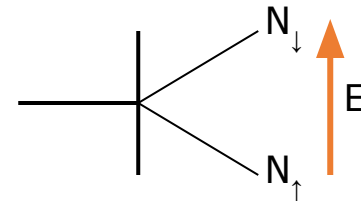
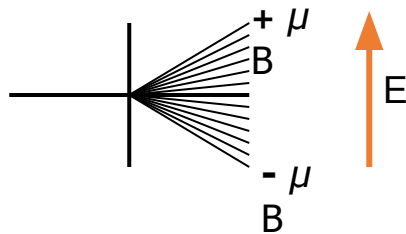
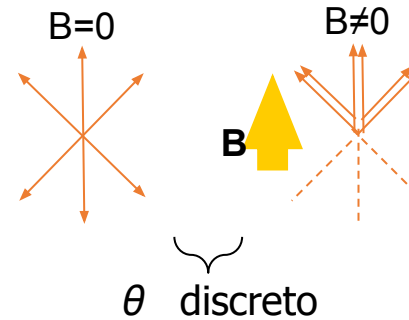
N : alta densidade de mom. mag.

μ : momento orbital
momento de spin

Clássico



Quântico



- Quantização do mom. angular:

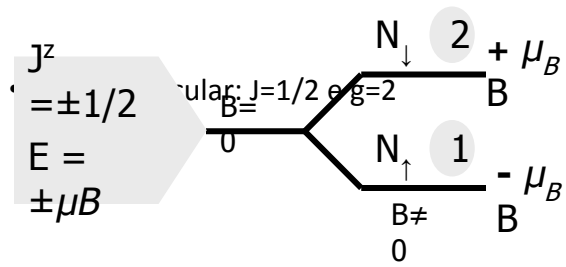
$$\underline{\mu} = -g \mu_B \underline{J}$$

$$E = -\underline{\mu} \cdot \underline{B} = g \mu_B J^z$$

B

μ
 J

$J^z: J,$
 $J-1,$
 $J-2,$
 $\dots -J$



- População $N_T = N_1 + N_2$

$$n_1 = N_1 / N_T = e^{-E_1/kT} / (e^{-E_1/kT} + e^{-E_2/kT})$$

$$n_2 = N_2 / N_T = e^{-E_2/kT} / (e^{-E_1/kT} + e^{-E_2/kT})$$

- Magnetização resultante:

$$M = \mu(N_1 - N_2) / V = N \mu \frac{e^x - e^{-x}}{e^x + e^{-x}}$$

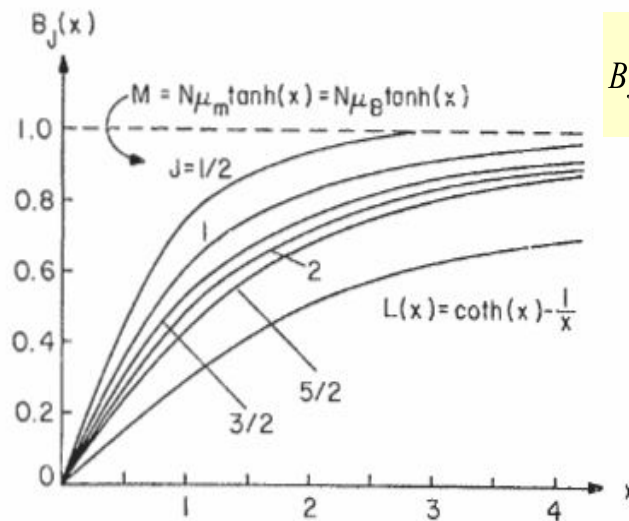
$$x = \frac{\mu B}{kT}$$

~~$e^x + e^{-x}$~~
 $\tanh(x)$

- Para qualquer J:
 $M = g \mu_B J N B_J(x)$

Função de Brillouin \int

$$B_J(x) = \frac{2J+1}{2J} \coth\left(\frac{(2J+1)x}{2J}\right) - \frac{1}{2J} \coth\left(\frac{x}{2J}\right)$$



- No limite de J muito grande:

$$B_J(x) \xrightarrow{J \rightarrow \infty} L(x)$$

Limite Clássico!!

$$B_J(x) = \frac{2J+1}{2J} \coth\left(\frac{(2J+1)x}{2J}\right) - \frac{1}{2J} \coth\left(\frac{x}{2J}\right)$$

- Para $x = \frac{\mu B}{kT} \ll 1$ temos:

$$\coth x = \frac{1}{x} + \frac{x}{3}$$

$$B_J(x) \xrightarrow{x \ll 1} \frac{J(J+1)}{3J^2} x$$

- Logo:

$$M = \frac{NJ(J+1)g^2 \mu_B^2 B}{3kT} = \frac{C}{T} B$$

$$\chi = \frac{M}{H} = \mu_0 \frac{Ng^2 \mu_B^2 J(J+1)}{3J^2 kT}$$

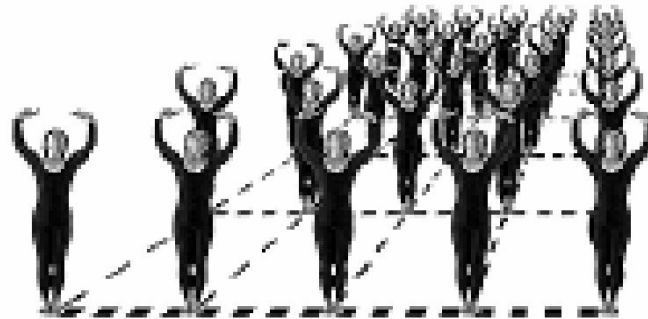
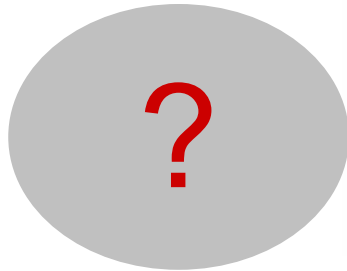
Ferromagnetismo



momento
dipolo magnético



Paramagnetismo



Ferromagnetismo

Ferromagnetismo : Campo Molecular

Hipótese de Weiss

- Cada momento de dipolo magnético sofre a ação de um campo magnético efetivo criado pelos vizinhos
- Campo molecular médio → Magnetização espontânea (M_s)

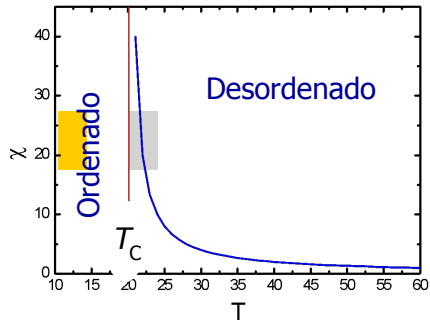
$$H_e = \lambda M$$

$$H_{tot} = H_a + H_e = H + \lambda M$$

$$M = \chi H = (C/T)H \quad \text{ou} \quad M = (C/T)(H + \lambda M)$$

$$\chi = \frac{M}{H} = \frac{C}{T - T_c} \quad \text{onde} \quad T_c = \lambda C$$

Lei de Curie-Weiss

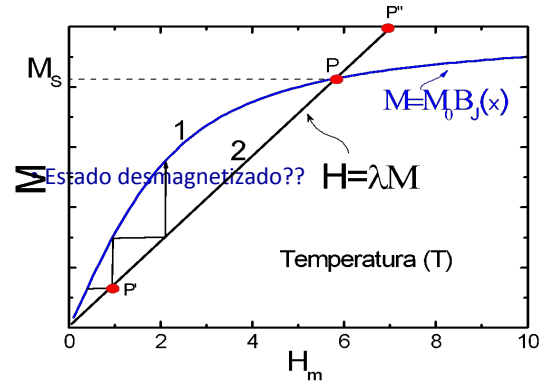


Magnetização pelo campo molecular

Soluções : origem e ponto P (estável)

Origem: $M=0$ (instável)

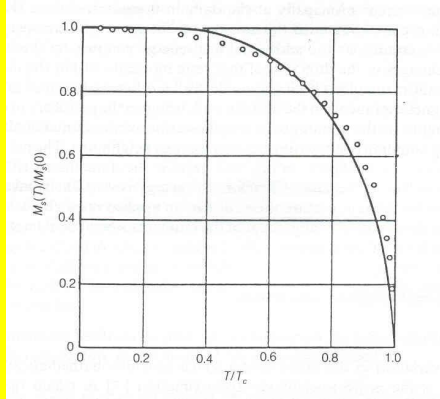
- distribuição aleatória de mom. magn.
- $\lambda M=0$
- aparecimento de um alinhamento local
- P' – desloca em direção a P (estável)



- Domínios magnéticos
- Processo de magnetização: **multidomínios** \Rightarrow **monodomínios**

Ferromagnetismo : Teoria de Weiss

$M \times T$ para o Ni



$$\chi = \frac{C}{T - \theta}$$

Lei de
Curie-Weiss

- Temperatura de Curie T_C :
 - indicação de λ
 - intensidade do campo molecular

$$\lambda = \frac{3kT_C}{N\mu^2}$$

- Para o Fe: $\mu = 2.2\mu_B$
 $N = 8.54 \times 10^{28} \text{ m}^{-3}$
 $T_C = 1063 \text{ K}$

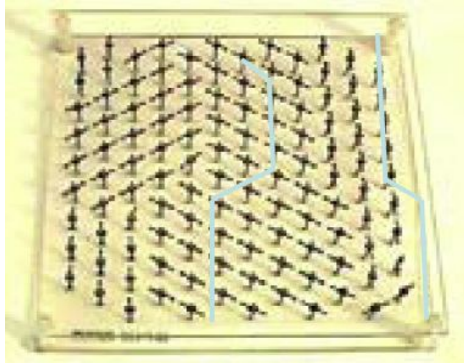
$$\lambda = 7.8 \times 10^8$$

$$H_m = \lambda M$$

$$H_m = \lambda N \mu_B$$

$$H_m = 1.7 \times 10^8 \text{ A/m} = 2.1 \times 10^7 \text{ Oe}$$

Ferromagnetismo : origem do campo molecular



~~$$E_{i \leftrightarrow j}(\vec{r} = \vec{r}_i - \vec{r}_j) = -\frac{\vec{m}_i \cdot \vec{m}_j}{r^3} - \frac{3(\vec{r} \cdot \vec{m}_i)(\vec{r} \cdot \vec{m}_j)}{r^5}$$~~

- Interação dipolar leva à formação de domínios magnéticos PORÉM é muito fraca para explicar a presença de um estado ordenado em temperatura ambiente

- INTERAÇÃO DE TROCA
- Interação QUÂNTICA

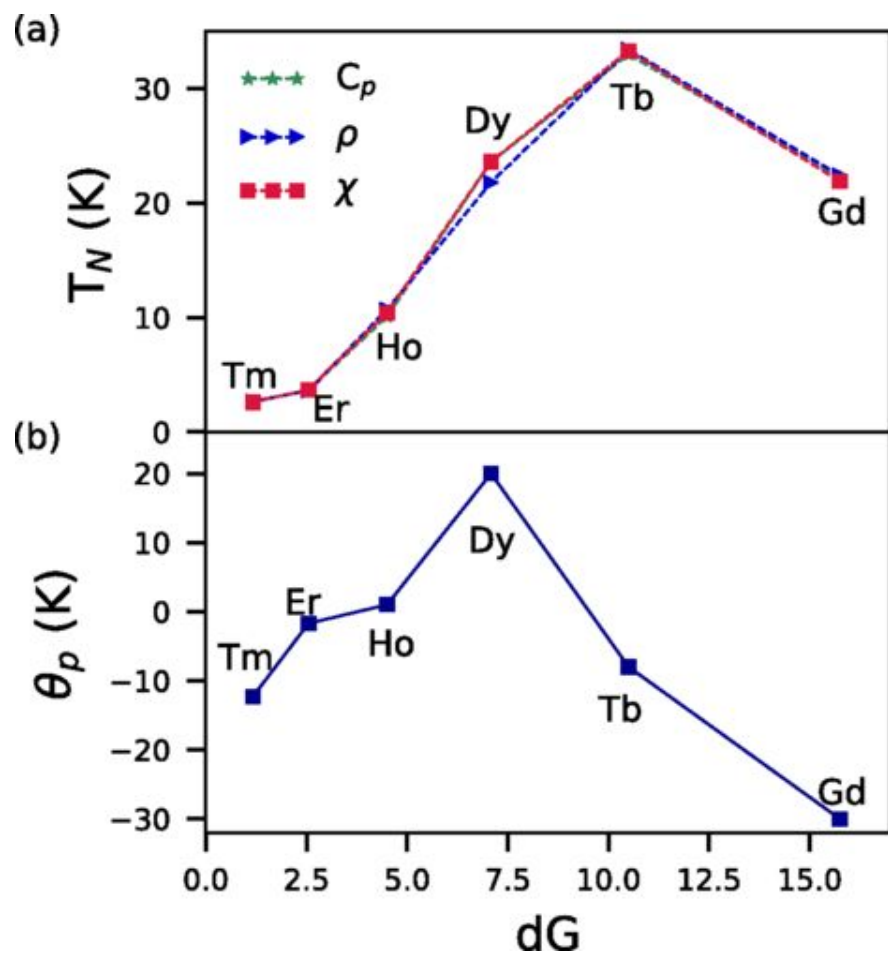
$$H = -2J \sum_{i,j} \mathbf{s}_i \otimes \mathbf{s}_j$$

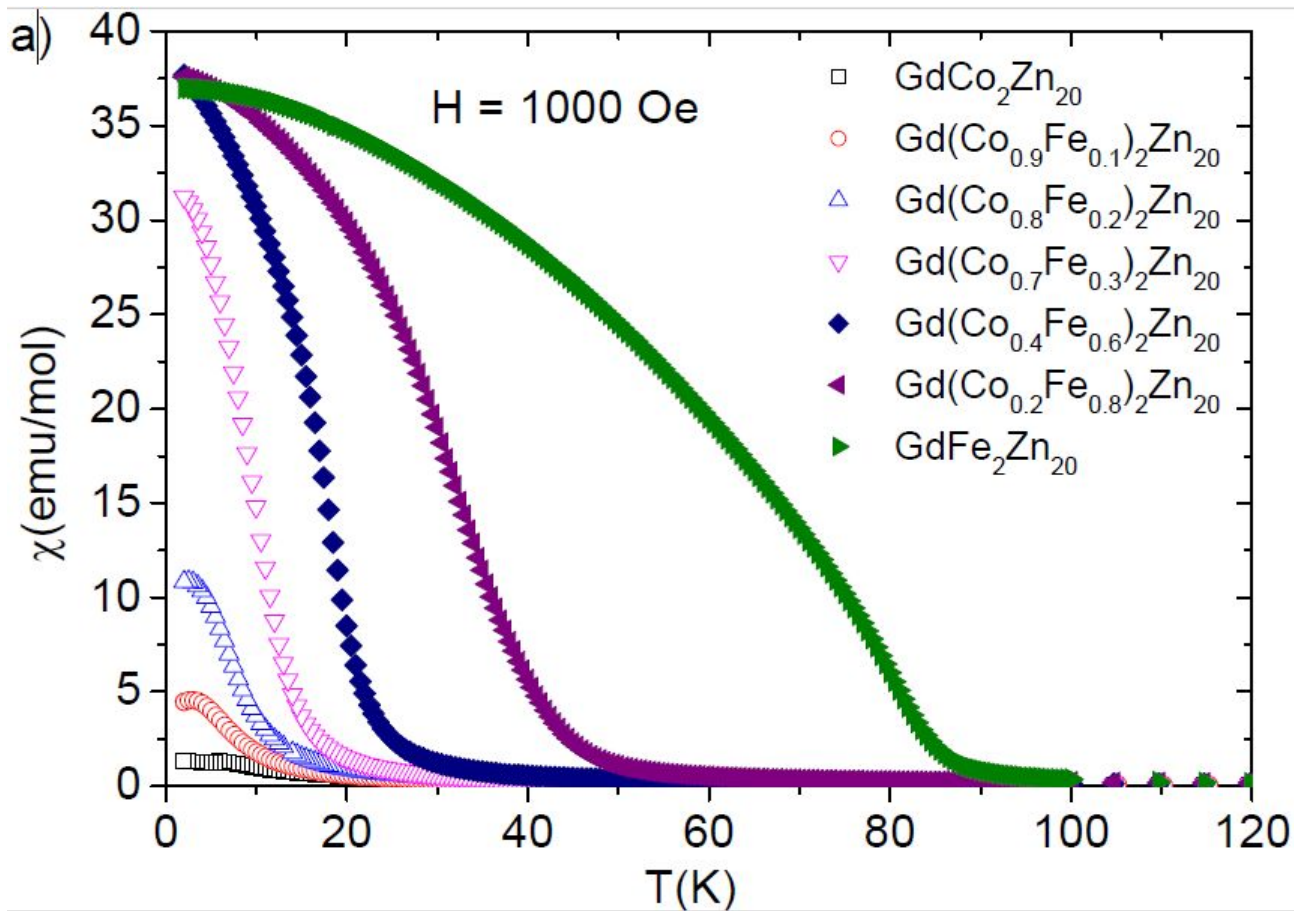
$J > 0$: Ferromagnetismo ↑↑↑↑↑↑

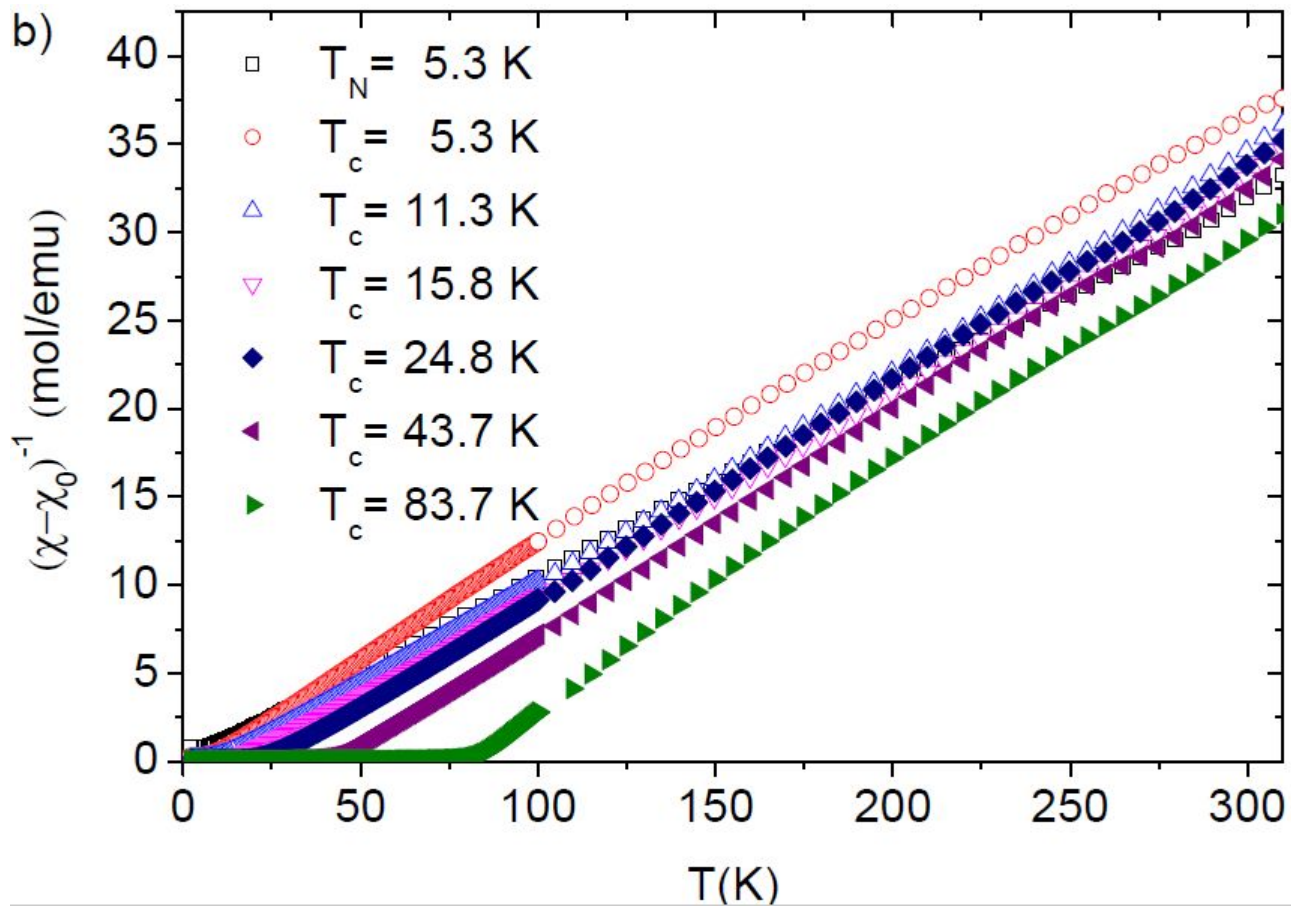
$J < 0$: Antiferromagnetismo ↑↓↑↓↑↓

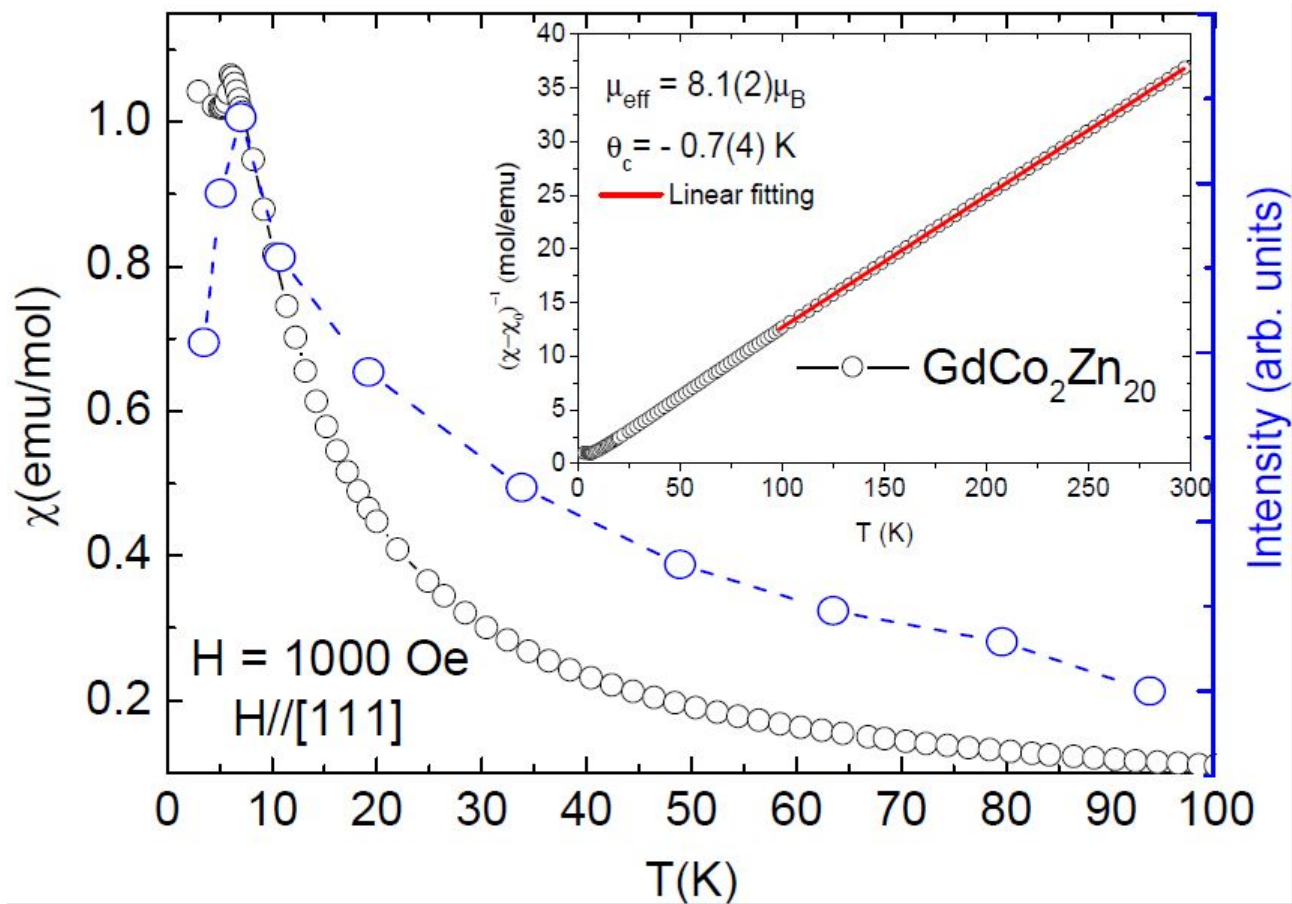
Table 5.2 The g-factors for 4f ions using Hund's rules.

ion	shell	S	L	J	g_J	$g_J - 1$	$(g_J - 1)^2 J(J + 1)$
Ce ³⁺	4f ¹	$\frac{1}{2}$	3	$\frac{5}{2}$	$\frac{6}{7}$	$-\frac{1}{7}$	0.18
Pr ³⁺	4f ²	1	5	4	$\frac{4}{5}$	$-\frac{1}{5}$	0.80
Nd ³⁺	4f ³	$\frac{3}{2}$	6	$\frac{9}{2}$	$\frac{72}{99}$	$-\frac{27}{99}$	1.84
Pm ³⁺	4f ⁴	2	6	4	$\frac{3}{5}$	$-\frac{2}{5}$	3.20
Sm ³⁺	4f ⁵	$\frac{5}{2}$	5	$\frac{5}{2}$	$\frac{2}{7}$	$-\frac{5}{7}$	4.46
Eu ³⁺	4f ⁶	3	3	0	-	-	-
Gd ³⁺	4f ⁷	$\frac{7}{2}$	0	$\frac{7}{2}$	2	1	15.75
Tb ³⁺	4f ⁸	3	3	6	$\frac{3}{2}$	$\frac{1}{2}$	10.50
Dy ³⁺	4f ⁹	$\frac{5}{2}$	5	$\frac{15}{2}$	$\frac{4}{3}$	$\frac{1}{3}$	7.08
Ho ³⁺	4f ¹⁰	2	6	8	$\frac{5}{4}$	$\frac{1}{4}$	4.50
Er ³⁺	4f ¹¹	$\frac{3}{2}$	6	$\frac{15}{2}$	$\frac{6}{5}$	$\frac{1}{5}$	2.55
Tm ³⁺	4f ¹²	1	5	6	$\frac{7}{6}$	$\frac{1}{6}$	1.17
Yb ³⁺	4f ¹³	$\frac{1}{2}$	3	$\frac{7}{2}$	$\frac{8}{7}$	$\frac{1}{7}$	0.32
Lu ³⁺	4f ¹⁴	0	0	0	-	-	-

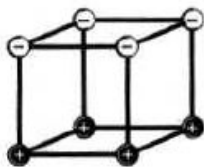




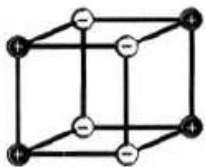




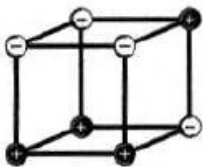
(a) type A



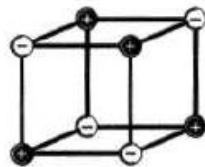
(b) type C



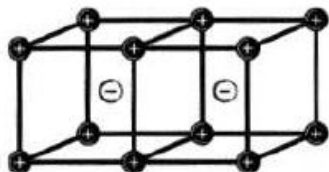
(c) type E



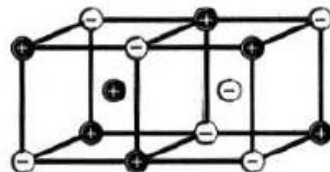
(d) type G



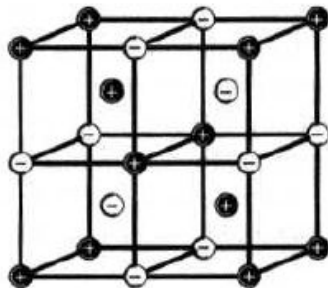
(a)



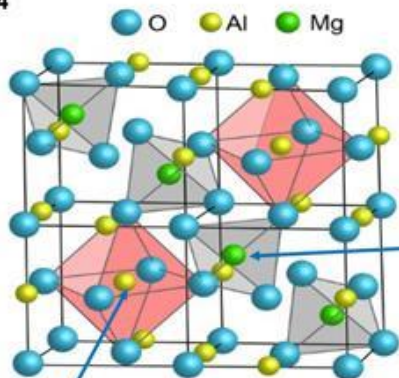
(b)



(c)

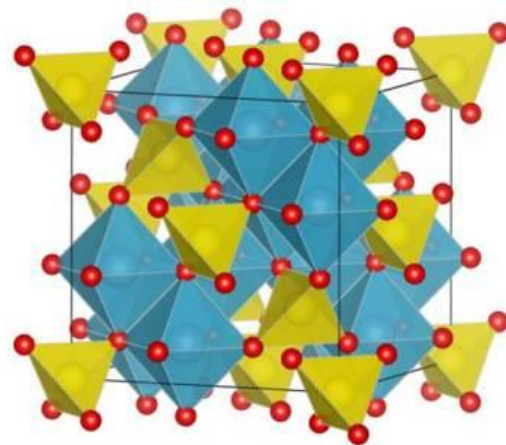
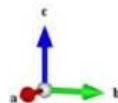


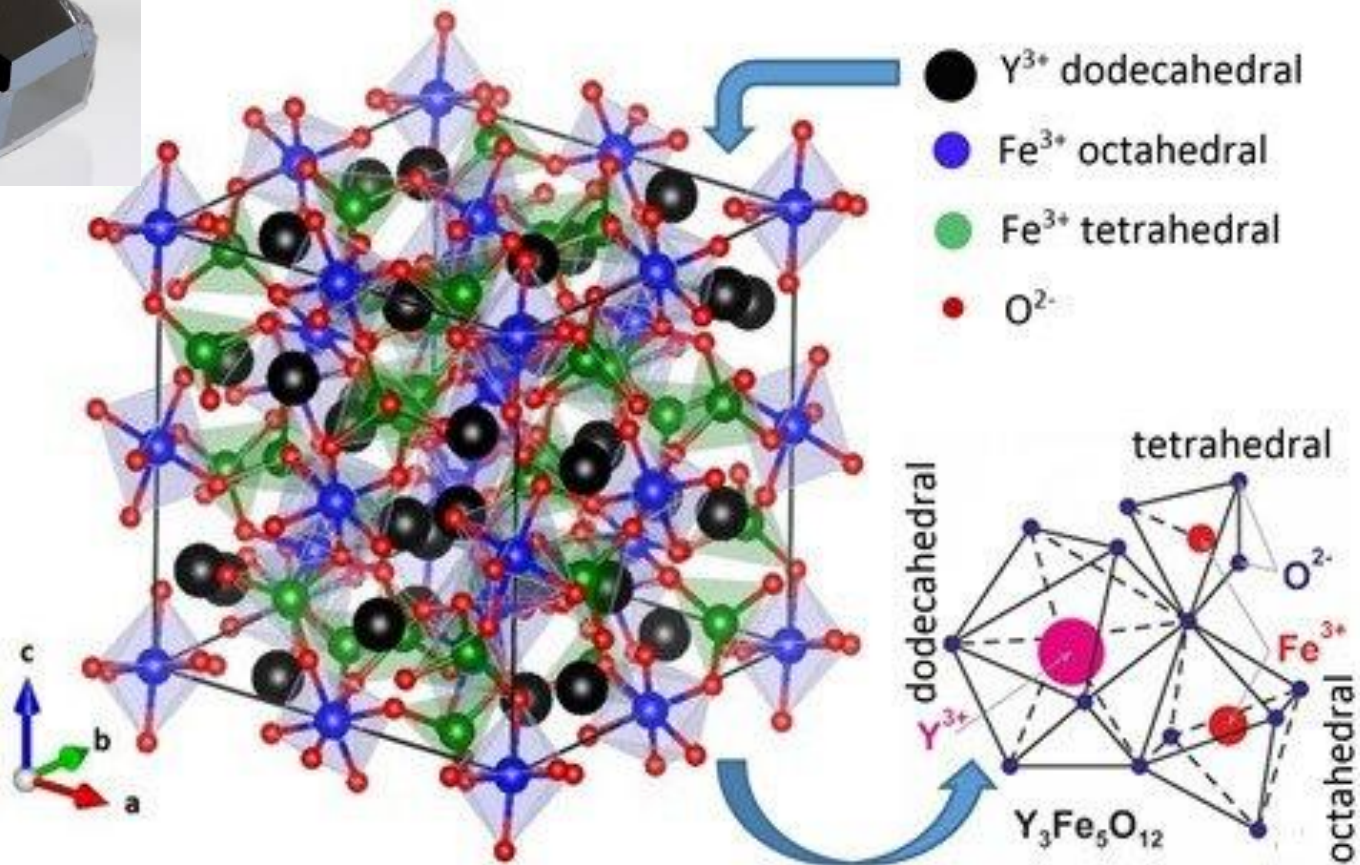
Spinel AB_2O_4

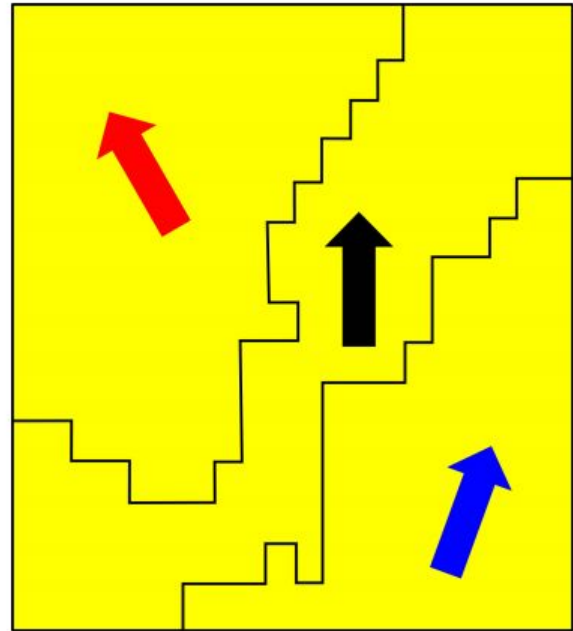
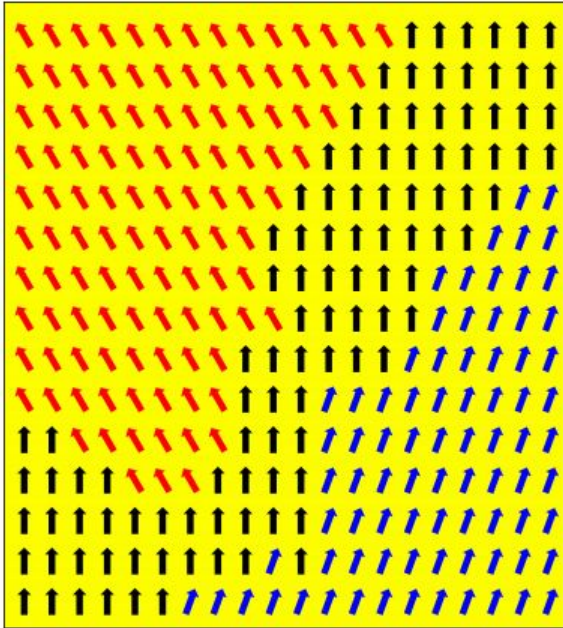


A Site – one metal with four nearest-neighbor oxygens.
Tetrahedral site

B site – one metal with six nearest-neighbor oxygens.
Octahedral site

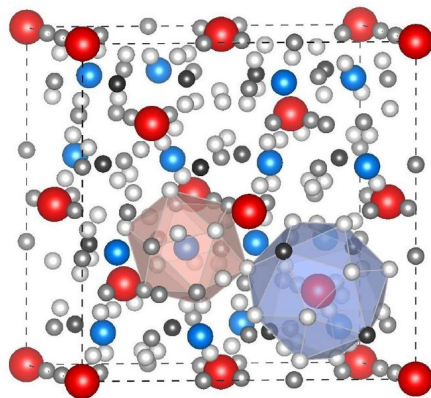






Results

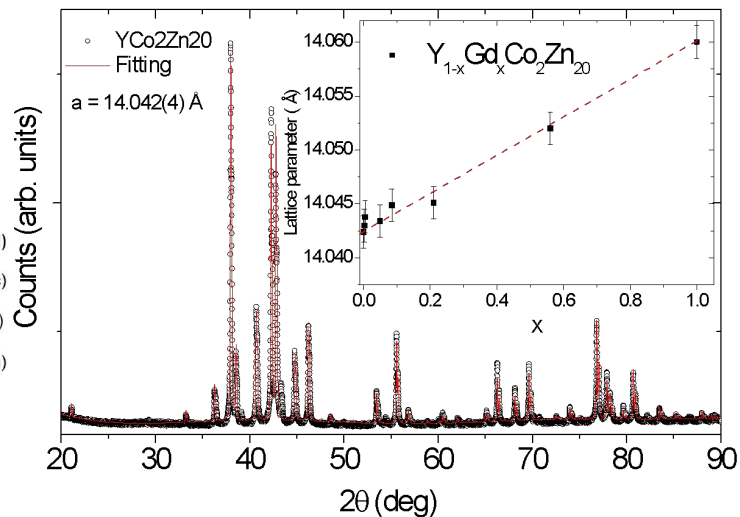
● Y-GdCo₂Zn₂₀



- Y (8a)
- Co (16d)
- Zn (16c)
- Zn (48f)
- Zn (96g)



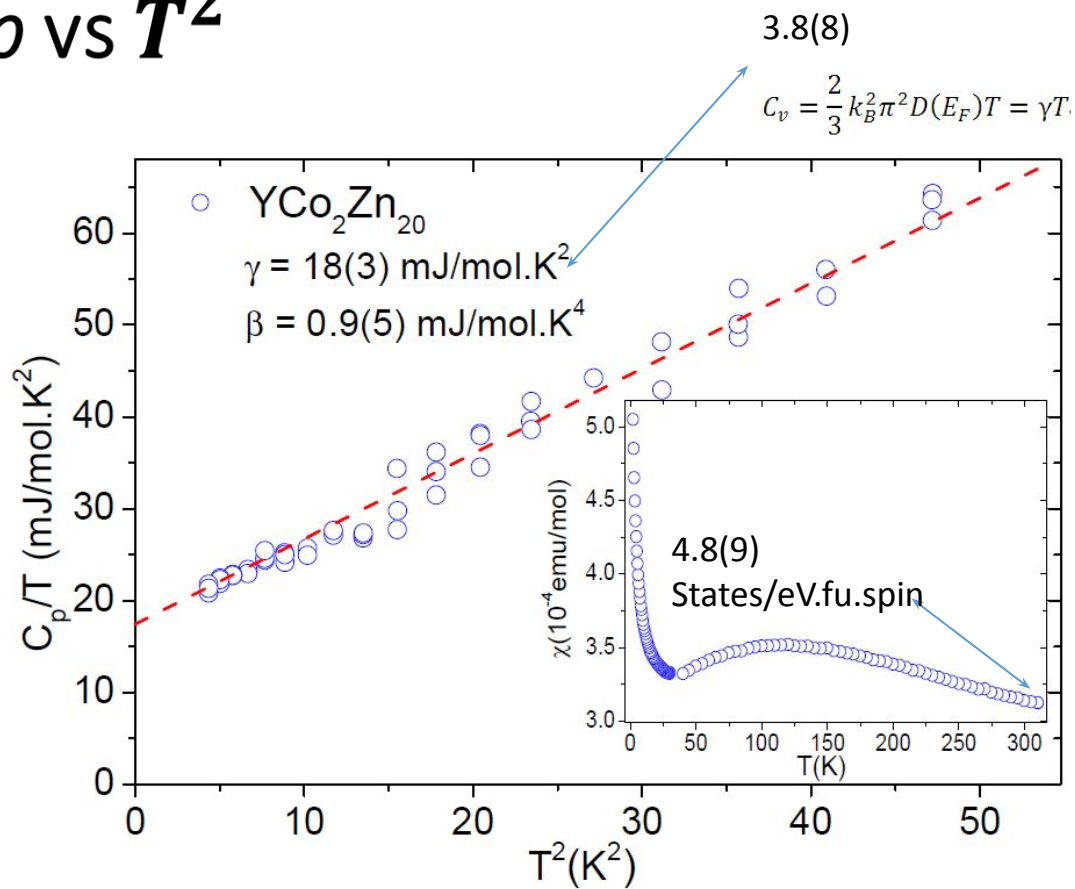
● Features



- Cubic (space group No. 227 CeCr₂Al₂₀-type)
- $a = 14.042(4) \text{ \AA}$

Results

C_p vs T^2

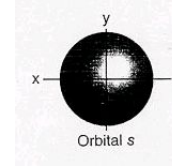
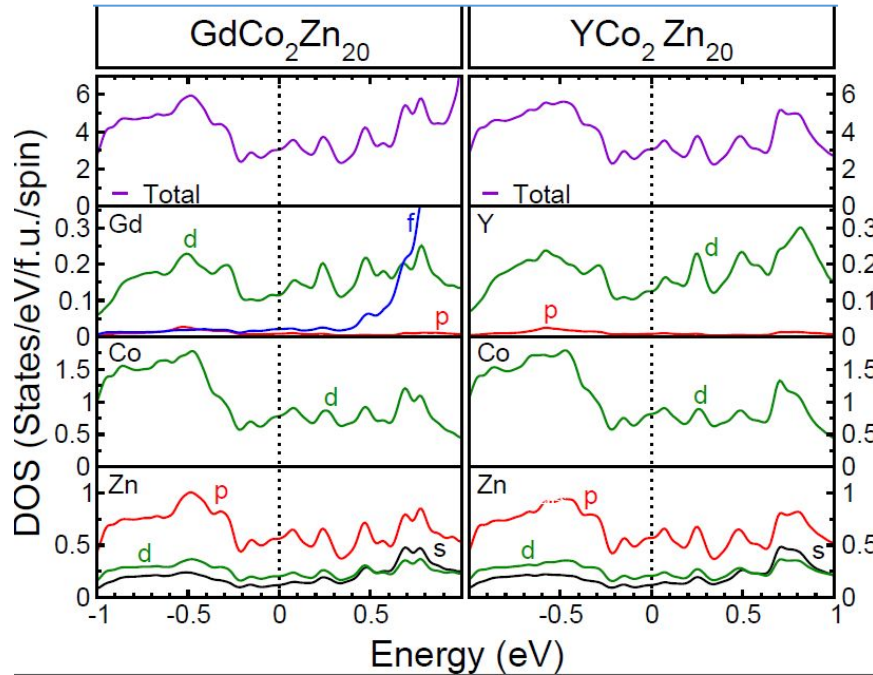


Results

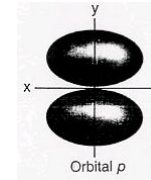
Partial density of states (DFT)

3.01(1)

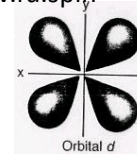
States/eV.fu.spin



Type s 0.13(1)
States/eV.fu.spin



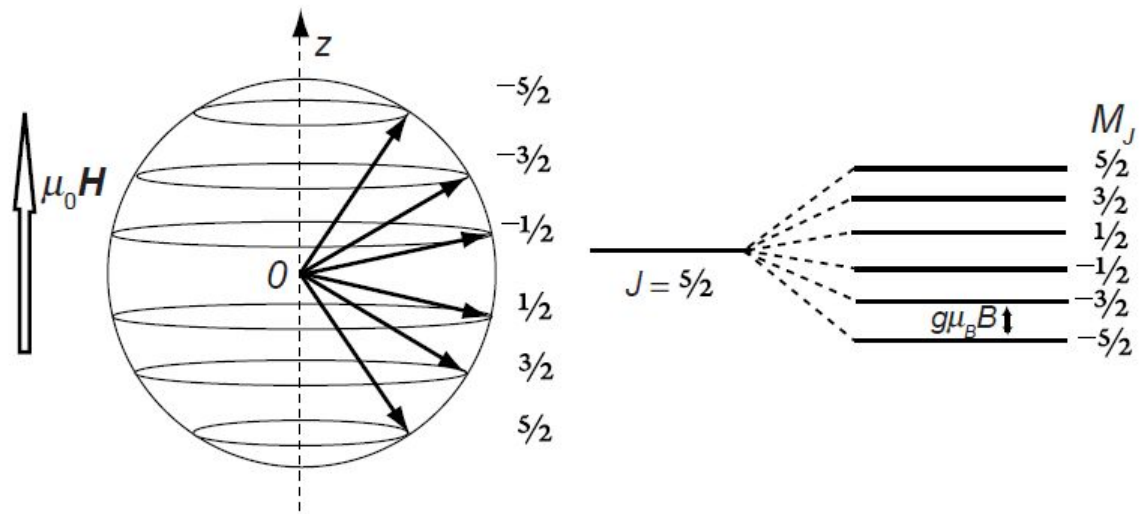
Type p 0.59(1)
States/eV.fu.spin

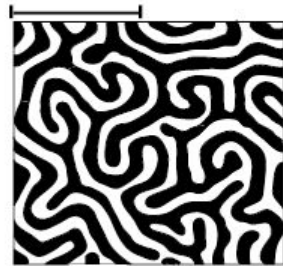
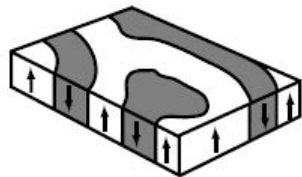
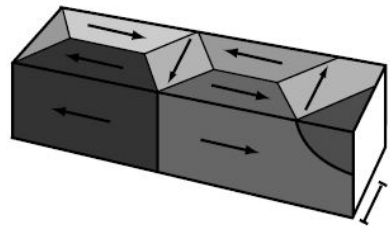
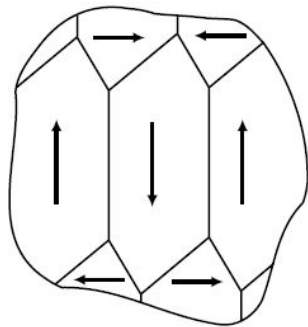
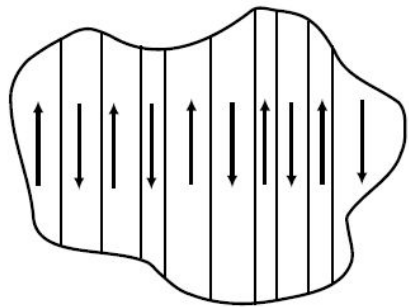


Type d 1.09(1)
States/eV.fu.spin

Table 3.6. Summary of localized and delocalized magnetism

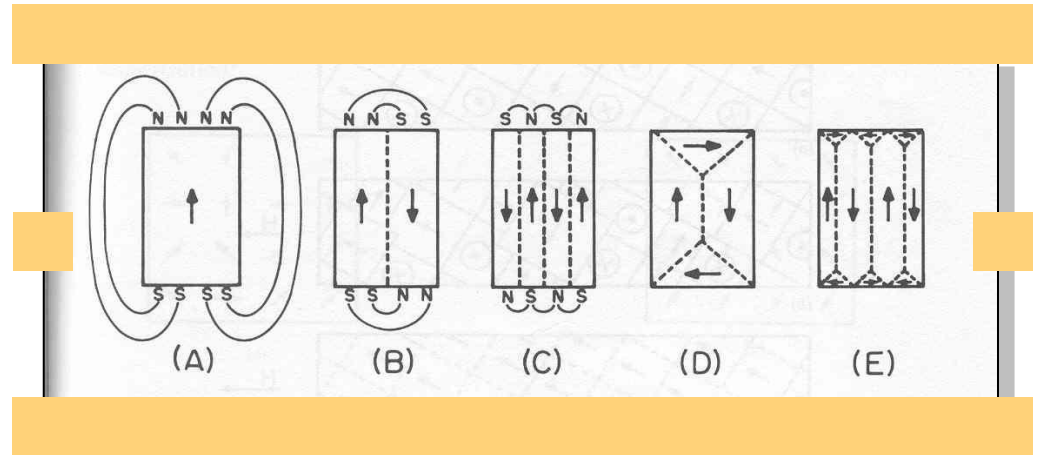
Localized magnetism	Delocalized magnetism
Integral number of $3d$ or $4f$ electrons	Nonintegral number of unpaired spins on the ion core
Integral number of unpaired spins per atom	
Discrete energy levels	Spin polarized energy bands with strong correlations
$\text{Ni}^{2+} 3d^8 \quad m = 2 \mu_B$	$\text{Ni} 3d^{9.4}4s^{0.6} \quad m = 0.6 \mu_B$
$\Psi \approx \exp(-r/a_0)$	$\Psi \approx \exp(-i\mathbf{k} \cdot \mathbf{r})$
Boltzmann statistics	Fermi–Dirac statistics
$4f$ metals and compounds; some $3d$ compounds	$3d$ metals; some $3d$ compounds



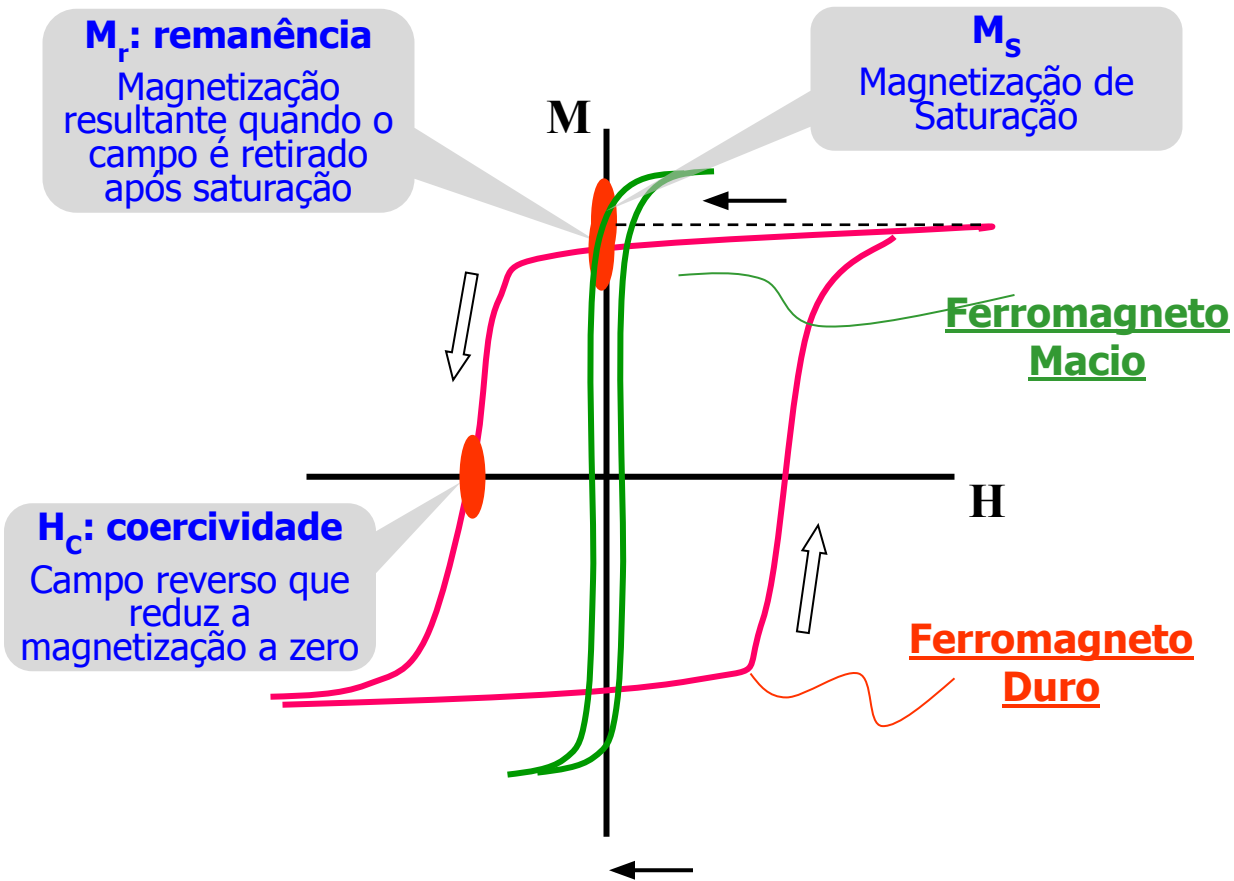


Domínios

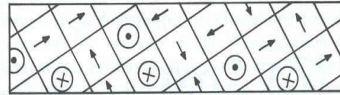
- Balanço Energético
- um único domínio - mono domínio
 - alta energia magnetostática
- Divisão em estruturas
 - fechamento do fluxo magnético
 - minimiza energia



Histerese e Processos de Magnetização



Domínios



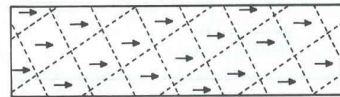
(a)



(b)



(c)



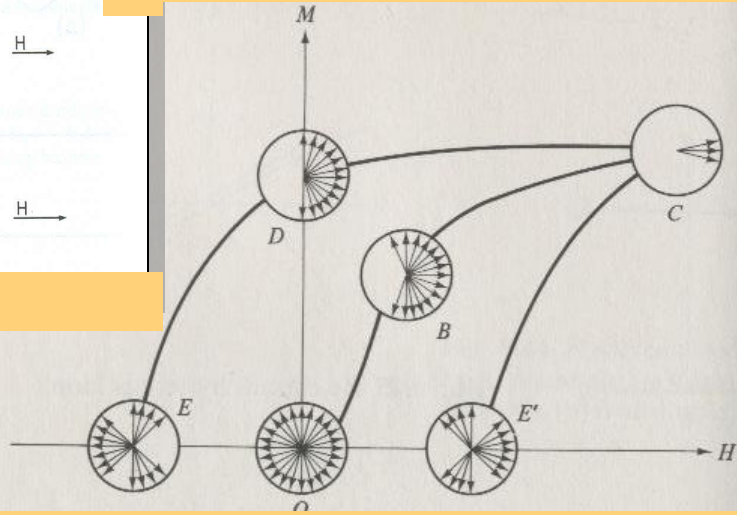
(d)

H →

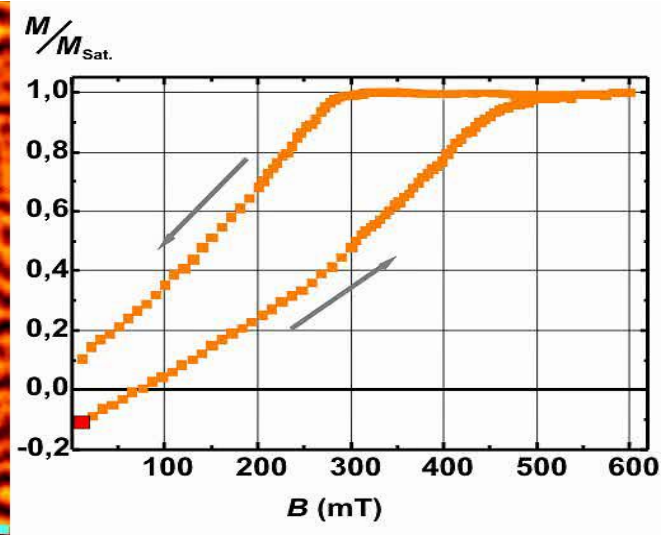
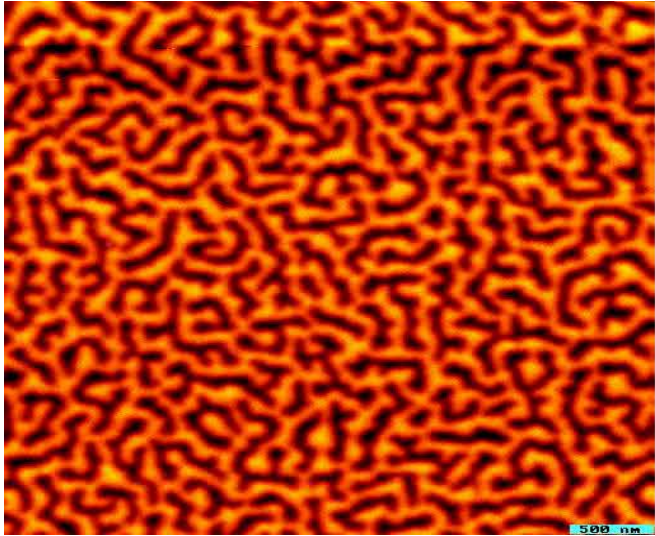
H →

H →

H →



Movimento de Paredes de Domínio



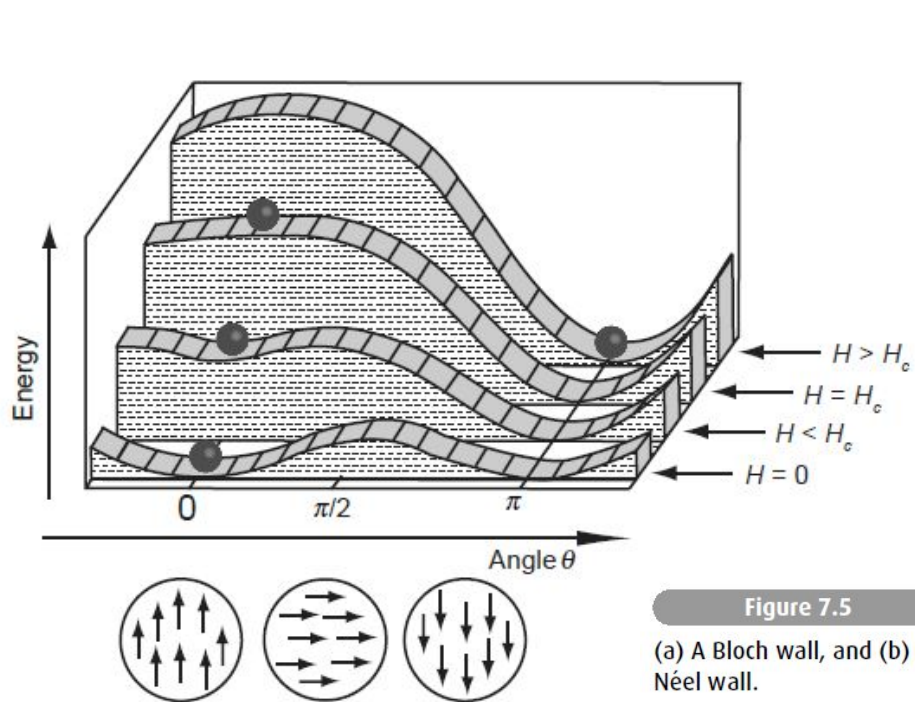
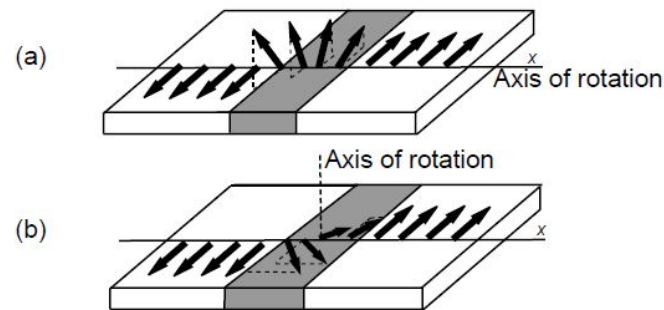
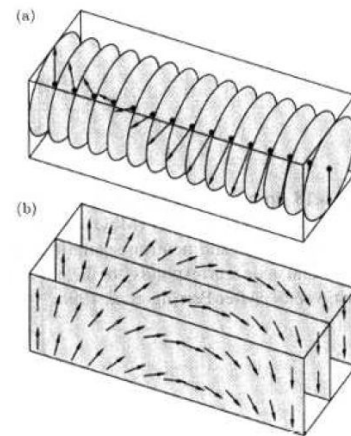


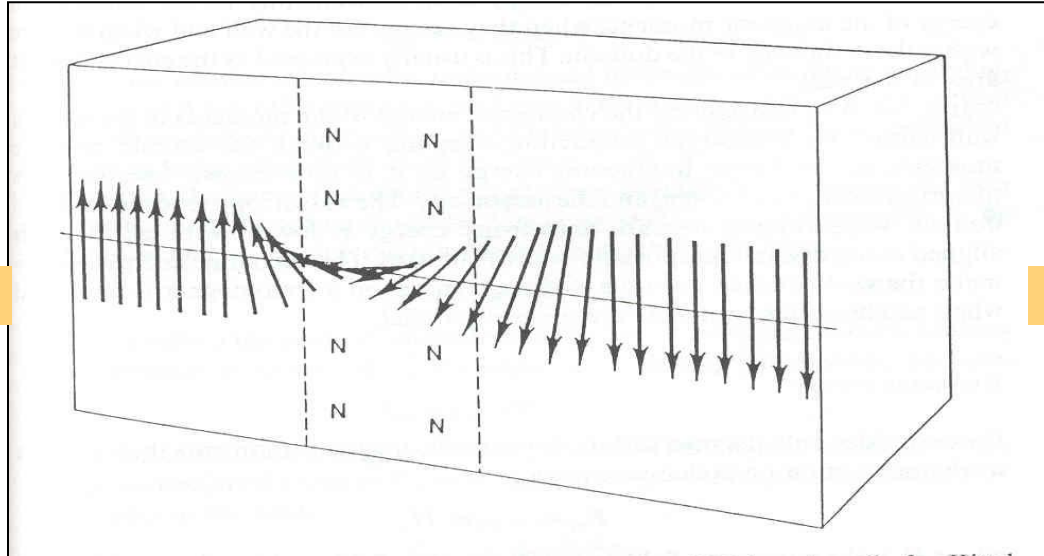
Figure 7.5

(a) A Bloch wall, and (b) a Néel wall.



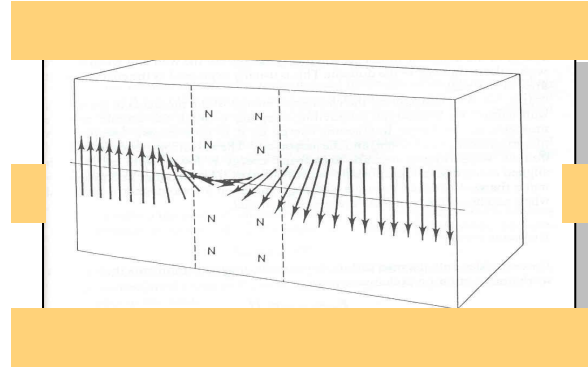
Parede de domínio

- Qual é o custo de energia?
- Qual é a largura?



- Definição:

- Diferença de energia dos momentos
 - dentro da parede
 - dentro do domínio



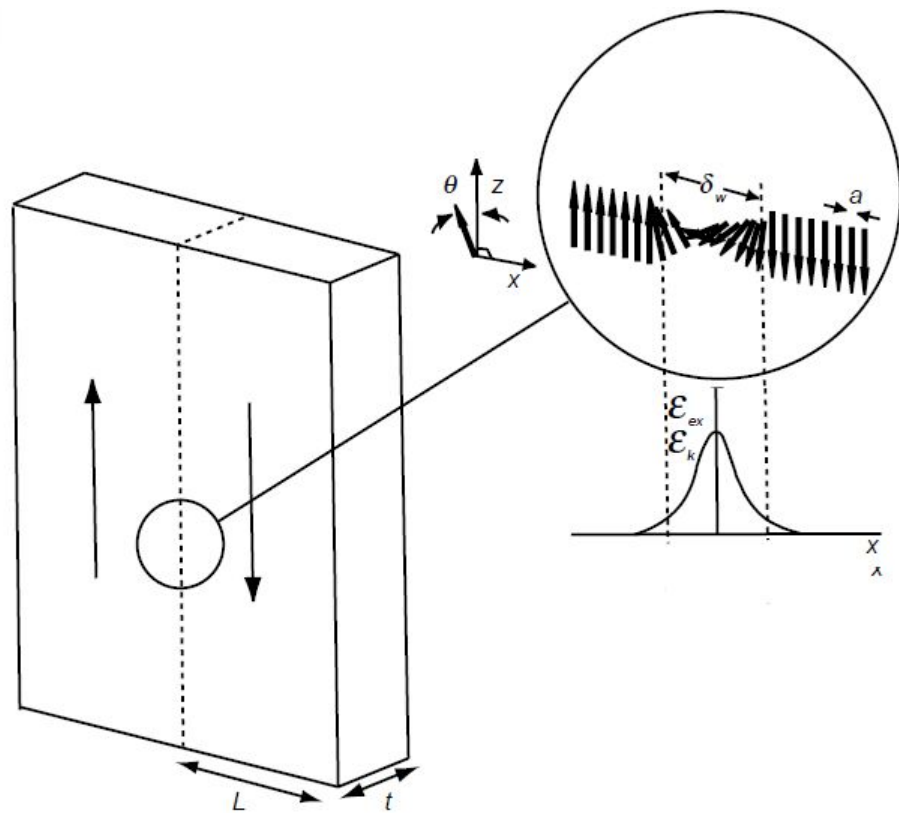
- Dois termos

- Energia de troca
 - momentos paralelos
- Anisotropia
 - momento em uma direção

$$\delta_{wall} \approx \pi \left(\frac{A}{K_u} \right)^{1/2} \text{ Fe: } 30 \text{ nm}$$
$$\sigma_{wall} \approx a \left(AK_u \right)^{1/2} \text{ Fe: } 0.7 \text{ mJ/m}^2$$

Figure 7.6

Detail of the 180° Bloch wall.



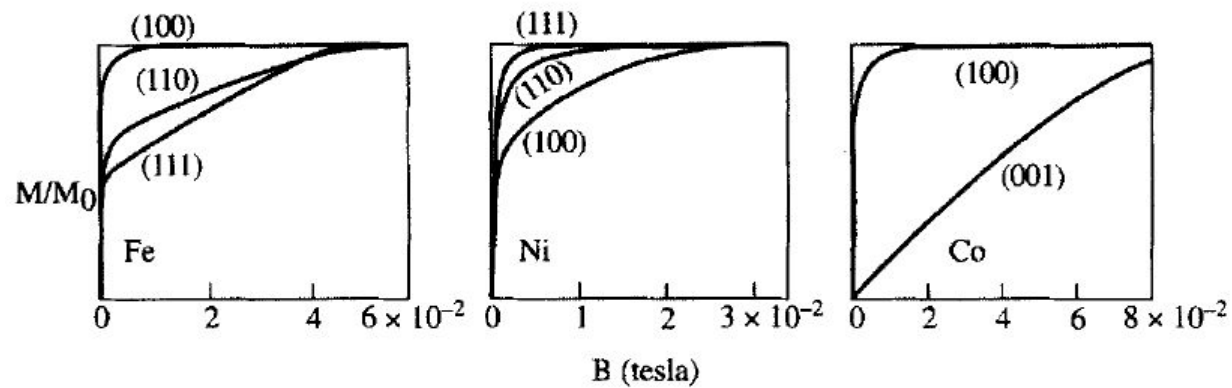


Fig. 6.22 Magnetization in Fe, Co and Ni for applied fields in different directions showing anisotropy. After Honda and Kaya 1926, Kaya 1928.

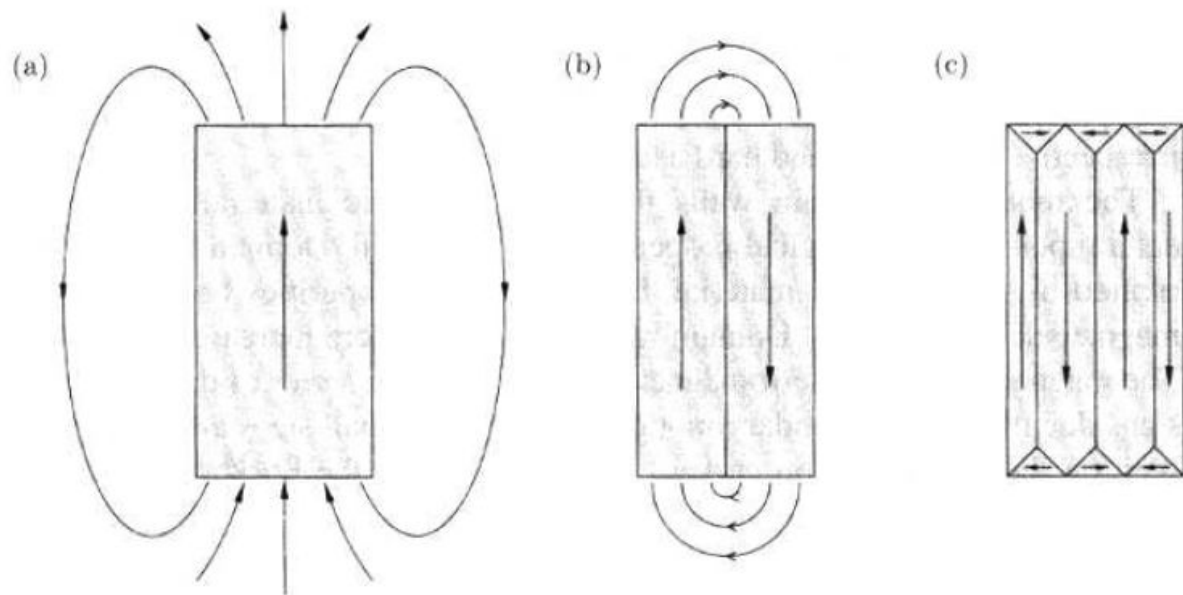
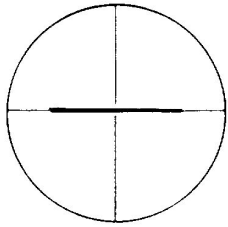


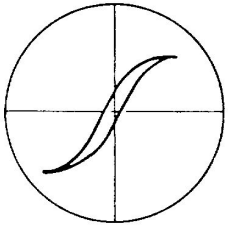
Fig. 6.23 A sample which is (a) uniformly magnetized, (b) divided into two domains, and (c) with a simple closure domain structure.

Ferromagnetos - Classificação

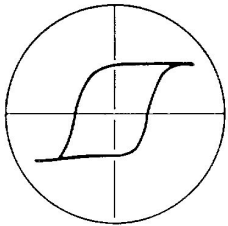


Paramagnético

- Os materiais ferromagnéticos podem ser separados basicamente em três classes, dependendo de sua resposta ao campo magnético aplicado (curva de histerese):



- Ferromagnetos Moles, ou doces

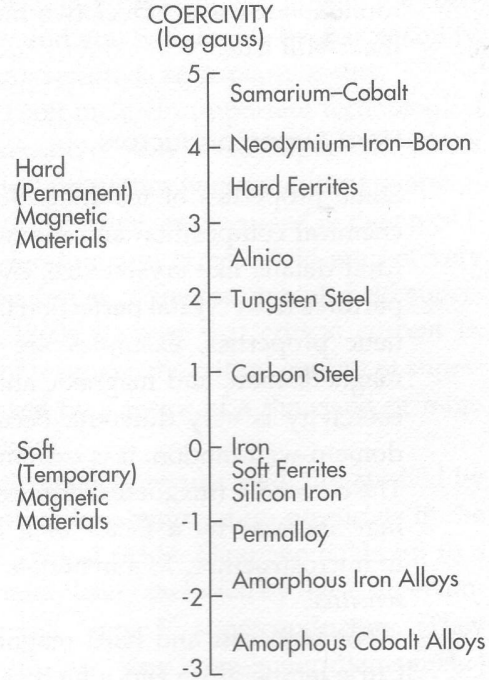


- Ferromagnetos Duros

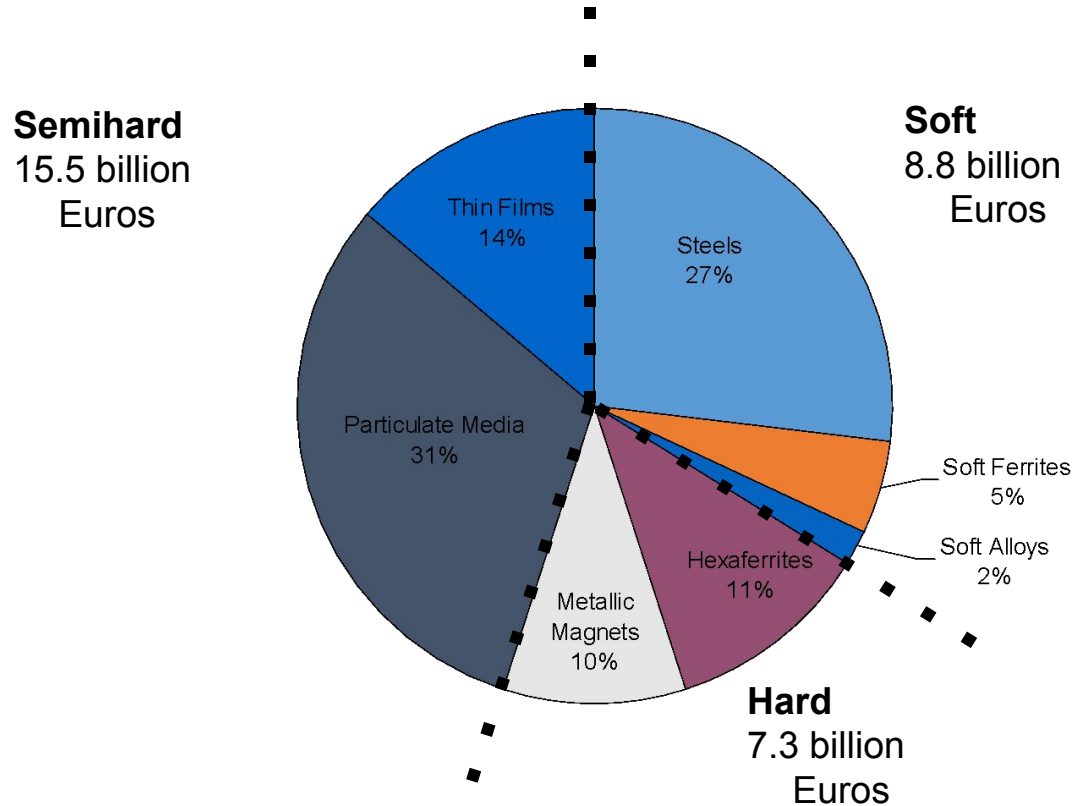
- Ferromagnetos intermediários

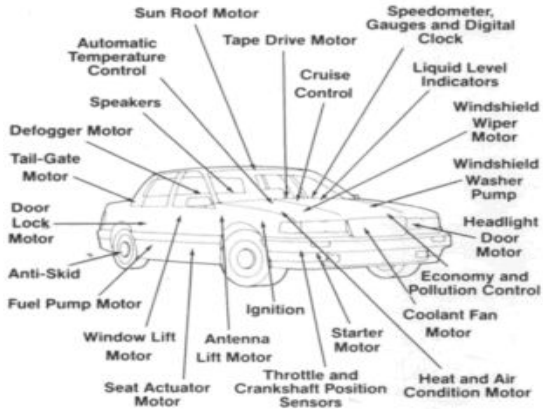
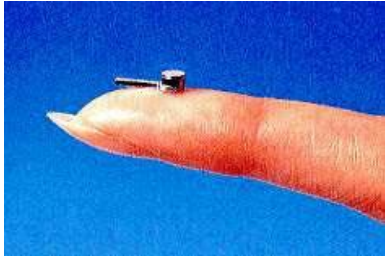
Ferromagnetos

Figure 6.5 The coercivity—the strength of an applied field needed to demagnetize a magnetic material—of various hard and soft magnets, on a logarithmic scale. Amorphous metals (see Chapter 8) may be demagnetized by a field of a milligauss (10^{-3} gauss), whereas rare-earth permanent magnets (see Chapter 4) require fields of tens of kilogauss (10^4 gauss and more) to be demagnetized.



Materiais Magnéticos no mercado Mundial





Ferromagnetos Duros

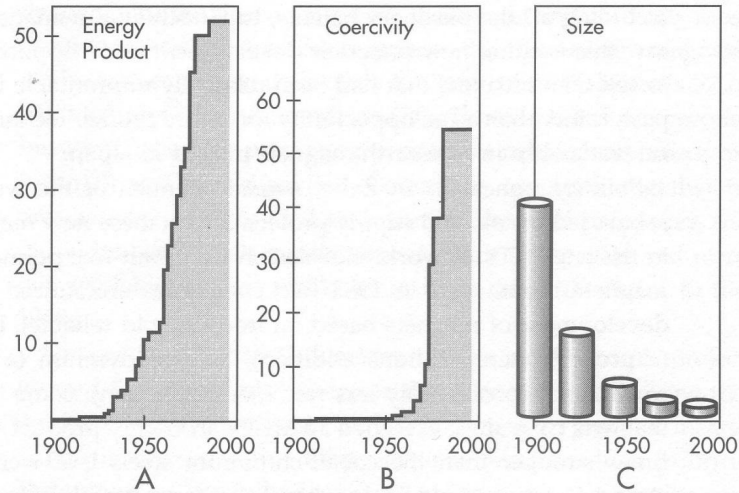
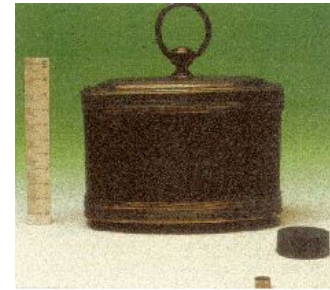


Figure 4.1 The remarkable increases in (A) energy product (in megagauss-oersted) and (B) coercivity (in kilogauss) of permanent-magnet materials in this century. As magnets became more powerful, the size and length of a magnet required for a specific application (C) decreased.

Brass bound lodestone, ferrite block and NdFeB magnet: each store the same magnetic energy (~0.4J) & contain ~70% iron by weight, yet the mass has decreased a thousand fold.



Automotive:

Starter motors, Anti-lock braking systems (ABS), Motor drives for wipers, Injection pumps, Fans and controls for windows, seats etc, Loudspeakers, Eddy current brakes, Alternators.

Telecommunications:

Loudspeakers, Microphones, Telephone ringers, Electro-acoustic pick-ups, Switches and relays.

Data Processing:

Disc drives and actuators, Stepping motors, Printers.

Consumer Electronics:

DC motors for showers, Washing machines, Drills, Low voltage DC drives for cordless appliances, Loudspeakers for TV and Audio, TV beam correction and focusing device, Compact-disc drives, Home computers, Video Recorders, Clocks.

Electronic and Instrumentation:

Sensors, Contactless switches, NMR spectrometer, Energy meter disc, Electro-mechanical transducers, Crossed field tubes, Flux-transfer trip device, Dampers.

Industrial:

DC motors for magnetic tools, Robotics, Magnetic separators for extracting metals and ores, Magnetic bearings, Servo-motor drives, Lifting apparatus, Brakes and clutches, Meters and measuring equipment.

Astro and Aerospace:

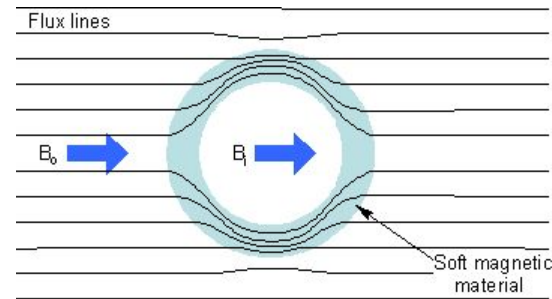
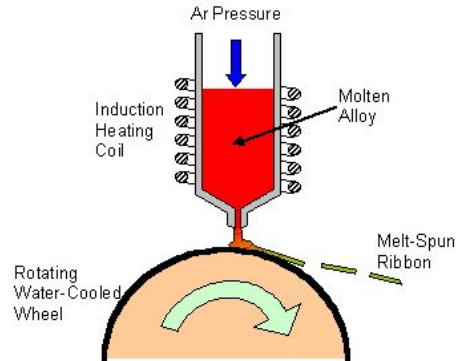
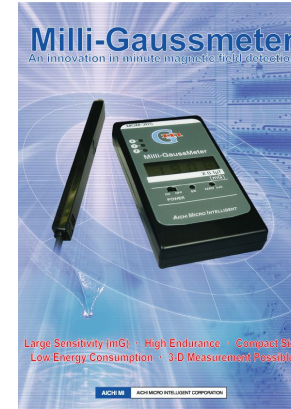
Frictionless bearings, Stepping motors, Couplings, Instrumentation, Travelling wave tubes, Auto-compass.

Biosurgical:

Dentures, Orthodontics, Orthopaedics, Wound closures, Stomach seals, Repulsion collars, Ferromagnetic probes, Cancer cell separators, Magnetomotive artificial hearts, NMR / MRI body scanner.

Ferromagnetos Doces

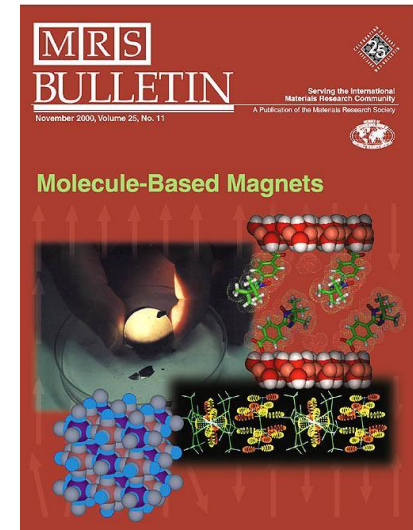
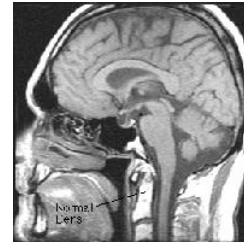
- Transformadores
- Cabeçotes de leitura e gravação
- Sensores (Fluxgate)



http://www.aacg.bham.ac.uk/magnetic_materials/soft_magnets.htm

Ferromagnetos – Outras Aplicações

- Magnetoresistência gigante
- Magnetostricção gigante
- Efeito Hall extraordinário
- Refrigeração magnética
- Magnetos moleculares
- Ressonância magnética



<http://electronics.howstuffworks.com/mri.htm>

- Refinamento do grão
 - \uparrow interação de troca
 - \uparrow remanência

- Propriedades magnéticas
 - tamanho de grão
 - fração volumétrica das fase

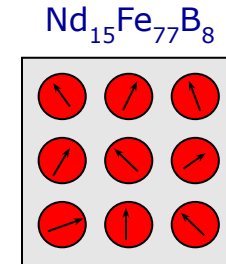
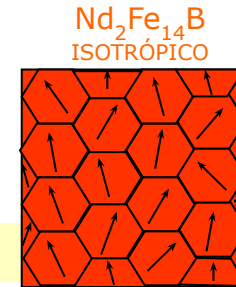
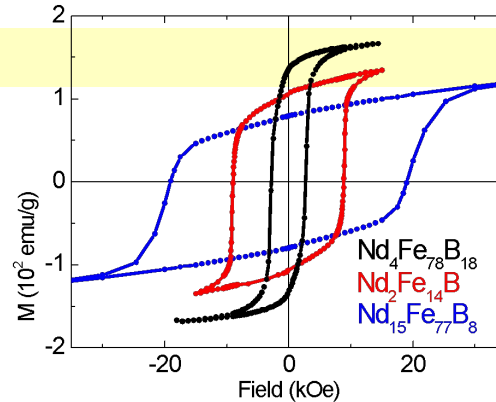
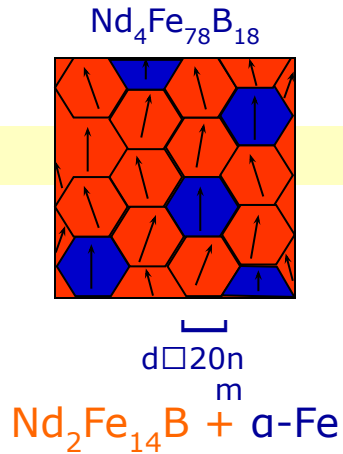
Nanocompósitos de NdFeB (ímãs nanoestruturados)

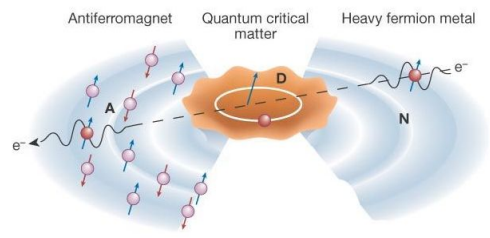
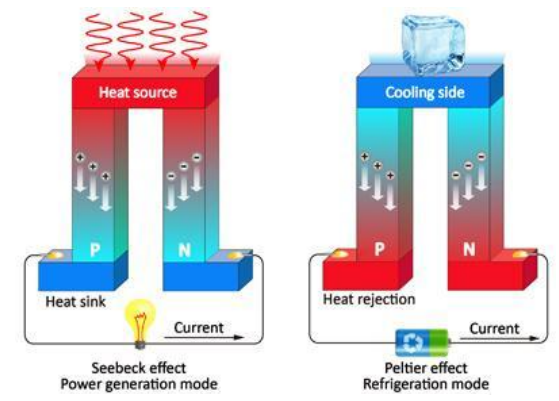
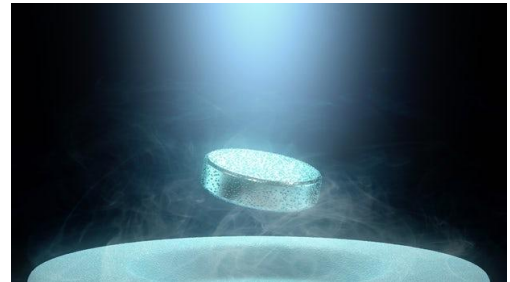
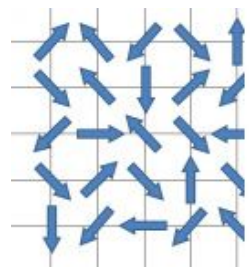
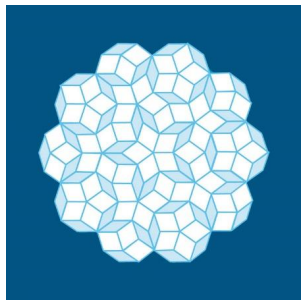
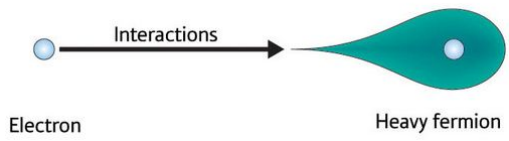
Acoplamento de troca



Aumento da remanência

$$M_r \approx 0.8M_s$$





<https://chem.au.dk/forskning/forskningscentre/center-for-materials-crystallography/research/energy-materials/thermoelectrics/>

<https://www.nature.com/articles/nature032>

Tabela Periódica dos Elementos

1 IA Novo Original												18 VIIIA																																																																																																	
1 H 1.00784	2 He 4.002602											3 Li 6.941	4 Be 9.012182											19 K 39.0983	20 Ca 40.078	21 Sc 44.955912	22 Ti 47.88	23 V 50.9415	24 Cr 51.9961	25 Mn 54.938049	26 Fe 55.845	27 Co 58.933200	28 Ni 58.6934	29 Cu 63.546	30 Zn 65.38	31 Ga 69.723	32 Ge 72.64	33 As 74.92160	34 Se 78.96	35 Br 79.904	36 Kr 83.798	37 Rb 85.4678	38 Sr 87.62	39 Y 88.90585	40 Zr 91.224	41 Nb 92.90638	42 Mo 95.94	43 Tc 98	44 Ru 101.07	45 Rh 102.90550	46 Pd 106.42	47 Ag 107.8682	48 Cd 112.411	49 In 114.818	50 Sn 118.710	51 Sb 121.760	52 Te 127.60	53 I 126.90447	54 Xe 131.293	55 Cs 132.90545	56 Ba 137.327	57 La 138.90547	58 Ce 140.12	59 Pr 140.90765	60 Nd 144.24	61 Pm 145	62 Sm 150.36	63 Eu 151.964	64 Gd 157.25	65 Tb 158.92534	66 Dy 162.500	67 Ho 164.93032	68 Er 167.259	69 Tm 168.93421	70 Yb 173.054	71 Lu 174.967	72 Hf 178.49	73 Ta 180.9479	74 W 183.84	75 Re 186.207	76 Os 190.23	77 Ir 192.217	78 Pt 195.078	79 Au 196.96657	80 Hg 200.59	81 Tl 204.3833	82 Pb 207.2	83 Bi 208.98038	84 Po 209	85 At 210	86 Rn 222	87 Fr 223	88 Ra 226	89 to 103	104 Rf 261	105 Db 262	106 Sg 266	107 Bh 264	108 Hs 277	109 Mt 268	110 Ds 271	111 Rg 272	112 Uub 285	113 Uut 284	114 Uuq 289	115 Uup 288	116 Uuh 292	117 Uus 294	118 Uuo 294

Massas atômicas em parênteses são aquelas do isótopo mais estável ou comum.

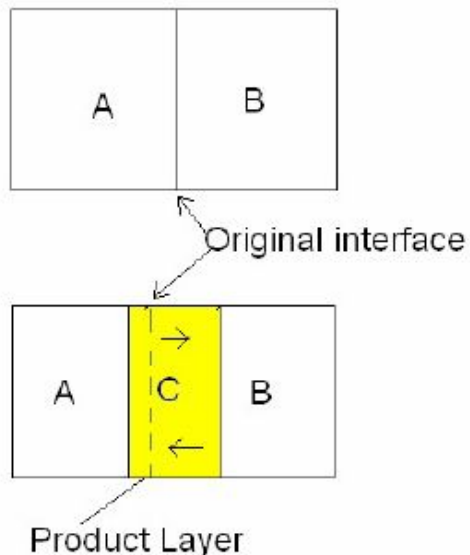
Direitos autorais de design: © 2013 Dayah (michael@dayah.com), http://www.dayah.com/periodico/

57 La 138.90547	58 Ce 140.12	59 Pr 140.90765	60 Nd 144.24	61 Pm 145	62 Sm 150.36	63 Eu 151.964	64 Gd 157.25	65 Tb 158.92534	66 Dy 162.500	67 Ho 164.93032	68 Er 167.259	69 Tm 168.93421	70 Yb 173.054	71 Lu 174.967
89 Ac 227	90 Th 232.0381	91 Pa 231.03689	92 U 238.02891	93 Np 237	94 Pu 239	95 Am 243	96 Cm 247	97 Bk 247	98 Cf 251	99 Es 252	100 Fm 257	101 Md 258	102 No 259	103 Lr 262

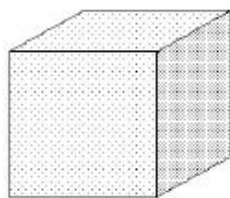
Nota: Os números de subgrupo 1-18 foram adotados em 1984 pela International Union of Pure and Applied Chemistry (União Internacional de Química Pura e Aplicada). Os nomes dos elementos 112-118 são os equivalentes latinos desses números.



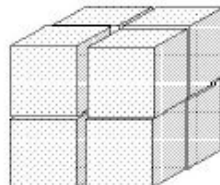
Solid State Reactions



- Diffusion controlled: Fick's 1st Law
 $J = -D(dc/dx)$
- Small particle sizes that are well mixed are needed to maximize the surface contact area.
- **Tamman's Rule** suggests a temperature of about two-thirds of the melting point (K) of the lower melting reactant is needed to have reaction to occur in a reasonable time.

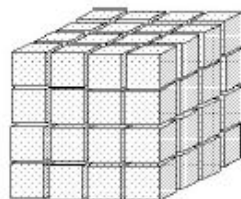


$$A = 6\text{cm}^2$$



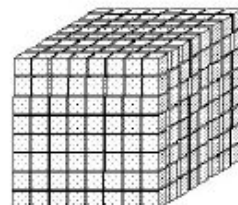
Pieces half the original size.
Twice the surface area

$$A = 12\text{cm}^2$$



Pieces one quarter the original size.
Four times the surface area

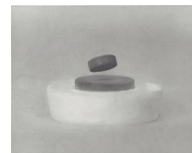
$$A = 24\text{cm}^2$$



Pieces one eighth the original size.
Eight times the surface area

$$A = 48\text{cm}^2$$

- Thorough grinding is necessary to achieve a **homogenous** mixture of reactants.
- The number of crystallites in contact may be increased by **pelletizing** the powders using a hydraulic press.
- The reaction mixture is typically removed and reground to bring **fresh surfaces** in contact, which speeds up the reaction.
- **Reaction times** are sometimes hours, but may range into several days or weeks for a complete reaction, with intermediate grinding.
- Sample purity is typically examined using powder X-ray diffraction.
- Furnaces use **resistance heating** with metal, SiC, or MoSi₂ heating elements.
- Conversion of electrical energy into heat (to 2300 K). An electrical arc directed at the sample may achieve 3300 K. A CO₂ laser can give temperatures up to 4300 K.
- Containers for the reaction (**crucibles**) must be able to withstand high temperatures and be **sufficiently inert to the reactants**. Common crucibles are silica (to 1430 K), alumina (to 2200 K), zirconia (to 2300 K), or magnesia (2700 K). Platinum (m.p. 2045 K) and silver (m.p. 1235 K) are also used for some reactions.



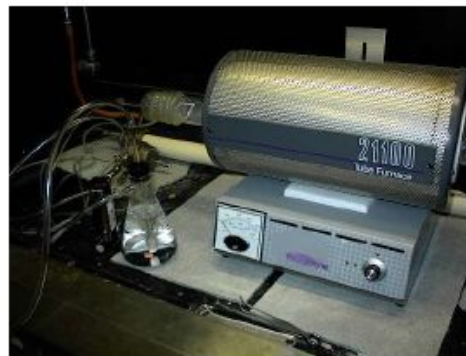
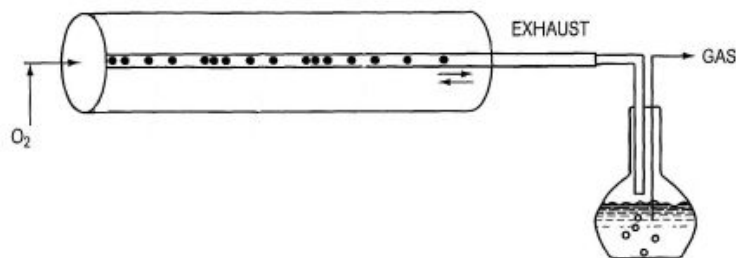
Special Atmosphere

Synthesis of some compounds must be carried out under a special atmosphere.

- an **noble gas**, argon, may be used to prevent oxidation to higher oxidation state.
- an **oxidizing gas**, oxygen, might be used to form a **high** oxidation state.
- a **reducing gas**, hydrogen, might be used to form a **low** oxidation state.

Reactions usually take place in a small boat crucible placed in a tube in a horizontal tube furnace.

• Gas is passed of a period of time to expel all air from the apparatus, then continues to flow during the heating and cooling cycle. A bubbler is used to ensure positive pressure is maintained.



Microwave Synthesis

In a liquid or solid, the molecules of ions are not free to rotate.

The alternating electric field of the radiation:

1.If **charged particles** are present, these move under the influence of the field and produce an oscillating electric current. Resistance to the movement causes energy to be transferred to the surroundings as heat, known as **conduction heating**.

2.If no particles are present that can move freely, but molecules or units with **dipole moments** are present, then the electric field acts to align the dipole moments. This is **dielectric heating**. This is the type of heating that acts on water molecules in food.

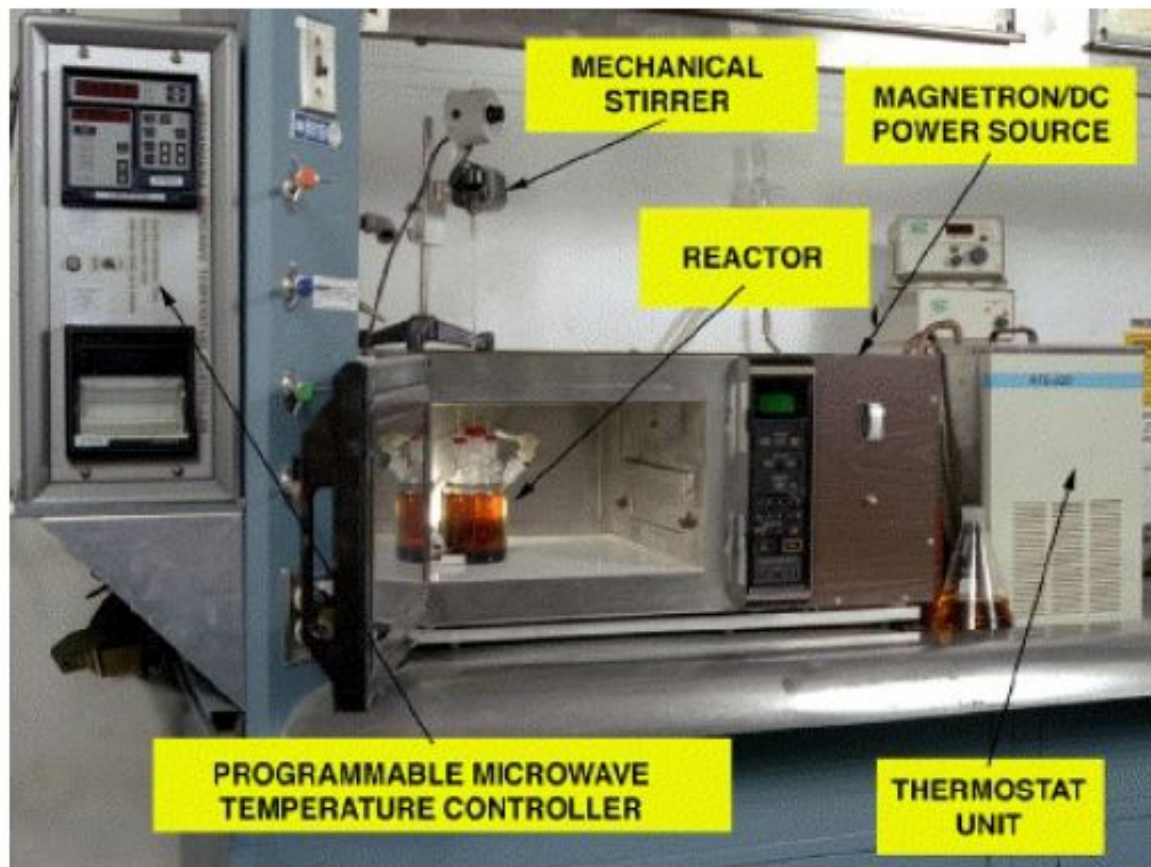
The electric field of the microwave radiation is oscillating at the frequency of the radiation, but the electric dipoles in solids do not change their alignment instantaneously, but with a characteristic time, τ .

The oscillating electric field changes its direction rapidly so that the time between changes is much smaller than τ , then the dipoles cannot respond fast enough and do not realign (lags behind).

The solid absorbs some of the microwave radiation and the energy is converted to heat.

Depends on the dielectric constant and the dielectric loss.

To use microwave heating, **at least one component of the reaction mixture must absorb microwave radiation**.

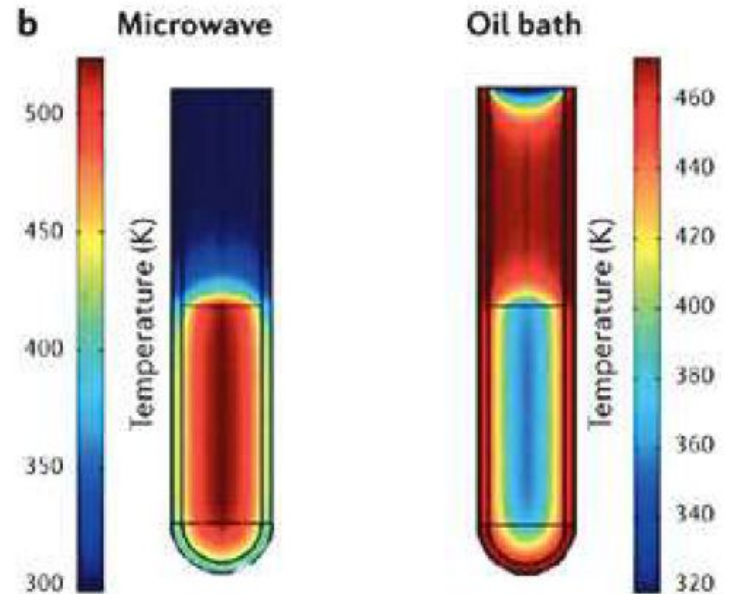


High Temperature Superconductor $\text{YBa}_2\text{Cu}_3\text{O}_{7-x}$

Conventional method takes about 24 hours to complete, whereas it takes approximately 2 hours using [microwave synthesis](#).

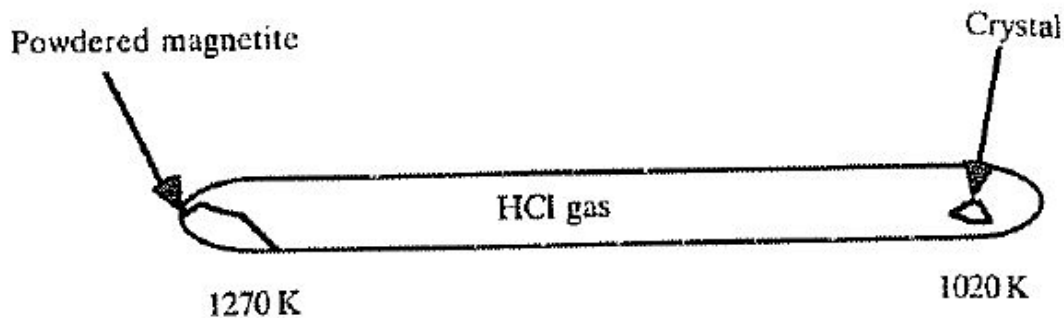
- A stoichiometric mixture of CuO , $\text{Ba}(\text{NO}_3)_2$, Y_2O_3 are placed in a modified microwave oven that allows the safe removal of nitrogen oxides formed during the reaction.
- The reaction mixture is treated with 500 watts of microwave radiation for five minutes, then reground and exposed to microwave radiation between 130-500 watts for 15 minutes. The reaction mixture is ground again and exposed to microwave radiation for 25 minutes.

Microwave irradiation raises the temperature of the whole volume simultaneously (i.e. bulk heating).

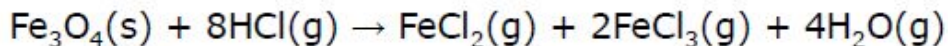


Chemical Vapor Transport

In CVT, a solid or solids interact with a volatile compound and a solid product is deposited in different part of the apparatus.



Growth of magnetite crystals using chemical vapour transport



The reaction is endothermic, so the equilibrium moves to the right as the temperature is raised. At the cooler end of the tube, the equilibrium shifts to the left and magnetite is deposited.

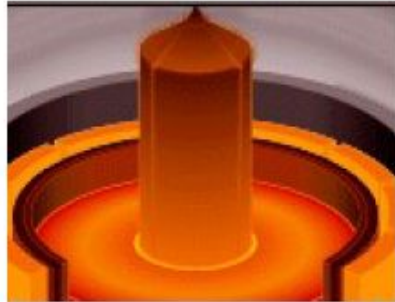
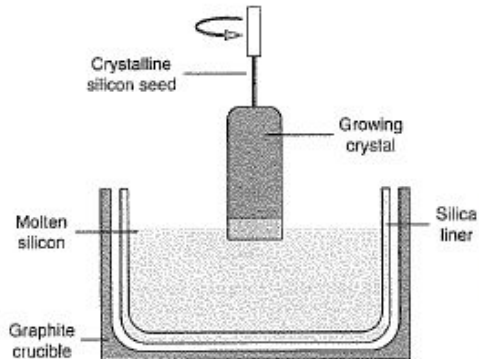
Czochralski Process

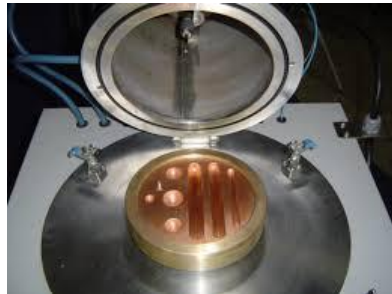
Silicon for the electronics industry has to have low levels of impurities, less than one impurity atom in 10^{10} Si.

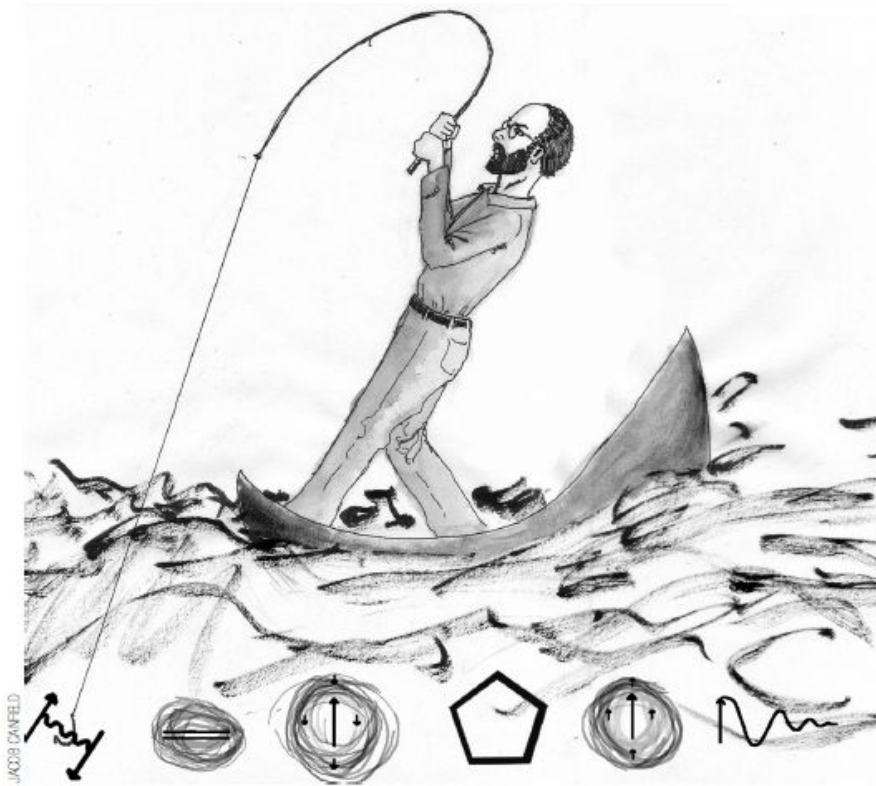
SiHCl_3 is highly volatile and distilled and decomposed as polycrystalline material onto rods of high purity silicon at 1300 K.

Large single crystals are made by the **Czochralski** process.

- The silicon is melted in an atmosphere of Ar, then a single crystal seed rod is used as a seed which is dipped into the melt.
- The crystal is slowly withdrawn, pulling an ever lengthening single crystal in the same orientation as the original seed.







PHILOSOPHICAL MAGAZINE B, 1992, VOL. 65, No. 6, 1117–1123

Growth of single crystals from metallic fluxes

By P. C. CANFIELD and Z. FISK

Los Alamos National Laboratory,
Los Alamos, New Mexico 87545, USA

[Received 4 October 1991]

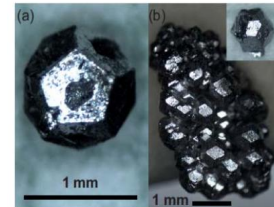
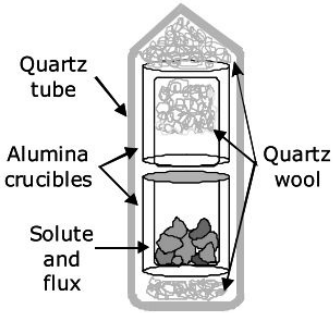
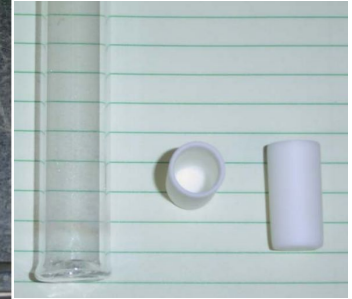
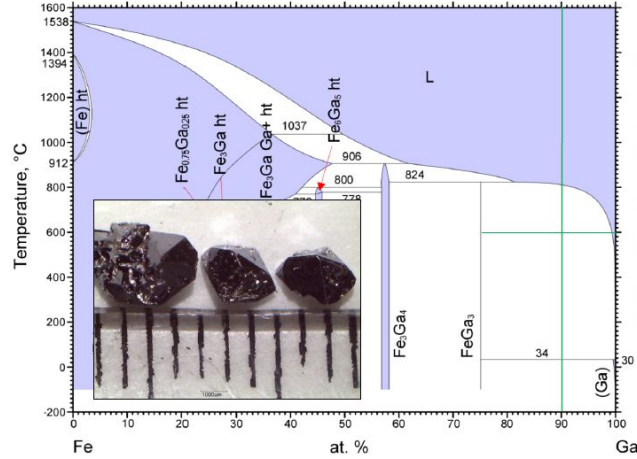
ABSTRACT

Our experience with the growth of a wide variety of intermetallic compounds from molten fluxes is reviewed. Common problems associated with this method of sample growth are discussed, as are problems and advantages of particular fluxes.

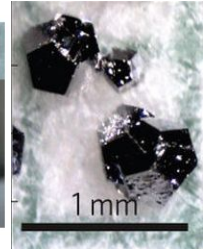
Desenhar e criar o sistema

Tabla periódica de los elementos

Fe 26



Zc-Zn



Gd-Cd



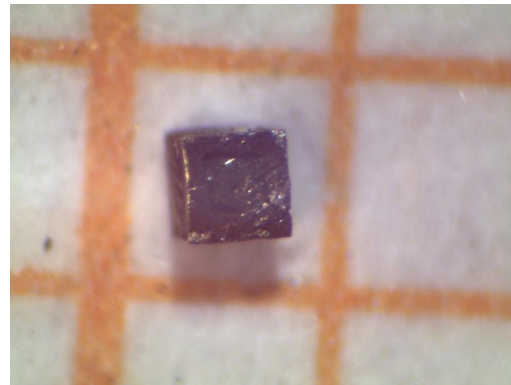


*

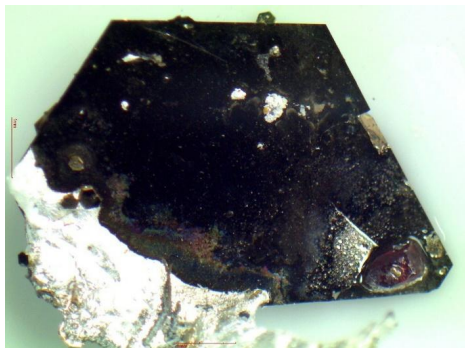
TbFe_2Ge_2



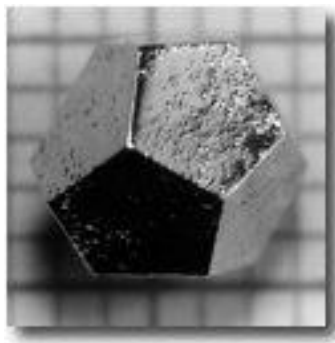
FeGa_3



GdPb_3

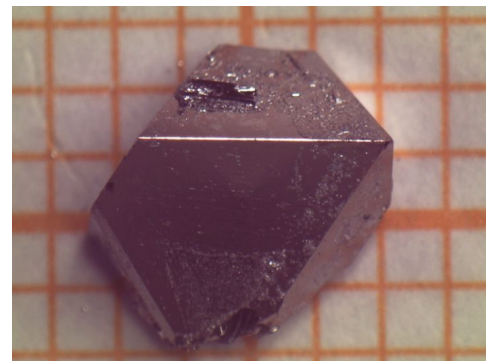


AlB_2



*

Ho-Mg-Zn



$\text{YbFe}_2\text{Zn}_{20}$

* Canfield's

Rudolf L. MOSSBAUER

discovers the “Recoilless Nuclear Resonance Absorption of γ -Radiation” in 1958
and receives the Nobel Prize in 1961



R.L. Mössbauer made his first observation of recoilless nuclear resonant absorption in ^{191}Ir !

R.L. Mössbauer,
Z. Physik, 1958, 151, 124.

R.L. Mössbauer,
Naturwissenschaften, 1958, 45, 538

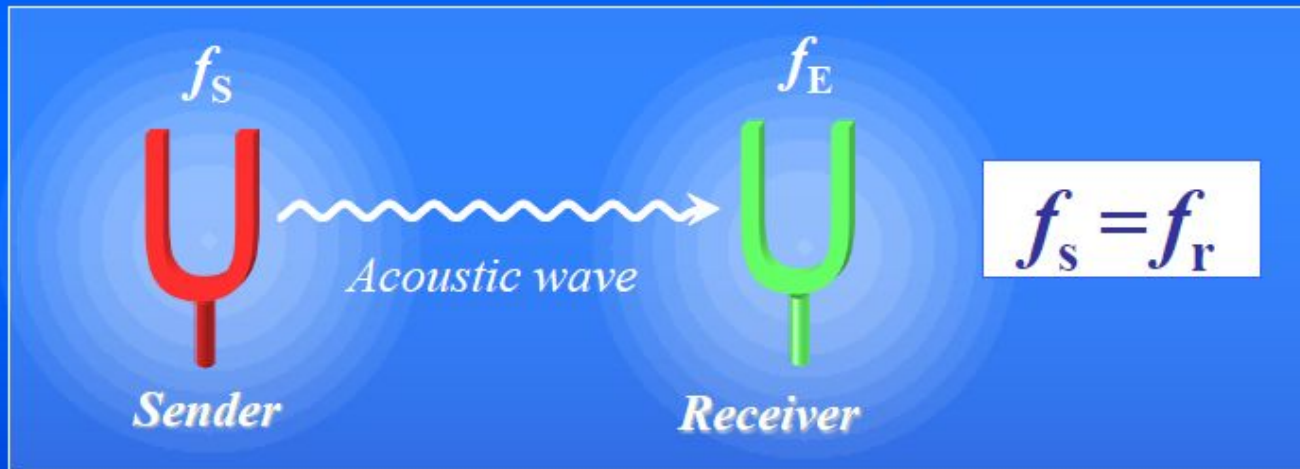
Mössbauer effect:

“Recoilless nuclear resonance absorption of γ -rays”

similar to

Acoustic resonance between two tuning forks with

same frequency $f_s = f_r$



Mössbauer effect: Atomic nuclei instead of tuning forks

Nucleus 1

Nucleus 2

Excited state

E_e

Z,N

Ground state

E_g

Z,N



E_e

Z,N

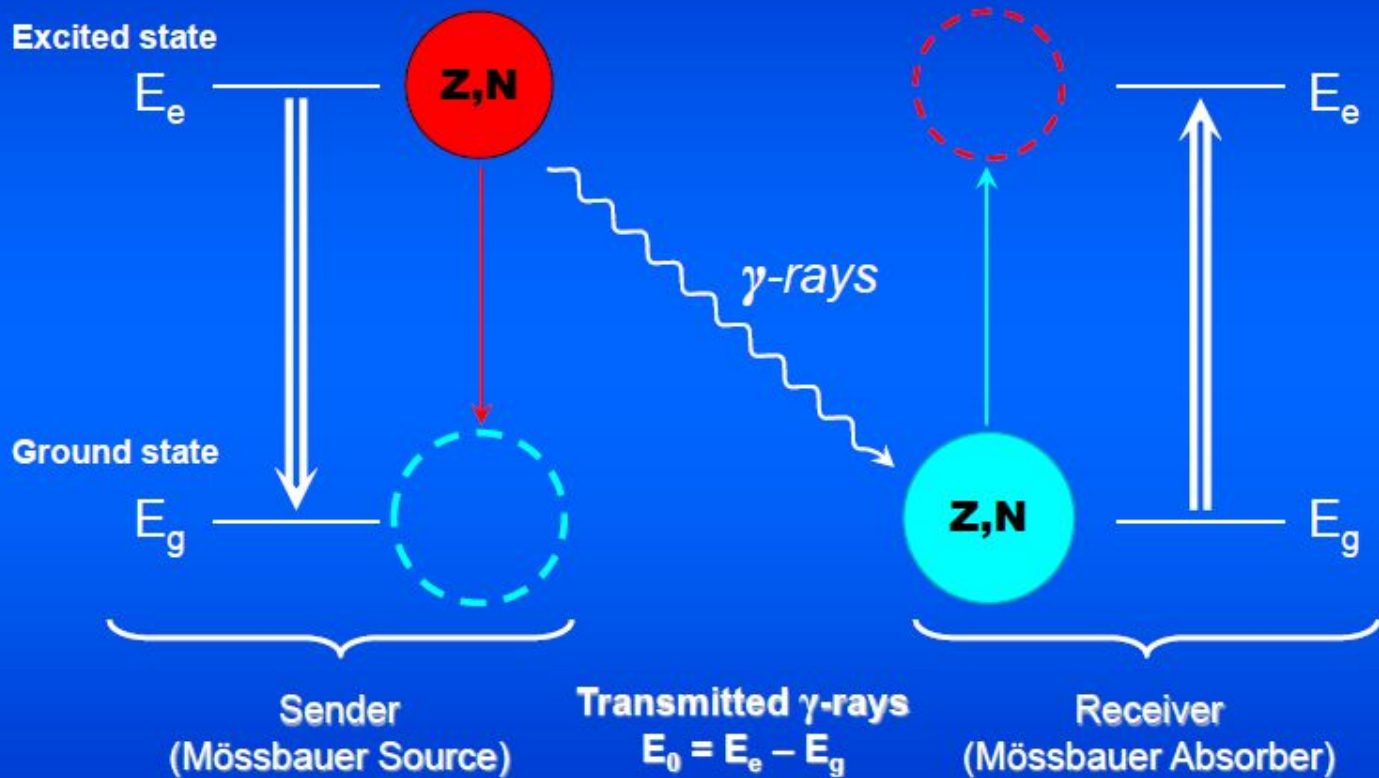
E_g

γ -rays

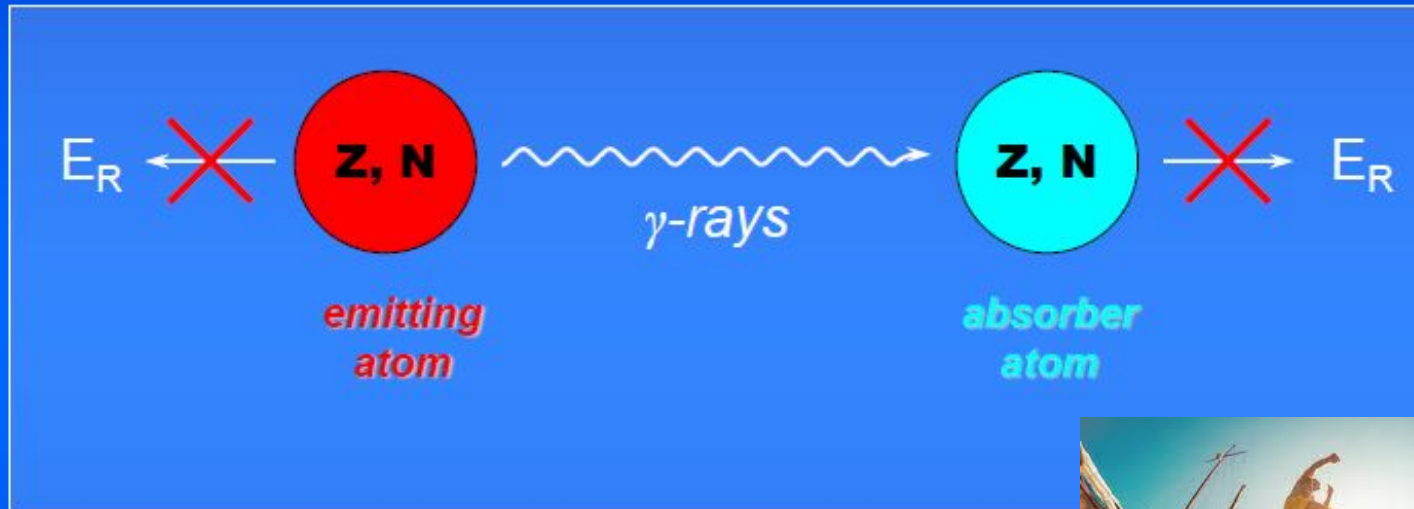
Sender
(Mössbauer Source)

Transmitted γ -rays
 $E_0 = E_e - E_g$

Receiver
(Mössbauer Absorber)



Important:
Elimination of recoil effect
upon emission and absorption of γ -rays!



$$E_R = E_\gamma^2 / 2mc^2$$

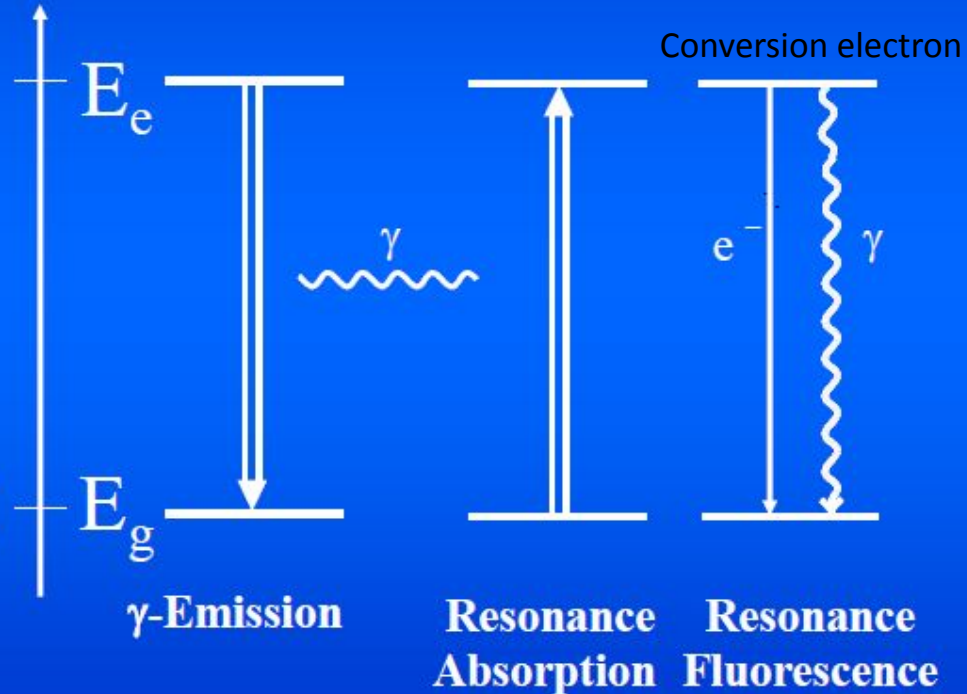


Recoilless Nuclear Resonance Absorption and Fluorescence of γ -Radiation

Nucleus in
Excited
State



Nucleus in
Ground
State



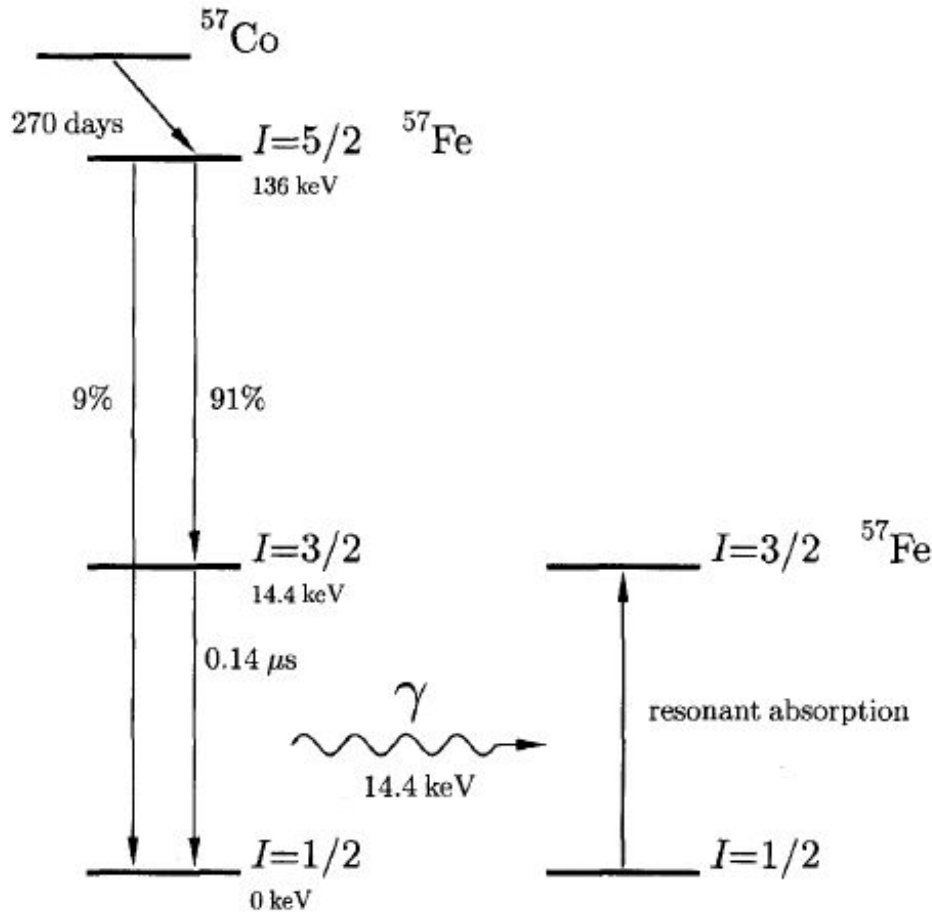
The preparation of narrow-line Mössbauer sources of ^{57}Co in metallic matrices

G. LONGWORTH and B. WINDOW

Materials Physics Division, AERE, Harwell, Berks

MS. received 1st March 1971

Abstract. The merits of various cubic matrices for the preparation of high-activity small-area sources of ^{57}Co are discussed. The useful areal density of activity is limited to about 150 mCi cm^{-2} for all matrices owing to resonance broadening, and the thickness of the source foil is determined by self absorption and the generation of fluorescence x rays. Electrostatic broadening and the change of isomer shift with age are shown to be relatively unimportant for sources of the above density of activity on chromium, rhodium and palladium. Rhodium is the best choice for a strong, unsplit source for use at 4.2 K. Methods of preparation which give linewidths close to natural linewidths are discussed.



Radioactive ^{57}Co with 270 days half-life, which may be generated in a cyclotron and diffused into a noble metal like rhodium, serves as the gamma radiation source for ^{57}Fe Mössbauer spectroscopy. ^{57}Co decays by electron capture (EC from K-shell, thereby reducing the proton number, from 27 to 26 corresponding to ^{57}Fe) and initially populates the 136 keV nuclear level of ^{57}Fe with nuclear spin quantum number $I = 5/2$. This excited state decays after ca. 10 ns and populates, with 85 % probability the 14.4 keV level by emitting 122 keV gamma quanta, with 15 % probability the 136 keV level decays directly to the ground state of ^{57}Fe . The 14.4 keV nuclear state has a half-life of ca. 100 ns. Both the half-life and the emitted gamma quanta of 14.4 keV energy are ideally suited for ^{57}Fe Mössbauer spectroscopy.

Nuclear parameters for selected Mössbauer isotopes

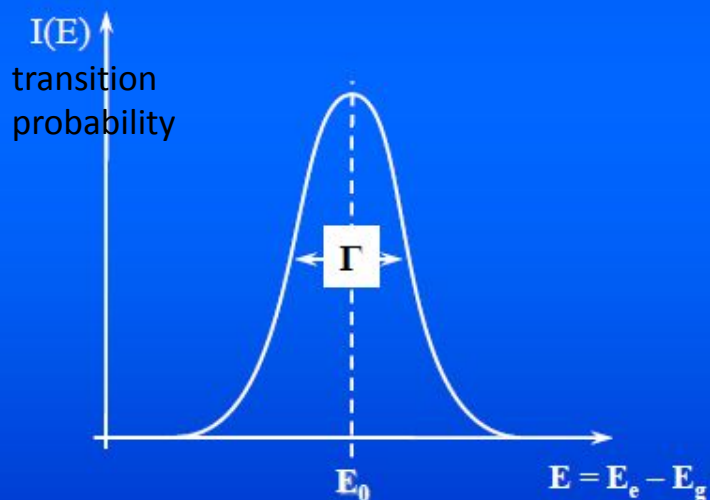
Isotope	E_{γ}/keV	$\Gamma_r/(\text{mm s}^{-1})$ $= 2 \Gamma_{\text{nat}}$	I_g	I_e	α	Natural abundance %	Nuclear decay*
^{57}Fe	14.41	0.192	1/2-	3/2-	8.17	2.17	$^{57}\text{Co}(\text{EC } 270 \text{ d})$
^{61}Ni	67.40	0.78	3/2-	5/2-	0.12	1.25	$^{61}\text{Co}(\beta^- 99 \text{ m})$
^{119}Sn	23.87	0.626	1/2+	3/2+	5.12	8.58	$^{119\text{m}}\text{Sn}(\text{IT } 50 \text{ d})$
^{121}Sb	37.15	2.1	5/2+	7/2+	~ 10	57.25	$^{121\text{m}}\text{Sn}(\beta^- 76 \text{ y})$
^{125}Te	35.48	5.02	1/2+	3/2+	12.7	6.99	$^{125}\text{I}(\text{EC } 60 \text{ d})$
^{127}I	57.60	2.54	5/2+	7/2+	3.70	100	$^{127\text{m}}\text{Te} (\beta^- 109 \text{ d})$
^{129}I	27.72	0.59	7/2+	5/2+	5.3	nil	$^{129\text{m}}\text{Te} (\beta^- 33 \text{ d})$
^{149}Sm	22.5	1.60	7/2-	5/2-	~ 12	13.9	$^{149}\text{Eu}(\text{EC } 106 \text{ d})$
^{151}Eu	21.6	1.44	5/2+	7/2+	29	47.8	$^{151}\text{Gd}(\text{EC } 120 \text{ d})$
^{161}Dy	25.65	0.37	5/2+	5/2-	~ 2.5	18.88	$^{161}\text{Tb}(\beta^- 6.9 \text{ d})$
^{193}Ir	73.0	0.60	3/2+	1/2+	~ 6	61.5	$^{193}\text{Os}(\beta^- 31 \text{ h})$
^{197}Au	77.34	1.87	3/2+	1/2+	4.0	100	$^{197}\text{Pt}(\beta^- 18 \text{ h})$
^{237}Np	59.54	0.067	5/2+	5/2-	1.06	nil	$^{241}\text{Am}(\alpha 458 \text{ y})$

*EC = electron capture, β^- = beta-decay, IT = isomeric transition, α – alpha-decay

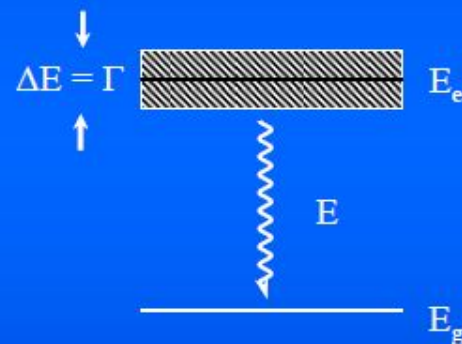
Mean lifetime τ of excited state and natural line width Γ

An excited state (nuclear or electronic) of mean lifetime τ can never be assigned a sharp energy value, but only a value within the energy range ΔE , which correlates with the uncertainty in time Δt via the **Heisenberg Uncertainty Principle**: $\Delta E \Delta t \geq \hbar$. Weisskopf and Wigner have shown that in general $\Gamma \cdot \tau = \hbar$.

$$\Gamma = \hbar/\tau = \text{natural line width, } \hbar = h/2\pi \text{ Planck's constant}$$



Intensity as function of transition energy E of nuclear (or optical) transitions.

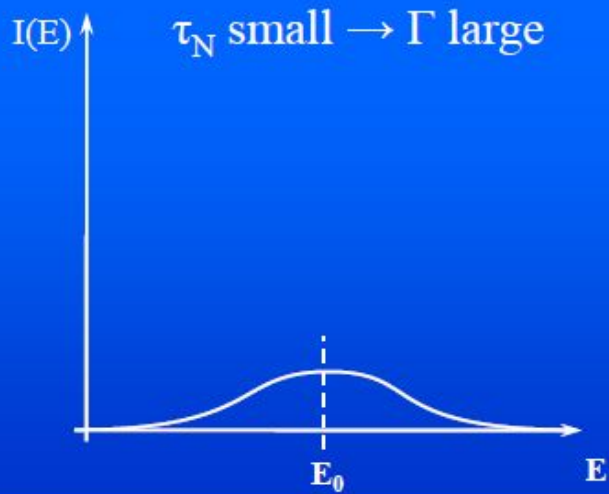
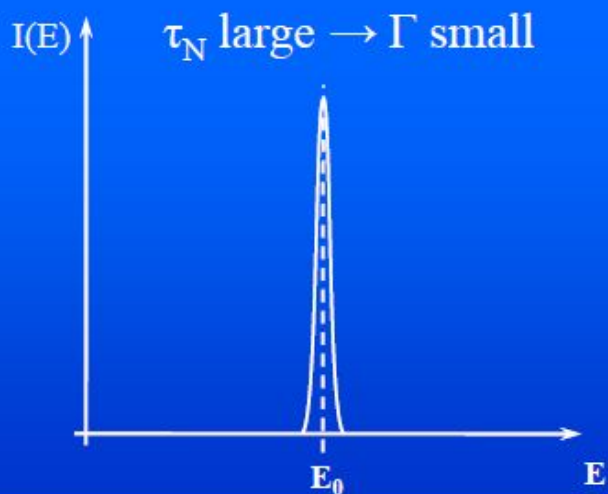


Transitions from an excited state (e) to the ground state (g) or vice versa involve all possible energies within the range of ΔE . The transition probability or intensity as a function of E yields a spectral line centered around the most probable transition energy E_0 .

According to Weisskopf and Wigner the distribution of energies about the energy E_0 (= transition probability as function of transition energy E) is given by the **Breit-Wigner (or Lorentzian) formula**:

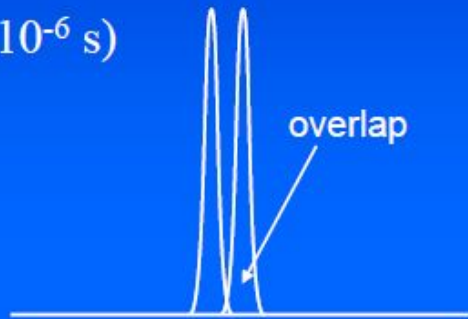
$$I(E) = \frac{(\Gamma/2)^2}{(E - E_0)^2 + (\Gamma/2)^2}$$

The mean lifetime τ determines the width of the resonance lines ($\Gamma \cdot \tau = \hbar$).
The mean lifetime τ is related to the half-life $t_{1/2}$ by the relation $\tau = \ln 2 \cdot t_{1/2}$.

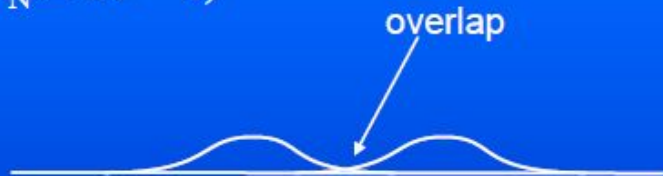


Resonance absorption is observable only if the emission and absorption lines **overlap sufficiently**. This is not the case when the lines are:

- too narrow ($\tau_N \geq 10^{-6}$ s)



- too broad ($\tau_N \leq 10^{-11}$ s)



**Resonance
absorption
is “hidden
in the noise”**

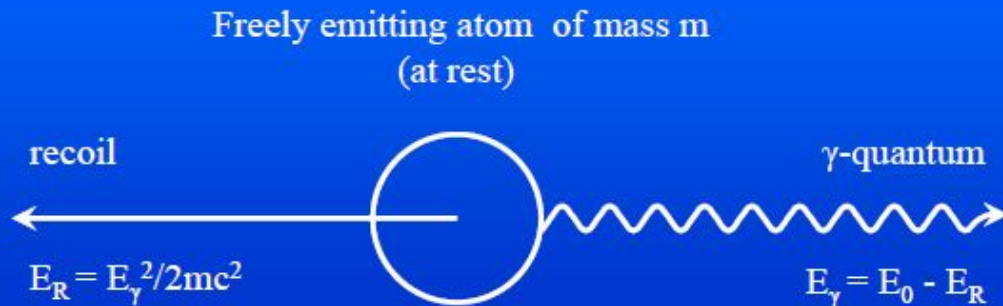
Suitable for Mössbauer spectroscopy: 10^{-6} s $\geq \tau_N \geq 10^{-11}$ s

Recoil Effect

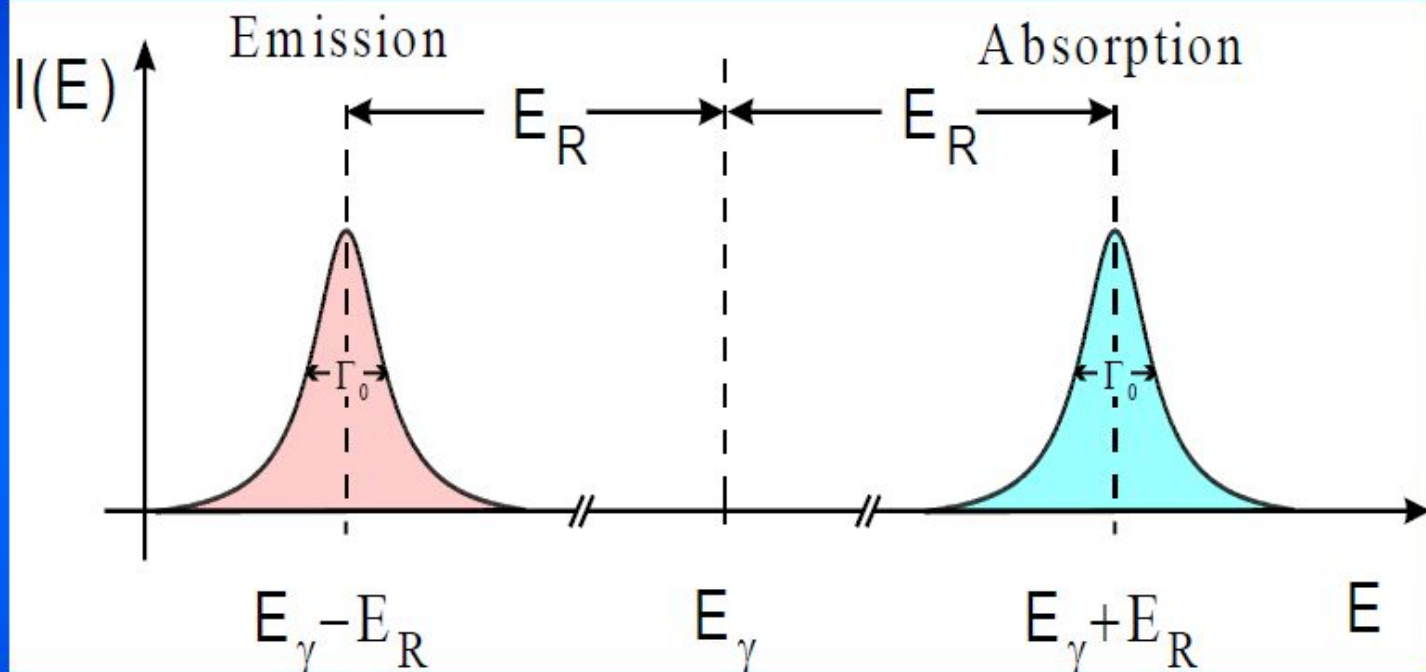
By emission or absorption of γ -quanta with energy E_γ in a **free atom or molecule** (gas, liquid) the atom (molecule) of mass **m** suffers a recoil effect with energy E_R given by the equation

$$E_R = E_\gamma^2 / 2mc^2$$

which is much larger (5-6 orders of magnitude) than the natural line width $\Gamma \rightarrow$ no resonance possible between free atoms or molecules



Recoil Effect



$$E_R = \frac{E_\gamma^2}{2mc^2}$$

$${}^{57}\text{Fe} : E_R = 2 \cdot 10^{-3} \text{ eV}$$
$$\Gamma_0 = 4.7 \cdot 10^{-9} \text{ eV}$$

Free-atom Recoil and Thermal Broadening

We consider the emission of a γ -quantum of initial energy E_0 from an atom with mass m moving with velocity v_N in the direction of the γ -ray propagation.

Before emission: $E_0 + \frac{1}{2} m v_N^2$

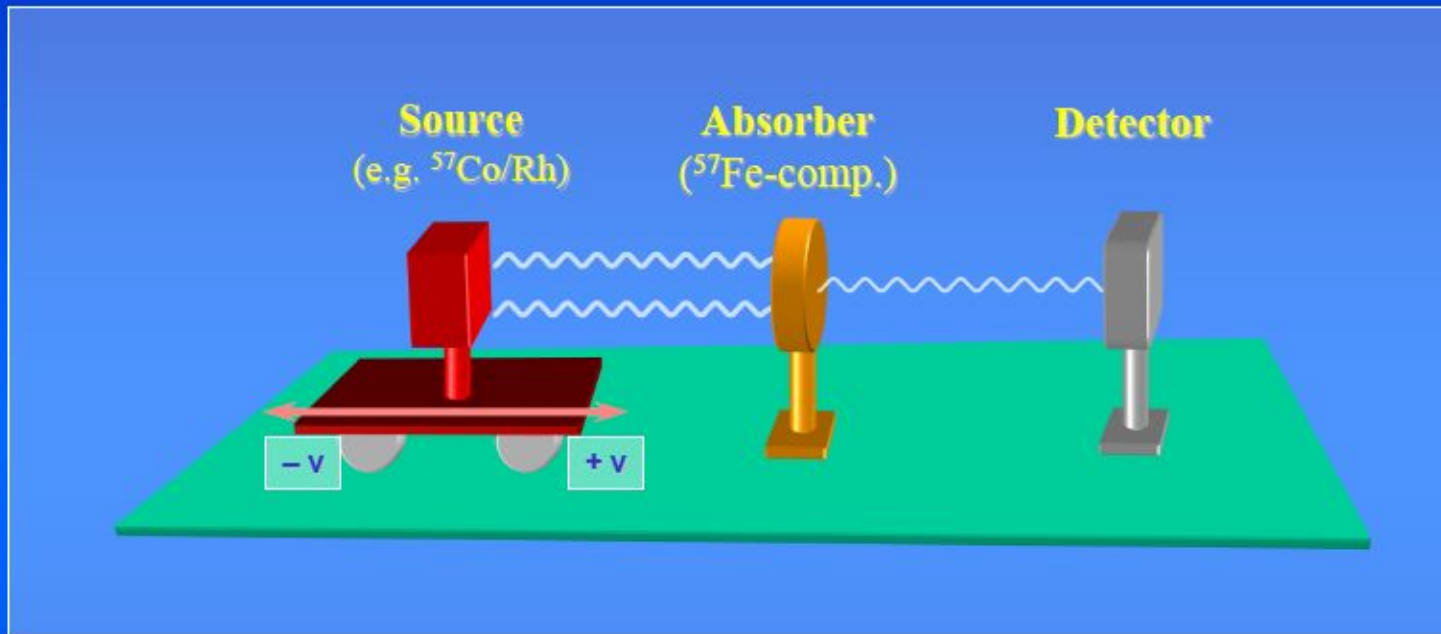
After emission: $E_\gamma + \frac{1}{2} m (v_N + v_R)^2$ $v_R =$ velocity due to recoil
(opposite to v_N)

Conservation of energy: $E_0 + \frac{1}{2} m v_N^2 = E_\gamma + \frac{1}{2} m (v_N + v_R)^2$

Difference between nuclear transition energies before and after emission:

$$\delta E = E_0 - E_\gamma = \underbrace{\frac{1}{2} m v_R^2}_{\text{Recoil energy } E_R} + \underbrace{m v_N v_R}_{\text{Doppler energy } E_D}$$

Mössbauer-Experiment



Source and absorber are moved relative to each other with

Doppler velocity $v = c (\Gamma_0/E_\gamma)$

$c =$ velocity
of light

$^{57}\text{Fe} : \Gamma_0 = 4.7 \cdot 10^{-9} \text{ eV}, E_\gamma = 14400 \text{ eV}, v = 0.096 \text{ mm s}^{-1}$



Hyperfine Interactions between Nuclei and Electrons and Mössbauer Parameters

- Electric Monopole Interaction
⇒ Isomer Shift δ
- Electric Quadrupole Interaction
⇒ Quadrupole Splitting ΔE_Q
- Magnetic Dipole Interaction
⇒ Magnetic Splitting ΔE_M

Hyperfine Interactions and Mössbauer Parameters

Mössbauer Parameter	Type of Interaction	Information for Chemistry
Isomer Shift δ (mm/sec)	Electric Monopole (Coulombic) interaction between nucleus (protons) and electrons	Oxidation state Electronegativity of ligands Character of bonds Spin state (HS, IS, LS)
Quadruple splitting ΔE_Q (mm/sec)	Electric quadrupole interaction between nuclear quadrupole moment and inhomogeneous electric field	Molecular symmetry Oxidation state Character of bonds Spin state (HS, IS, LS)
Magnetic splitting ΔE_M (mm/sec)	Magnetic dipole interaction between nuclear magnetic dipole moment and magnetic field	Magnetic interactions e.g. ferromagnetism, antiferromagnetism

Conditions for Hyperfine Interactions

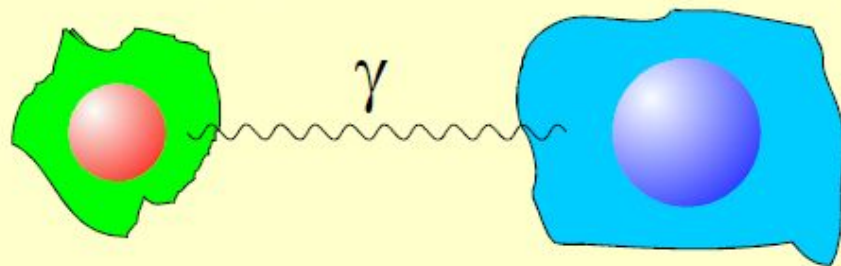
Type of Interaction	Nuclear Condition	Electronic Condition	Consequence
Electric Monopole interaction	$R_e^2 \neq R_g^2$	$ \Psi(0) _A^2 \neq \Psi(0) _S^2$	Different shift of nuclear levels \rightarrow Isomer shift δ
Electric Quadrupole interaction	Electric quadrupole moment $eQ \neq 0$ ($I > 1/2$)	EFG $\neq 0$	Nuclear states split into $I + 1/2$ substates $ I, \pm m_I\rangle$ (twofold degenerate) \rightarrow Quadrupole Splitting ΔE_Q
Magnetic dipole interaction	Magn. dipole moment $\mu \neq 0$ ($I > 0$)	$H \neq 0$	Nuclear states $ I\rangle$ split into $2I+1$ substates $ I, m_I\rangle$ with $m_I = +I, +I-1, \dots, -I$ \rightarrow Magnetic dipole splitting ΔE_M

Electric Monopole Interaction

Isomer Shift δ

Source (S)

Absorber (A)

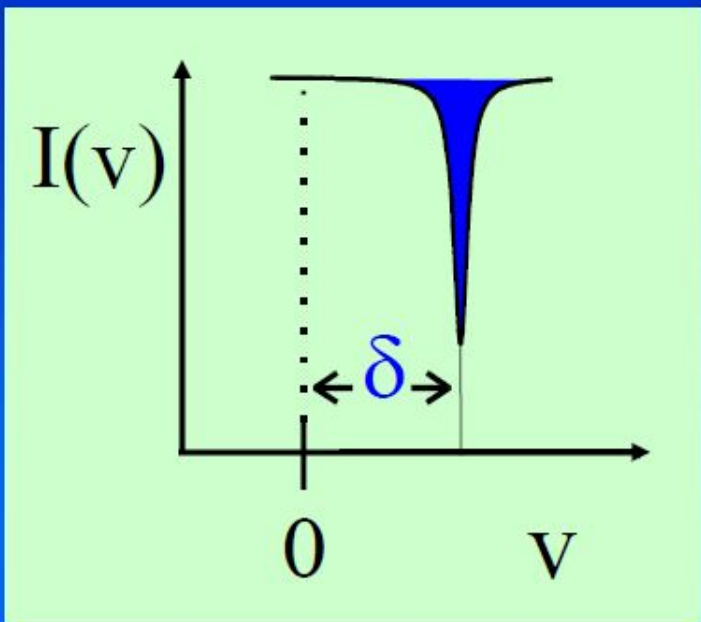
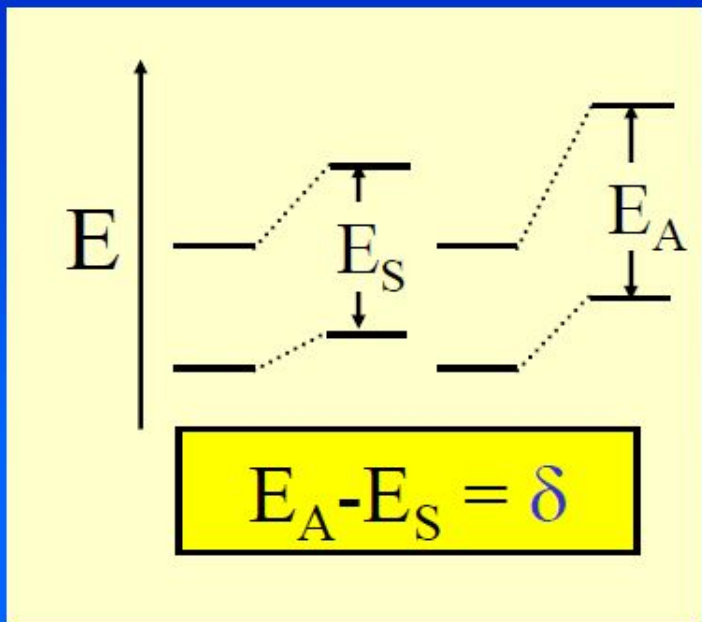


Nuclear radius

$$R_e \neq R_g$$

Electron density

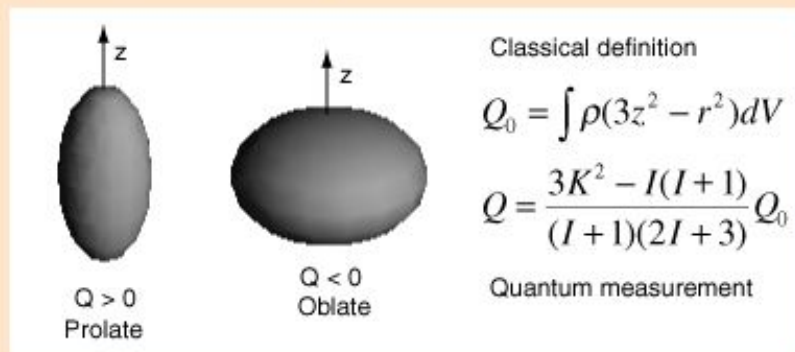
$$\rho_S \neq \rho_A$$



Oxidation state
Spin state
Bond properties
Covalency
Electronegativity

Electric Quadrupole Moments of Nuclei

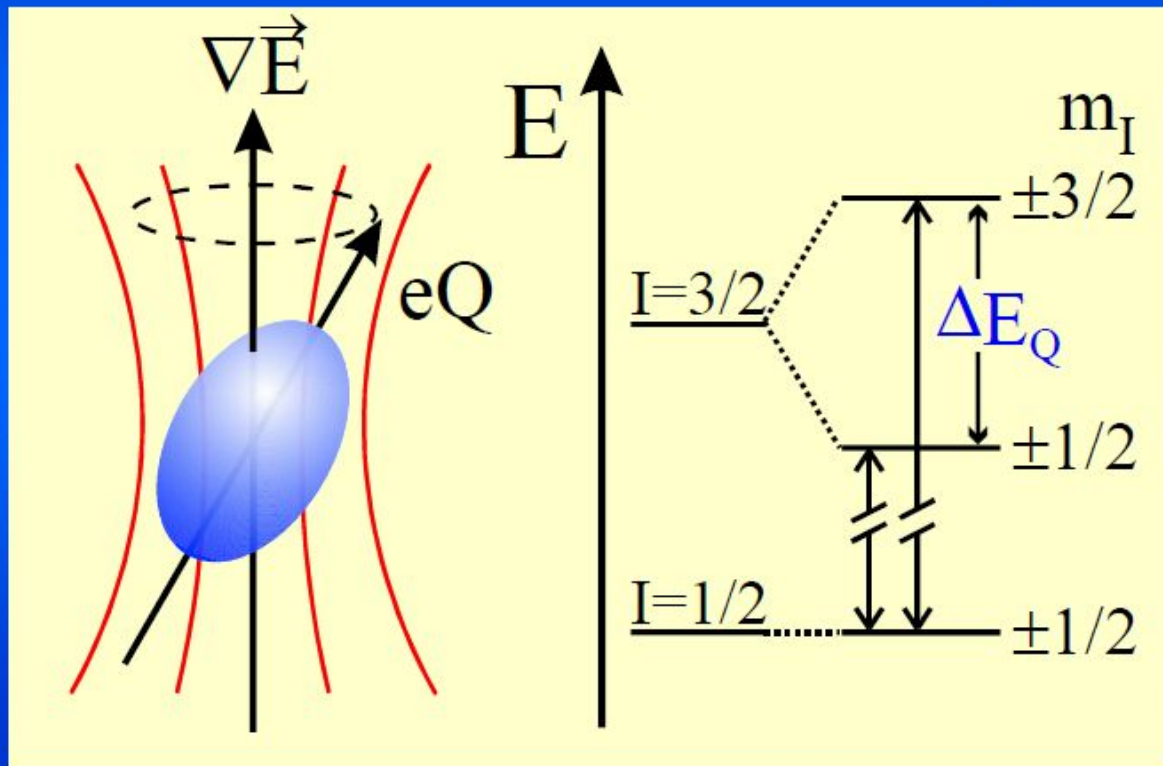
The nuclear [electric quadrupole moment](#) is a parameter which describes the effective shape of the ellipsoid of nuclear charge distribution. A non-zero quadrupole moment Q indicates that the charge distribution is not spherically symmetric. By convention, the value of Q is taken to be positive if the ellipsoid is prolate and negative if it is oblate.



The quantity Q_0 is the classical form of the calculation represents the departure from spherical symmetry in the rest frame of the nucleus. The expression for Q is the quantum mechanical form which takes into account the [nuclear spin](#) I and the projection K in the z -direction.

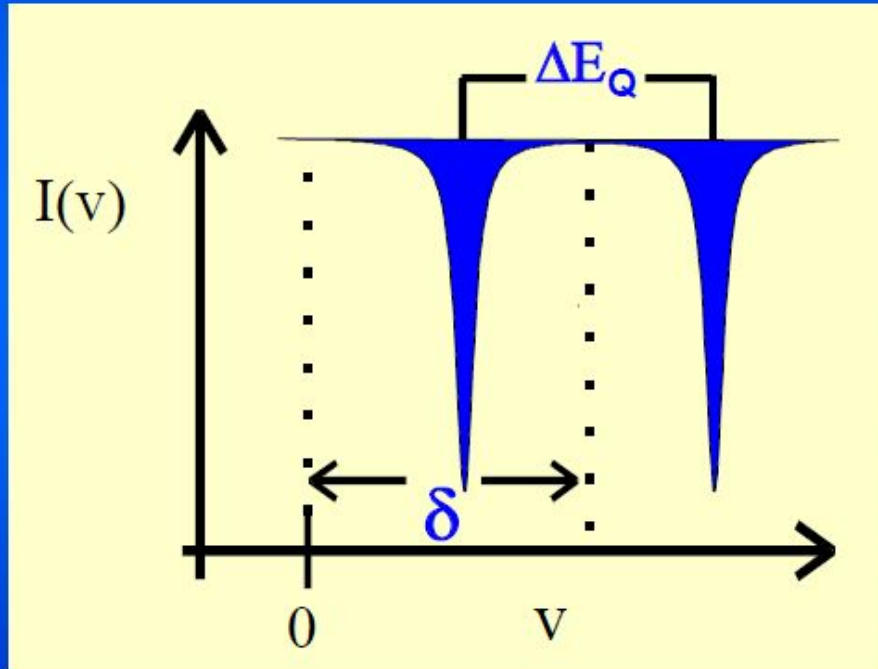
Electric Quadrupole Interaction

Quadrupole Splitting ΔE_Q



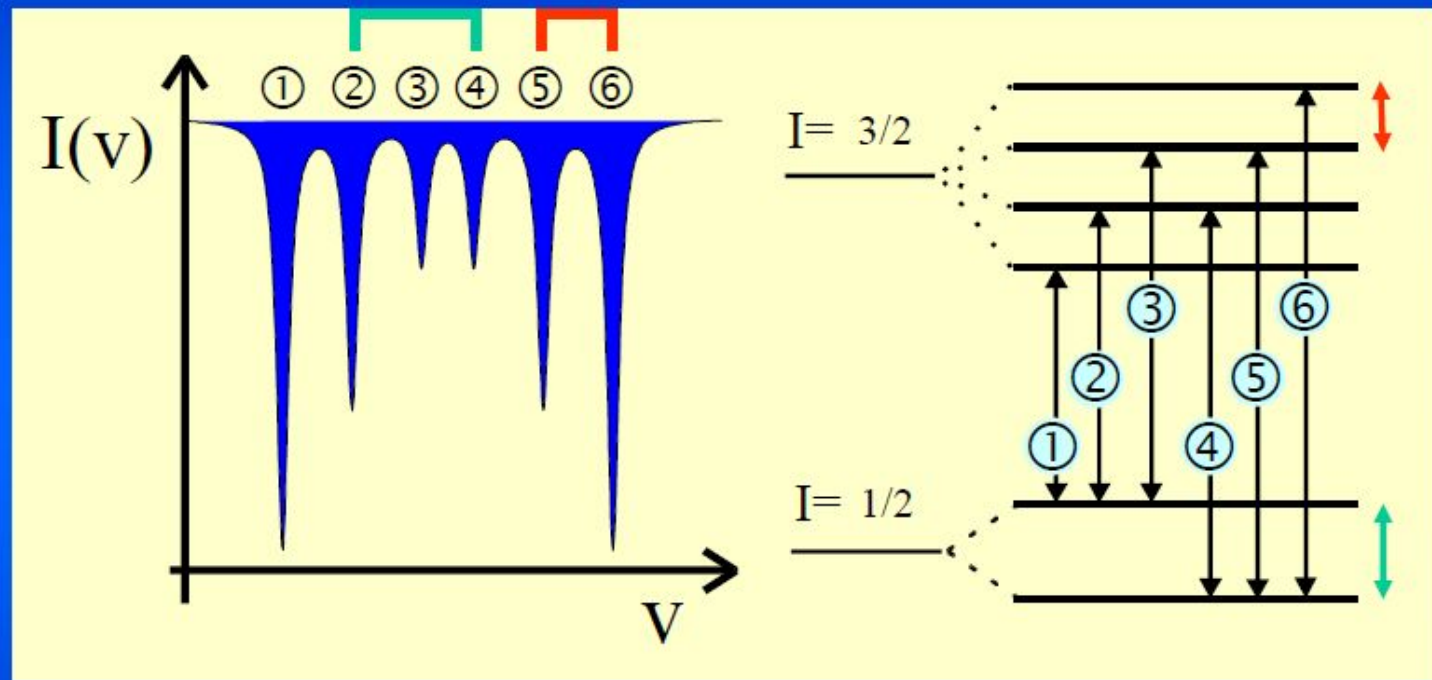
Electric Quadrupole Interaction

Quadrupole Splitting $\Delta E_Q \sim eQ \cdot \nabla E$



Oxidation state
Spin state,
Symmetry

$$E_M(m_I) = -\mu H m_I / I$$



**Ferro-, Antiferro-,
Ferri -magnetism**

Pure magnetic dipole interaction

Magnetic dipole interaction (Zeeman effect) is described by the Hamiltonian

$$\hat{H}_M = -\hat{\boldsymbol{\mu}} \cdot \hat{\mathbf{H}} = -g_N \beta_N \hat{\mathbf{I}} \cdot \vec{H}$$

g_N : nuclear Landé-factor

$\beta_N = e\hbar/2Mc$ nuclear Bohr magneton

If $\vec{H} \parallel \vec{z}$:

$$\hat{H}_M = -g_N \beta_N H \hat{I}_z$$

First order perturbation theory yields the matrix (elements) equations:

$$\left\| \left\langle I, m'_I \left| \hat{H}_M \right| I, m_I \right\rangle - E_M \delta_{m'_I m_I} \right\| = 0 \quad \text{with eigenvalues} \quad \mathbf{E}_M(\mathbf{I}, \mathbf{m}_I) = -g_N \beta_N H m_I$$

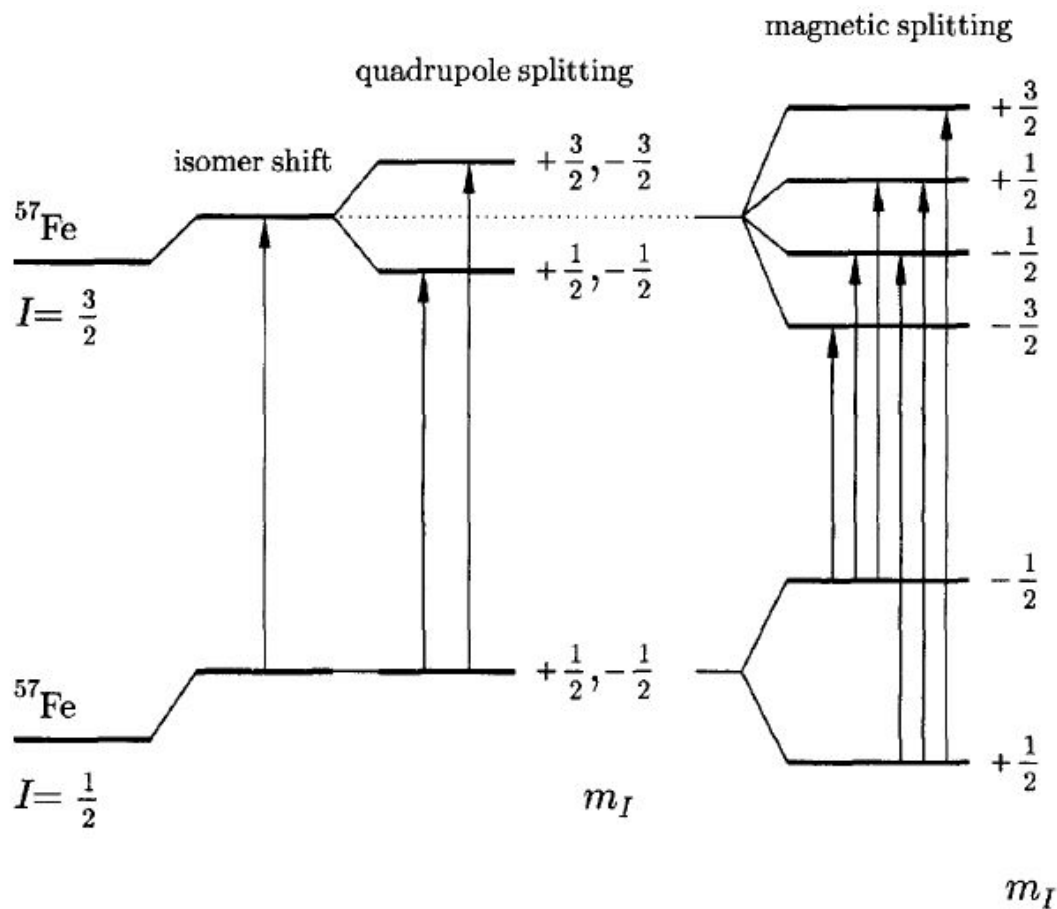


Fig. 3.20 The effects of chemical shift, quadrupole splitting and magnetic splitting on the nuclear energy levels of ^{57}Fe . The arrows show the Mössbauer absorption transitions. The difference in the size of the transitions is greatly exaggerated; in reality they typically differ from each other by less than 1 part in 10^{11} .



ELSEVIER

Journal of Alloys and Compounds 317–318 (2001) 44–51

Journal of
ALLOYS
AND COMPOUNDS

www.elsevier.com/locate/jallcom

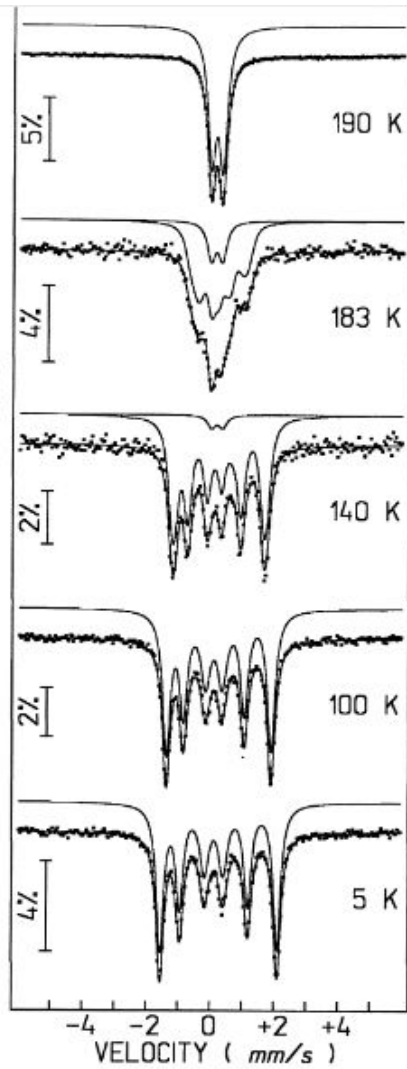
^{57}Fe Mössbauer spectroscopy study of the $\text{AFe}_x\text{Al}_{12-x}$ intermetallics
($\text{A}=\text{Y}$, Tm, Lu and U, $4 \leq x \leq 4.3$)

J.C. Waerenborgh^{a,*}, P. Salamakha^a, O. Sologub^a, A.P. Gonçalves^a, S. Sérgio^b, M. Godinho^b,
M. Almeida^a

^a*Departamento de Química, Instituto Tecnológico e Nuclear, P-2686-953 Sacavém, Portugal*

^b*Departamento de Física, Faculdade de Ciências da Universidade de Lisboa, P-1749-016 Lisboa, Portugal*

RELATIVE TRANSMISSION

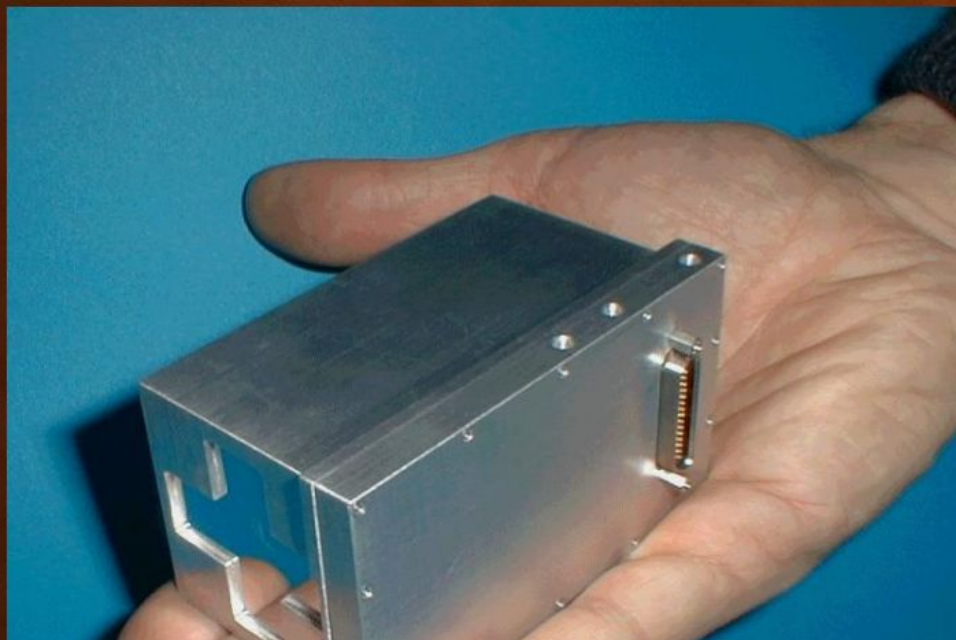


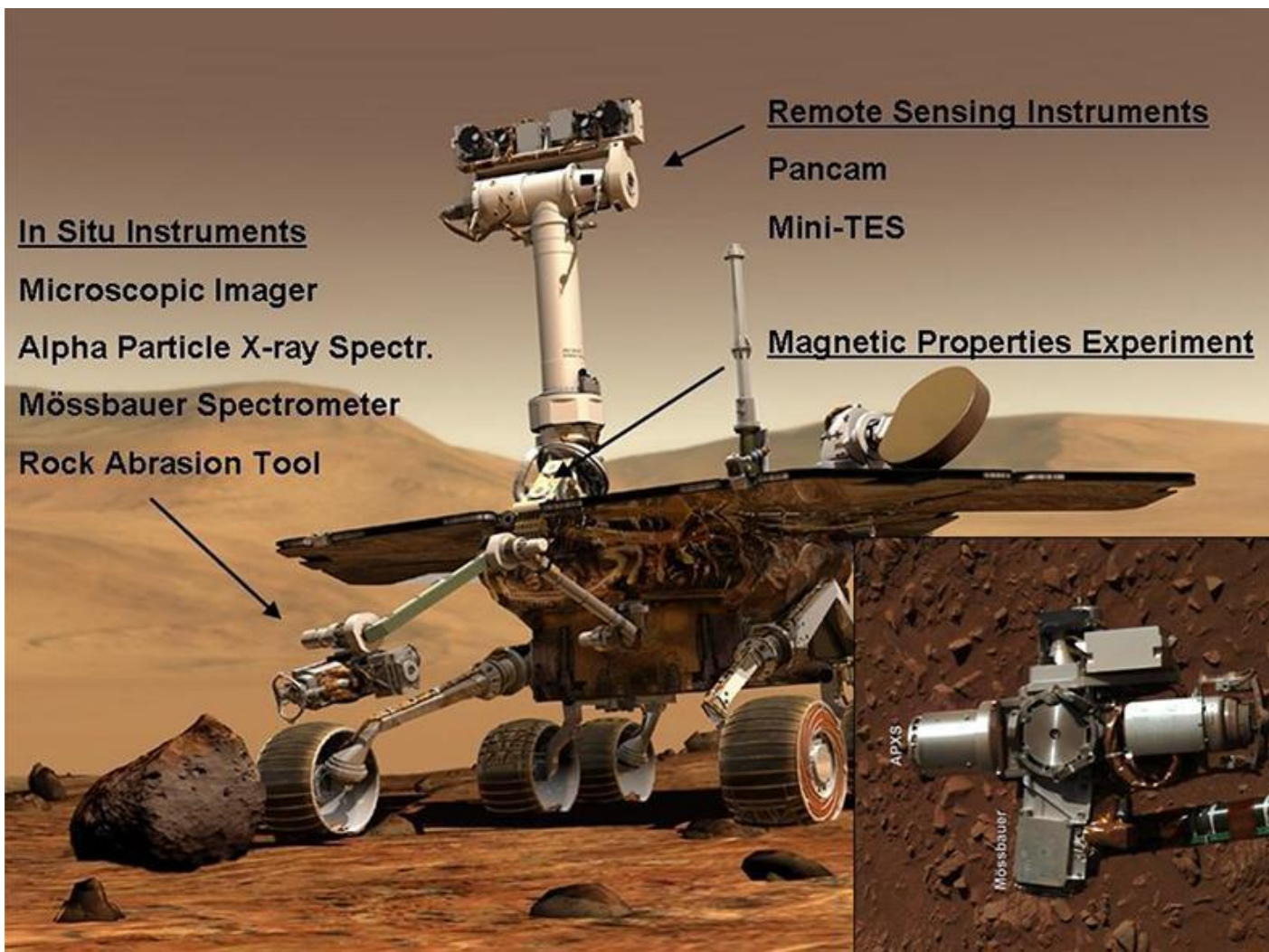


MB



The Mössbauer Spectrometer on the Mars Exploration Rovers, Spirit and Opportunity, is known as MB. The MB determines the makeup and quantities of iron-bearing minerals in geological samples studied by the rover. MB can be placed right up to rock and soil samples for close-up study, and it also examines magnetic dust samples





Remote Sensing Instruments

Pancam

Mini-TES

Magnetic Properties Experiment

In Situ Instruments

Microscopic Imager

Alpha Particle X-ray Spectr.

Mössbauer Spectrometer

Rock Abrasion Tool

APXS

Mössbauer



Propriedades Magnéticas



Propriedades Magnéticas